



Seventh Framework Programme FP7-SPACE-2010-1  
Stimulating the development of downstream GMES services

Grant agreement for: Collaborative Project. Small- or medium scale focused research project

Project acronym: **SIDARUS**

Project title: Sea Ice Downstream services for Arctic and Antarctic Users and Stakeholders

Grant agreement no. 262922

Start date of project: 01.01.11

Duration: 36 months

Project coordinator: Nansen Environmental and Remote Sensing Center, Bergen, Norway

**D6.1: Measurements of Arctic sea ice thickness  
by UK submarines**

Due date of deliverable: 31.12.2011

Actual submission date: 07.02.2012

Organization name of lead contractor for this deliverable: UCAM

Project co-funded by the European Commission within the Seventh Framework Programme, Theme 6 SPACE		
Dissemination Level		
PU	Public	X
PP	Restricted to other programme participants (including the Commission)	
RE	Restricted to a group specified by the consortium (including the Commission)	
CO	Confidential, only for members of the consortium (including the Commission)	

ISSUE	DATE	CHANGE RECORDS	AUTHOR
1	06/12/2012	Version 1	J. Rodrigues
1	06/01/2012	Version 4	J. Rodrigues
1	10/01/2012	Version 7	J. Rodrigues
1	15/01/2012	Version 8	J. Rodrigues
1	21/01/2012	Version 10	J. Rodrigues
1	01/02/2012	Version 11	J. Rodrigues
1	06/02/2012	Version 12	J. Rodrigues
1	07/02/2012	Version 13	J. Rodrigues

### **SIDARUS CONSORTIUM**

Participant no.	Participant organisation name	Short name	Country
1 (Coordinator)	Nansen Environmental and Remote Sensing Center	NERSC	NO
2	Alfred-Wegener-Institut für Polar-und Meeresforschung	AWI	DE
3	Collecte Localisation Satellites SA	CLS	FR
4	University of Bremen, Institute of Environmental Physics	UB	DE
5	The Chancellor, Masters and Scholars of the University of Cambridge	UCAM	UK
6	Norwegian Meteorological Institute, Norwegian Ice Service	Met.no	NO
7	Scientific foundation Nansen International Environmental and Remote Sensing Centre	NIERSC	RU
8	B.I. Stepanov Institute of Physics of the National Academy of Sciences of Belarus	IPNASB	BR

No part of this work may be reproduced or used in any form or by any means (graphic, electronic, or mechanical including photocopying, recording, taping, or information storage and retrieval systems) without the written permission of the copyright owner(s) in accordance with the terms of the SIDARUS Consortium Agreement (EC Grant Agreement 262922).

All rights reserved.

This document may change without notice.

## Table of Contents

Table of Contents .....	3
1 Introduction.....	13
1.1 The rapid decline of the Arctic sea ice .....	13
1.2 From perennial to seasonal Arctic sea ice.....	14
1.3 The future of the Arctic sea ice .....	15
1.4 The importance of the sea ice thickness distribution .....	16
2 Theory and measurements of sea ice thickness .....	18
2.1 The ice thickness distribution.....	18
2.2 The pressure ridge distribution .....	19
2.3 The lead distribution .....	22
2.4 Submarine measurements .....	22
2.5 Satellite altimetry measurements .....	24
2.6 Electromagnetic sounding.....	26
2.7 Other methods of ice thickness determination .....	28
2.8 Conversion of draft and freeboard into thickness .....	29
3 Draft measurements with single-beam sonars .....	32
3.1 Analysis of Admiralty Pattern 780 sonar records.....	32
3.2 Beamwidth effects.....	37
3.3 Other errors and uncertainties.....	39
3.4 Analysis of Admiralty Pattern 2077 sonar records.....	39
3.5 Multibeam sonars.....	43
4 Previous Royal Navy cruises .....	45
4.1 The 1976 <i>Gurnard</i> Cruise.....	46
4.2 The 1976 <i>Sovereign</i> Cruise .....	47
4.3 The 1979 <i>Sovereign</i> Cruise .....	50
4.4 The 1985 Cruise .....	51
4.5 The 1987 <i>Superb</i> Cruise.....	53
4.6 The 1991 <i>Tireless</i> Cruise .....	55
4.7 The 1996 <i>Trafalgar</i> Cruise .....	56
5 The 2004 <i>Tireless</i> Cruise .....	58
5.1 Description of the cruise .....	58
5.2 Ice draft distribution: general results.....	61
5.3 Pressure ridge distribution: general results .....	65
5.4 Regional analysis .....	70
5.4.1 Fram Strait .....	71
5.4.2 Northeast Greenland and North Greenland.....	76
5.4.3 The GreenICE Survey .....	82
5.4.4 North Pole.....	82
5.5 AP2077 results.....	83
6 The 2007 <i>Tireless</i> Cruise .....	86
6.1 Description of the cruise – the outbound journey.....	86

---

6.2	Description of the cruise – the homebound journey .....	90
6.3	Ice draft distribution: general results – outbound journey.....	91
6.4	Ice draft distribution: general results – homebound journey.....	95
6.5	Pressure ridge distribution: general results .....	98
6.6	Regional analysis .....	108
6.6.1	South Fram Strait.....	110
6.6.2	Central Fram Strait .....	113
6.6.3	North Fram Strait.....	115
6.6.4	Northeast Greenland.....	116
6.6.5	North Greenland.....	120
6.6.6	The DAMOCLES Survey .....	122
6.6.7	North Ellesmere Island .....	122
6.6.8	Canadian Basin .....	123
6.6.9	Beaufort Sea .....	125
6.6.10	The SEDNA Survey .....	129
7	Long term changes in Arctic sea ice thickness .....	131
7.1	Fram Strait .....	131
7.2	North Greenland and Ellesmere Island .....	134
7.3	The North Pole.....	136
7.4	The Beaufort Sea .....	136
8	Comparison with other ice thickness measurements .....	138
8.1	Submarine vs ICESat measurements .....	138
8.2	Submarine vs electromagnetic sounding .....	141
9	Conclusion .....	142

### **List of Figures**

Figure 2-1. Sea ice thickness distribution in March 2007 from ICESat measurements.....	26
Figure 3-1. First example of a record of the bottom topography of the sea ice obtained with an AP780 sonar.....	32
Figure 3-2. Second example of a record of the bottom topography of the sea ice obtained with an AP780 sonar.....	33
Figure 3-3. Example of a dark hyperbolic shaped feature used to identify the water level. ....	35
Figure 3-4. The roll section shown in Figure 3-1 after processing is complete.....	36
Figure 3-5. The roll section shown in Figure 3-2 after processing is complete.....	36
Figure 3-6. Draft of the roll section shown in Figure 3-1. ....	37
Figure 3-7. Example of an AT2077 record. ....	40
Figure 3-8. Basic principle of sonar operation. ....	41
Figure 3-9. Locations of recent CTD measurements used in the determination of the speed of sound. ....	42
Figure 3-10. Speed of sound measurements in Fram Strait.....	42
Figure 3-11. Speed of sound measurements N of Greenland and Ellesmere Island.....	43
Figure 3-12. Speed of sound measurements in the N Beaufort Sea. ....	43
Figure 3-13. Computer generated image of the underside of the ice from multibeam data.....	44
Figure 4-1. Track of the 1976 Gurnard cruise in the Beaufort Sea (in red). The track of the 2007 Tireless cruise around the SEDNA ice camp is also marked (in blue).....	46
Figure 4-2. Mean draft (in metres) for each section of the 1976 Sovereign cruise. ....	48
Figure 4-3. Mean ice drafts from 50km sections obtained during the 1979 cruise (from (Wadhams, 1983)). ....	51
Figure 4-4. Mean ice drafts from 50-km track sections obtained during the 1985 cruise (from (Wadhams, 1989)). The top box at high latitude is expanded in the next figure. ....	52
Figure 4-5. Mean ice drafts from 50-km track sections obtained during the 1985 cruise (from (Wadhams, 1989)). ....	53
Figure 4-6. Regions where sonar data were collected in Fram Strait during the 1987 cruise. Dark boxes mark extreme E and W limits of submarine track within 1° latitude increments (from (Wadhams, 1992)). ....	54
Figure 4-7. Track of the April 1991 cruise. ....	56
Figure 4-8. Track of the September 1996 cruise (from (Wadhams and Davis, 2001)). ....	57
Figure 5-1. Track of the April 2004 cruise. ....	58
Figure 5-2. Track of the submarine in Fram Strait during the 2004 cruise. ....	59
Figure 5-3. Track of the GreenICE Survey on on 10-11 April 2004.....	60
Figure 5-4. Mean ice draft (in metres) for each section of the 2004 cruise.....	63
Figure 5-5. Mean (circles) and modal (crosses) ice drafts for each section of the 2004 cruise in Fram Strait. ....	71
Figure 5-6. Mean ice draft (in metres) for each section of the 2004 cruise in Fram Strait.....	72
Figure 5-7. Ice draft histograms for Central Fram Strait W (sections 1-18) in linear (L) and semi-logarithmic (R) scales.....	73
Figure 5-8. Ice draft histograms for Central Fram Strait E (sections 30-33) in linear (L) and semi-logarithmic (R) scales.....	73

Figure 5-9. Ice draft histograms for North Fram Strait (sections 34-37) in linear (L) and semi-logarithmic (R) scales.....	74
Figure 5-10. 5m (circles) and 9m (triangles) ridge keel frequency in each section of the 2004 cruise in Fram Strait. ....	74
Figure 5-11. Mean number of ridges per km for each section of the 2004 in Fram Strait. Left for 5m keels, right for 9m keels . ....	75
Figure 5-12. Mean number of 15m keels per km for each section of the 2004 in Fram Strait.....	75
Figure 5-13. Keel depth distribution histogram for sections 1-18. ....	76
Figure 5-14. Mean (circles) and modal (crosses) ice drafts for each section of the 2004 cruise in Northeast and North Greenland. ....	76
Figure 5-15. Mean ice draft (in metres) for each section of the 2004 cruise in Northeast Greenland and North Greenland.....	77
Figure 5-16. Ice draft histograms for Northeast Greenland (sections 38-43) in linear (L) and semi-logarithmic (R) scales.....	77
Figure 5-17. Ice draft histograms for North Greenland (sections 44-57) in linear (L) and semi-logarithmic (R) scales.....	78
Figure 5-18. Ice draft histograms for North Greenland (sections 59-62) in linear (L) and semi-logarithmic (R) scales.....	79
Figure 5-19. 5m (circles) and 9m (triangles) ridge keel frequency in each section of the 2004 cruise in Northeast Greenland and North Greenland. ....	79
Figure 5-20. Mean number of ridges per km for each section of the 2004 in Northeast Greenland and North Greenland. Top for 5m keels, middle for 9m keels and bottom for 15m keels.....	80
Figure 5-21. Ridge spacing distribution for keels deeper than 9m in North Greenland (sections 44-57). In violet the observed values, in yellow the best lognormal fit, both normalized to unity. ....	81
Figure 5-22. Distribution of the number of ridges deeper than 15m per km in North Greenland II (sections 59-62). In red the observed values, in blue the Poisson fit, both normalized to unity. ....	81
Figure 5-23. Ice draft histograms for the North Pole in linear (L) and semi-logarithmic (R) scales. ....	83
Figure 6-1. Track of the outgoing part of the March 2007 cruise. ....	86
Figure 6-2. Track of the submarine in Fram Strait during the outwards part of the 2007 cruise. ....	87
Figure 6-3. Track of the DAMOCLES Survey on 12-13 March 2007.....	88
Figure 6-4. Track of the SEDNA Survey on 18 March 2007. ....	89
Figure 6-5. Mean ice draft (in metres) for each 50km section of the outbound part of the 2007 cruise. ....	93
Figure 6-6. Mean ice draft (in metres) for each 50km section of the homebound part of the 2007 cruise. ....	97
Figure 6-7. Mean (circles) and modal (crosses) ice draft for each section of the outbound part of the 2007 cruise in Fram Strait.....	111
Figure 6-8. Mean ice draft for each section of the outbound (left) and homebound (right) parts of the 2007 cruise in Fram Strait.....	111
Figure 6-9. Ice draft histograms in linear (L) and semi-logarithmic (R) scales for the outbound part of the 2007 cruise in South Fram Strait (sections 2-5). ....	112
Figure 6-10. Ice draft histograms in linear (L) and semi-logarithmic (R) scales for the homebound part of the 2007 cruise in South Fram Strait (sections 60-63). ....	112
Figure 6-11. Ice draft histograms in linear (L) and semi-logarithmic (R) scales for the homebound part of the 2007 cruise in South Fram Strait (sections 64-67). ....	112

Figure 6-12. 5m (circles), 9m (triangles) and 15m (squares) ridge frequency in each section of the outbound part of the 2007 cruise in Fram Strait. ....	113
Figure 6-13. Mean number of 5m (L) and 9m (R) keels per km for each section of the outbound part of the 2007 cruise in Fram Strait. ....	113
Figure 6-14. Ice draft histograms in linear (L) and semi-logarithmic (R) scales for the outbound part of the 2007 cruise in Central Fram Strait (sections 6-10). ....	114
Figure 6-15. Ice draft histograms in linear (L) and semi-logarithmic (R) scales for the homebound part of the 2007 cruise in Central Fram Strait (sections 55-59). ....	114
Figure 6-16. Distribution of the number of ridges deeper than 15m per km in Central Fram Strait (sections 6-10) during the outbound part of the 2007 cruise. ....	115
Figure 6-17. Keel depth distribution histogram cruise in Central Fram Strait (sections 6-10) for the outbound part of the 2007. ....	115
Figure 6-18. Ice draft histograms in linear (L) and semi-logarithmic (R) scales for the outbound part of the 2007 cruise in North Fram Strait (sections 11-14). ....	116
Figure 6-19. Ice draft histograms in linear (L) and semi-logarithmic (R) scales for the homebound part of the 2007 cruise in North Fram Strait (sections 51-54). ....	116
Figure 6-20. Mean (circles) and modal (crosses) ice draft for each section of the outbound part of the 2007 cruise in Northeast Greenland, North Greenland and North Ellesmere Island. ....	117
Figure 6-21. Mean ice draft for each section of the outbound part of the 2007 cruise in Northeast Greenland, North Greenland and North Ellesmere Island. ....	117
Figure 6-22. Mean ice draft for each section of the homebound part of the 2007 cruise in North Ellesmere Island, North Greenland and Northeast Greenland. ....	118
Figure 6-23. Ice draft histograms in linear (L) and semi-logarithmic (R) scales for the outbound part of the 2007 cruise in Northeast Greenland (sections 15-18). ....	118
Figure 6-24. Ice draft histograms in linear (L) and semi-logarithmic (R) scales for the homebound part of the 2007 cruise in Northeast Greenland (sections 47-50). ....	118
Figure 6-25. 5m (circles) and 9m (triangles) ridge frequency in each section of the outbound part of the 2007 cruise in Northeast Greenland, North Greenland and North Ellesmere Island. ....	119
Figure 6-26. Mean number of 5m keels per km for each section of the outbound part of the 2007 cruise in Northeast Greenland, North Greenland and North Ellesmere Island. ....	119
Figure 6-27. Mean number of 9m keels per km for each section of the outbound part of the 2007 cruise in Northeast Greenland, North Greenland and North Ellesmere Island. ....	119
Figure 6-28. Ice draft histograms in linear (L) and semi-logarithmic (R) scales for the outbound part of the 2007 cruise N of Greenland (sections 19-32). ....	120
Figure 6-29. Ice draft histograms in linear (L) and semi-logarithmic (R) scales for the homebound part of the 2007 cruise N of Greenland (sections 37-46). ....	121
Figure 6-30. Ridge spacing distribution for keels deeper than 5m (L) and 9m (R) for the outbound part of the 2007 cruise in North Greenland (sections 19-32). Observations in violet, best lognormal fit in yellow. ....	121
Figure 6-31. Keel depth distribution histogram for the outgoing part of the 2007 cruise in North Greenland and North Ellesmere Island (sections 19-36). Observations in red, exponential fit in yellow. ....	122
Figure 6-32. Ice draft histograms for the DAMOCLES Survey in linear (L) and semi-logarithmic (R) scales. ....	122

Figure 6-33. Ice draft histograms in linear (L) and semi-logarithmic (R) scales for the outbound part of the 2007 cruise N of Ellesmere Island (sections 35-36). .....	123
Figure 6-34. Ice draft histograms in linear (L) and semi-logarithmic (R) scales for the homebound part of the 2007 cruise N of Ellesmere Island (sections 33-36). .....	123
Figure 6-35. Ice draft histograms in linear (L) and semi-logarithmic (R) scales for the outbound part of the 2007 cruise in the Canadian Basin (sections 38-52).....	124
Figure 6-36. Ice draft histograms in linear (L) and semi-logarithmic (R) scales for the homebound part of the 2007 cruise in the Canadian Basin (sections 18-32). .....	124
Figure 6-37. Mean number of 5m (L) and 9m (R) keels per km for each section of the outbound part of the 2007 cruise in the Canadian Basin. ....	125
Figure 6-38. Mean (circles) and modal (crosses) ice drafts for each section of the outbound of the 2007 cruise in the Beaufort Sea. ....	126
Figure 6-39. Mean ice draft for each section of the outbound (left) and homebound (right) parts of the 2007 cruise in the Beaufort Sea. ....	126
Figure 6-40. Ice draft histograms in linear (L) and semi-logarithmic (R) scales for the outgoing part of the 2007 cruise in the Beaufort Sea (sections 53-64). ....	127
Figure 6-41. Ice draft histograms in linear (L) and semi-logarithmic (R) scales for the homebound part of the 2007 cruise in the Beaufort Sea (sections 1-17). ....	127
Figure 6-42. Mean number of 5m (L) and 9m (R) keels per km for each section of the outbound part of the 2007 cruise in the Beaufort Sea. ....	128
Figure 6-43. Keel depth distribution histogram for the homebound part of the 2007 cruise in the Beaufort Sea (sections 1-16). Observations in red, exponential fit in yellow. ....	128
Figure 6-44. Comparison of the keel depth distribution in the Beaufort Sea and North Greenland in the outbound part of the 2007 cruise. ....	129
Figure 6-45. Comparison of the keel depth distribution in the Beaufort Sea (violet) and North Greenland (yellow) in the outbound part of the 2007 cruise (this time in semi-logarithmic scale). ....	129
Figure 6-46. Ice draft histograms for the SEDNA Survey in linear (L) and semi-logarithmic (R) scales. ....	130
Figure 6-47. Keel depth distribution of the SEDNA Survey in linear (L) and semi-logarithmic (R) scales. ....	130
Figure 7-1. Mean sea ice draft in Central Fram Strait between 1976 and 2007. ....	133
Figure 7-2. Mean sea ice draft in North Fram Strait between 1976 and 2007. ....	134
Figure 7-3. Ice draft histograms for North Greenland in 2004 (L) and 2007 outgoing (R). ....	134
Figure 7-4. Mean ice draft in each section of four cruises in North Greenland (latitude ~ 85°N). ....	136
Figure 8-1. Mean ice thickness from submarine and ICESat measurements for each section of the 2004 cruise. ....	139
Figure 8-2. Mean ice thickness from submarine and ICESat measurements for each section of the outgoing part of the 2007 cruise. ....	140
Figure 8-3. Histograms for the sea ice thickness distribution in the region N of Greenland in the winter of 2007 from ICESat measurements. ....	141

### **List of Tables**

Table 4-1. UK submarine cruises to Fram Strait and the Arctic Ocean. ....	45
Table 4-2. Centroid, length (in km) and average draft (in metres) of each section of the 1976 Gurnard cruise in the Beaufort Sea. ....	47
Table 4-3. Ice draft statistics for the 1976 Sovereign cruise. ....	49
Table 4-4. Regions covered by the 1976 Sovereign cruise, their boundaries, length (in km), sections involved and mean draft (in metres). ....	50
Table 4-5. Basic ice draft statistics for the 1979 cruise in Fram Strait. ....	51
Table 4-6. Basic ice draft statistics for the 1979 cruise in Fram Strait. ....	51
Table 4-7. Basic ice draft statistics for the 1985 cruise in Fram Strait. ....	53
Table 4-8. Mean drafts for latitude bins of 1° of latitude in the 1987 cruise in Fram Strait. ....	55
Table 4-9. Mean drafts for 50km sections in the N part of Fram Strait during the 1987 cruise. ....	55
Table 5-1. Regions covered by the 2004 cruise, their start and end times, sections involved and AP780 rolls used. ....	60
Table 5-2. Regions covered by the 2004 cruise, their boundaries, length of track with valid data (in km) and percentage of valid data. ....	61
Table 5-3. Ice draft statistics for the 2004 cruise, sections 1-37 (Fram Strait). Draft and coefficient $\alpha$ in metres. ....	62
Table 5-4. Ice draft statistics for the 2004 cruise, sections 38-102 (Northeast Greenland, North Greenland and North Pole). Draft and coefficient $\alpha$ in metres. ....	63
Table 5-5. Beamwidth corrections for the 2004 cruise, sections 1-37. Drafts and depths in metres, $\Delta d/d_{real}$ as a percentage. Not yet calculated. ....	64
Table 5-6. Beamwidth corrections for the 2004 cruise, sections 38-102. Drafts and depths in metres, $\Delta d/d_{real}$ as a percentage. ....	65
Table 5-7. 5m keel spacing statistics for the 2004 cruise, sections 1-37. Ridge frequency in $\text{km}^{-1}$ , mean draft, mean and modal spacings in metres. ....	66
Table 5-8. 5m keel spacing statistics for the 2004 cruise, sections 38-102. Ridge frequency in $\text{km}^{-1}$ , mean draft, mean and modal ridge spacing in metres. ....	67
Table 5-9. 9m keel spacing statistics for the 2004 cruise, sections 1-37. Ridge frequency in $\text{km}^{-1}$ , mean draft, mean and modal ridge spacing in metres. ....	67
Table 5-10. 9m keel spacing statistics for the 2004 cruise, sections 38-102. Ridge frequency in $\text{km}^{-1}$ , mean draft, mean and modal ridge spacing in metres. ....	68
Table 5-11. 15m keel spacing statistics for the 2004 cruise, sections 1-37. Ridge frequency in $\text{km}^{-1}$ , mean draft, mean and modal ridge spacing in metres. ....	69
Table 5-12. 15m keel spacing statistics for the 2004 cruise, sections 38-102. Ridge frequency in $\text{km}^{-1}$ , mean draft, mean and modal ridge spacing in metres. ....	70
Table 5-13. Ice draft statistics, before and after beamwidth corrections, for the regions of the 2004 cruise. Draft in metres, coefficient $\beta$ in $\text{metres}^{-1}$ . ....	70
Table 5-14. Numbers of keels deeper than 5, 9 and 15m for the regions of the 2004 cruise. ....	70
Table 5-15. Ice draft histograms for the GreenICE Survey in linear (L) and semi-logarithmic (R) scales. ....	82
Table 5-16. Ice draft statistics in the 2004 cruise from AP2077 records for sections 1-37. Draft, coefficient $\alpha$ and $\Delta D$ in metres. $\Delta D/D(2077)$ as a percentage. ....	84

Table 5-17. Ice draft statistics in the 2004 cruise from AP2077 records for sections 38-102. Draft, coefficient $\alpha$ and $\Delta D$ in metres. $\Delta D/D(2077)$ as a percentage. ....	85
Table 6-1. Regions covered by the outgoing part of the 2007 cruise, their start and end times, sections involved, and AP780 rolls used. ....	89
Table 6-2. Regions covered by outbound part of the 2007 cruise, their boundaries, length of track with valid data (in km), and percentage of valid data.....	90
Table 6-3. Regions covered by the homebound part of the 2007 cruise, their start and end times, sections involved, and AP780 rolls used. ....	91
Table 6-4. Regions covered by homebound part of the 2007 cruise, their boundaries, length of track with valid data (in km), and percentage of valid data.....	91
Table 6-5. Ice draft statistics for the outbound part of the 2007 cruise, sections 2-36 (Fram Strait, Northeast Greenland, North Greenland and North Ellesmere Island). Draft and coefficient $\alpha$ in metres. ....	92
Table 6-6. Ice draft statistics for the outbound part of the 2007 cruise, sections 38-64 (Canadian Basin and Beaufort Sea). Draft and coefficient $\alpha$ in metres. ....	93
Table 6-7. Beamwidth corrections for the outbound part of the 2007 cruise, sections 2-36. Drafts and depths in metres, $\Delta d/d_{real}$ as a percentage. ....	94
Table 6-8. Beamwidth corrections for the outbound part of the 2007 cruise, sections 38-64. Drafts and depths in metres, $\Delta d/d_{real}$ as a percentage. ....	95
Table 6-9. Ice draft statistics for the homebound part of the 2007 cruise, sections 1-32 (Beaufort Sea and Canadian Basin). Draft and coefficient $\alpha$ in metres. ....	96
Table 6-10. : Ice draft statistics for the homebound part of the 2007 cruise, sections 33-67 (North Ellesmere Island, North Greenland, Northeast Greenland and Fram Strait). Draft and coefficient $\alpha$ in metres. ....	97
Table 6-11. 5m keel spacing statistics for the outbound part of the 2007 cruise, sections 2-36. Ridge frequency in $\text{km}^{-1}$ , mean draft, mean and modal spacings in metres.....	99
Table 6-12. 5m keel spacing statistics for the outbound part of the 2007 cruise, sections 38-64. Ridge frequency in $\text{km}^{-1}$ , mean draft, mean and modal spacings in metres.....	100
Table 6-13. 9m keel spacing statistics for the outbound part of the 2007 cruise, sections 2-36. Ridge frequency in $\text{km}^{-1}$ , mean draft, mean and modal spacings in metres.....	100
Table 6-14. 9m keel spacing statistics for the outbound part of the 2007 cruise, sections 38-64. Ridge frequency in $\text{km}^{-1}$ , mean draft, mean and modal spacings in metres.....	101
Table 6-15. 15m keel spacing statistics for the outbound part of the 2007 cruise, sections 2-36. Ridge frequency in $\text{km}^{-1}$ , mean draft, mean and modal spacings in metres.....	102
Table 6-16. 15m keel spacing statistics for the outbound part of the 2007 cruise, sections 38-64. Ridge frequency in $\text{km}^{-1}$ , mean draft, mean and modal spacings in metres.....	103
Table 6-17. 5m keel spacing statistics for the homebound part of the 2007 cruise, sections 1-32. Ridge frequency in $\text{km}^{-1}$ , mean draft, mean and modal spacings in metres.....	104
Table 6-18. 5m keel spacing statistics for the homebound part of the 2007 cruise, sections 33-67. Ridge frequency in $\text{km}^{-1}$ , mean draft, mean and modal spacings in metres.....	105
Table 6-19. 9m keel spacing statistics for the homebound part of the 2007 cruise, sections 1-32. Ridge frequency in $\text{km}^{-1}$ , mean draft, mean and modal spacings in metres.....	105
Table 6-20. 9m keel spacing statistics for the homebound part of the 2007 cruise, sections 33-67. Ridge frequency in $\text{km}^{-1}$ , mean draft, mean and modal spacings in metres.....	106

---

Table 6-21. 15m keel spacing statistics for the homebound part of the 2007 cruise, sections 1-32. Ridge frequency in $\text{km}^{-1}$ , mean draft, mean and modal spacings in metres.....	107
Table 6-22. 15m keel spacing statistics for the homebound part of the 2007 cruise, sections 33-67. Ridge frequency in $\text{km}^{-1}$ , mean draft, mean and modal spacings in metres.....	108
Table 6-23. Ice draft statistics before and after beamwidth corrections for the regions of the outgoing part of the 2007 cruise. Draft in metres, coefficient $\beta$ in $\text{metres}^{-1}$ .....	109
Table 6-24. Ice draft statistics before and after beamwidth corrections for the regions of the homebound part of the 2007 cruise. Draft in metres, coefficient $\beta$ in $\text{metres}^{-1}$ .....	109
Table 6-25. Numbers of keels deeper than 5, 9 and 15m for the regions of the outbound part of the 2007 cruise. ....	110
Table 6-26. Numbers of keels deeper than 5, 9 and 15m for the regions of the homebound part of the 2007 cruise. ....	110
Table 7-1. Mean ice drafts in Fram Strait in 2004 and the outbound part of 2007. ....	132
Table 7-2. Mean ice drafts (in metres) in Fram Strait in 1976, 1979, 1985, 1987 and 1996. ....	132
Table 7-3. Mean ice draft (in metres) in the region north of Greenland ( $85^{\circ}\text{N}$ ). ....	135
Table 7-4. Mean ice draft in the vicinity of the North Pole (latitude $>89\text{N}$ ). ....	136
Table 7-5. Basic ice draft statistics for the location of the AIDJEX and SEDNA ice camps. ....	137
Table 8-1. Mean ice thickness (in metres) from submarine and ICESat measurements in the winters of 2004 and 2007 for the region North of Greenland ( $84^{\circ}30'-85^{\circ}30'\text{N}$ , $22-70^{\circ}\text{W}$ ). ....	140

**SUMMARY**

We present the results of all sea ice thickness measurements made with upward-looking single-beam sonars installed in Royal Navy submarines during Arctic cruises between 1976 and 2007 and the yet unpublished complete study of the full draft distribution and the pressure ridge distribution of the last two cruises, in the winters of 2004 and 2007.

We compare the observations of these two cruises with those of earlier voyages in an attempt to establish how the Arctic Ocean sea ice cover has evolved in the past few decades. However, our analysis is inconclusive and we are not able to state unequivocally that there has been a decline in the sea ice thickness in the regions most visited by British submarines, namely Fram Strait, North Greenland and the North Pole.

The results of the submarine measurements are compared with sea ice thickness determinations made with other techniques, such as satellite altimetry and airborne electromagnetic sounding.

# 1 Introduction

## 1.1 The rapid decline of the Arctic sea ice

The decline of the Arctic sea ice cover of the past few decades is one of the most conspicuous climatic alterations that are happening in our planet. Sea ice is not only very sensitive to changes in the atmosphere and the ocean, and as such considered a good indicator of global climate change, it is also an active component of the Arctic climate. Its well-documented reduction in area and thickness is likely to have a significant impact in the regional (and even global) climate due to some typical high-latitude amplification mechanisms such as the ice albedo feedback.

Continuous monitoring of the Arctic Ocean sea ice began in the late 1970s with the launch of the first satellites equipped with sensors that operate in the microwave band. These are especially suitable for the determination of sea ice concentrations because of the possibility of discrimination between ice and water due to their different emissivities at these frequencies. Passive microwave imagery, as this technique is known, provides unequivocal evidence of the recent sharp decline of sea ice extent in all sectors of the Arctic (e.g. Stroeve *et al.*, 2007), which culminated with the historical minima of September 2007 and September 2011, believed to be lower than at any other time in the last 8000 years (Heygster, 2011).

The time series of the monthly averaged Arctic sea ice extent (usually defined as the area limited by the 15% ice concentration contour) shows that its current value for the month of September is about two thirds of the typical value of the late 1970s for the same month. The decline has not been monotonic, though. In fact, the sea ice cover possesses a notorious stochastic interannual variability and, it has been argued, a vague periodicity due to a (weak) coupling to vaguely periodic atmospheric conditions such as the Arctic Oscillation. But even if we artificially attenuate the year-to-year fluctuations by a suitable smoothing procedure we observe that the evolution of the last 30 years or so has been far from linear. In fact, a linear fit to the time series of the September ice extent for the 10 year period between 2001 and 2011 would lead to a rate of decline of approximately 200,000 km<sup>2</sup>/year, about four times the value for the 1979-2000 period. In view of this non-linearity, Eisenman (2010) proposed a higher order polynomial fit to the data which appears to be a much better approximation to the real curve than a linear fit.

We may prefer to avoid selecting a particular time of the year, namely the very popular time of the seasonal minimum, either because we are not attracted to media headlines or because we are aware that the September ice cover may be affected by particular weather conditions during the preceding summer, as occurred in 2007. In this case the length of the ice-free season (LIFS) can be taken as a good indicator of the disappearance of the Arctic sea ice. The average increase of the Arctic LIFS during the 1979-2006 period was roughly 1.1 days/year while in the 2001-2007 period it was about five times faster (Rodrigues, 2009). This acceleration in the pace at which the LIFS is growing is observed almost everywhere in the Arctic. Two regions where the situation has been changing faster are the Barents Sea and the Greenland Sea. For instance in the eastern (northern) sector of the Barents Sea the rate of increase was 2.9 days/year (3.0 days/year) in the 1979-2008

period and 10.0 days/year (18.5 days/year) in the 2001-2007 period. In the Greenland Sea the growth was 1.7 and 2.8 days/year, respectively.

## 1.2 From perennial to seasonal Arctic sea ice

The northwards retreat of the Arctic sea ice has been accompanied by an overall thinning. Basin-wide observations of ice thickness, considerably more challenging than those of ice concentrations, are currently made from submarines, satellites and, to a less extent, from aircrafts.

After their first excursions to the Arctic, submarines were soon recognized as unique platforms for the observation and study of the properties of sea ice cover across the whole Arctic basin (well, possibly with the exception of Soviet/Russian territorial waters). In a remote place where in-situ measurements are particularly difficult, these voyages have always been cherished by the scientific community, who was presented with a wealth of data of great importance for the understanding of the Arctic climate. For instance, studies of several thousands of kilometres of under-ice profiles led to the conclusion that there has been a significant thinning of the sea ice layer in the past few decades. Rothrock *et al.* (1999) and, independently, Wadhams and Davis (2000) report a drop of more than 40% in sea ice thickness between the mid-1970s and the mid-1990s. Such results were among the earliest to provide hard evidence that something remarkable was happening to the Arctic.

Then came the satellites, equipped with altimeters of increasing degree of sophistication, and with them the possibility of a continuous, global coverage of the Arctic, and the ambition of being able to measure accurately the thickness of the sea ice in the Arctic Ocean and surrounding seas, and to detect any possible trends. First were ESA's ERS-1, launched in 1991 and active until March 2000, and ERS-2, in orbit since April 1995; they were followed by ESA's Envisat, operational since March 2002; then came NASA's ICESat, launched in January 2003 and decommissioned in August 2010; and finally ESA's CryoSat, in operation since April 2010.

Convincing analyses of satellite altimetry data by Laxon *et al.* (2003), Giles *et al.* (2008), Farrell *et al.* (2009) and Kwok *et al.* (2009), among others, showed that the thinning of the Arctic sea ice first detected by the submarines continued into the 21st century.

It then became clear that the decrease in the mean ice thickness of the Arctic Ocean was associated with the reduction in the mean ice thickness of the multi-year ice and with the decline of the area covered by multi-year ice (Kwok *et al.*, 2009). Differentiation between first- and multi-year ice is achieved with scatterometers such as the SeaWinds instrument on board NASA's QuikSCAT satellite. Other techniques, such as satellite tracking of parcels of ice or the use of drifting buoys, confirm that the Arctic ice cover is getting younger and younger. There is now much more first-year ice in the Arctic than multi-year ice and most of the latter is two or three years old. Not so long ago (in the mid-1980s) the situation was the opposite (Maslanik *et al.*, 2007).

The younger and thinner the ice is, the more vulnerable it becomes to further melt, dynamical desintegration and drift towards lower latitudes. Special weather conditions or simply the natural variability of the Arctic climate may then trigger rapid reductions in the ice cover such as the one that occurred in the summer of 2007.

The Arctic Ocean may partially recover from such rapid ice loss events but a return to the conditions of just a few decades ago is ruled out by all climate models simulations. We are moving towards an Arctic of thinner ice in the winter and almost no ice in the summer. In other words, we are currently in a period of transition between a perennially ice covered Arctic Ocean and a seasonally ice covered one. The causes and consequences of this transformation are what matter for the scientist. The question of the exact timing of the first totally ice-free summer in the northern hemisphere for at least 8000 years is of little relevance. In fact, we are aware that, due to the chaotic nature of the climate system and other unknowns, we shall never have the answer in advance.

What we can do is to run climate models with slightly different initial conditions and generate an ensemble of possible future trajectories whose statistical analysis should give us an idea of...

### 1.3 The future of the Arctic sea ice

In view of the complexity of the climate system, the incomplete knowledge of the physical processes involved, the uncertainty in the initial state, notably in the sea ice thickness distribution, and the impossibility of predicting the future concentration of greenhouse gases in the atmosphere, there is little hope of finding the exact (or even approximately exact) evolution of the Arctic sea ice cover until, say, the end of the century. The projections of most global climate models taken into account for AR4 (IPCC, 2007) are for an on-going decline and an ice-free Arctic Ocean (at the end of the melt season) some time in the late 21<sup>st</sup> century (Stroeve *et al.*, 2007). A much faster disappearance of the Arctic sea ice, conceivably as early as 2040, was first suggested by Holland *et al.* (2006) after identifying several periods of abrupt ice loss in simulations of the NCAR CCSM model (Collins *et al.*, 2006) for the 21<sup>st</sup> century. Shortly after, Maslowski *et al.* (2007b) used their high-resolution coupled ice-ocean model (Maslowski *et al.*, 2007a) to put forward the possibility of an ice-free Arctic during the summer in the next few years.

From the 23 models that are part of the World Climate Research Programme's Coupled Model Intercomparison Project phase 3 (CMIP3) multi-model data set (Meehl, 2007), Wang and Overland (2009) selected the six that most successfully simulate the seasonal sea ice cycle and most faithfully reproduce the observed September ice extent between 1980 and 1999. These are the Community Climate System Model version 3.0 (CCSM3), developed by a consortium led by the National Center for Atmospheric Research (NCAR) in Boulder, USA; the model of the Centre National de Recherches Meteorologiques, version 3 (CNRM-CM3); the German ECHO-G model, which comprises the atmospheric component ECHAM-4 developed at the Max Planck Institute for Meteorology in Hamburg and the ocean component HOPE-G, also developed in Hamburg; the model of the Institute Pierre Simon Laplace (IPSL), France; the Japanese MIROC model; and finally the HadGEM1 model, created at the UK Met Office Hadley Centre.

Such a selection gives the necessary confidence to make acceptable, if not completely reliable, projections for future trajectories of the Arctic sea ice. Incidentally, these are also models that predict a faster future decline of the September ice extent. And yet, there is still a large dispersion between the projections of these models and even between different runs of the same model (namely because of the intrinsic variability of the climate system). Considering all available runs for

these six models, Wang and Overland calculated that the mean and median time needed for the September sea ice extent to be reduced from  $4.6\text{Mkm}^2$  to  $1.0\text{Mkm}^2$  are both approximately 30 years for the A1B scenario (and about 35 years for A2). We remark that CNRM-CM3 predicts the ice to be gone in just over 10 years while according to the UKMO-HadGEM1 we have to wait for 45 years (in A1B). The lower threshold of  $1.0\text{Mkm}^2$  was chosen because there are strong indications that the waters adjacent to the north shores of Greenland and the Canadian Archipelago will keep some ice for themselves even when it is gone everywhere else. On the other hand, the value  $4.6\text{Mkm}^2$  was the approximate value of the observed ice extent in September 2008.

## 1.4 The importance of the sea ice thickness distribution

The determination of the thickness of the sea ice layer in the Arctic Ocean and surrounding seas is an essential component of the study of the Arctic climate. On the one hand, the Arctic environment and, in particular, sea ice respond quickly to global climatic changes due to amplification processes that exist in the polar regions. Hence, a decline in the volume of sea ice can be regarded as one of the best signs of the warming of the planet. On the other hand, because sea ice acts as a regulator of heat and moisture transfer between the ocean and the atmosphere, changes in its thickness are likely to affect significantly the climate of the Arctic and nearby regions.

The second reason why it is important to have an accurate knowledge of the Arctic sea ice thickness is that it is a crucial piece of the initial state in climate simulations for the 21<sup>st</sup> century. The capability of global climate models to predict the future of the Arctic sea ice is hampered by our comparatively poor knowledge of the current sea ice thickness distribution. Simulations of future Arctic climate and, specifically, of Arctic sea ice extent, are known to be very sensitive to the initial sea ice thickness input (Gerdes, 2011). For example, simulations with the NAOSIM coupled ocean/sea ice model (Karcher *et al.*, 2003; Kauker *et al.*, 2003) initialized with comparatively thin ice exhibit a much quicker decline of the summer sea ice than those with an initially thicker ice cover. This appears to be also the case with other models and, for instance, it is likely to be one of the reasons why the Hadley Centre HadGEM1 (Johns *et al.*, 2006) and HadGEM2 (Collins *et al.*, 2008) models, which have different sea ice thickness distributions as inputs, generate very different future trajectories of the Arctic sea ice.

And yet, this apparent importance of the initial conditions has been questioned by the recent work of Tietsche and collaborators (Tietsche *et al.*, 2011). Using the ECHAM5/MPI-OM global climate model (Roeckner *et al.*, 2003; Marsland *et al.*, 2003), the authors simulated the effect of artificially removing all ice from the Arctic Ocean at the beginning of the summer. The unexpected outcome was that within a few years the ice would return to approximately the same state that it would have reached under the usual external forcing. This result indicates that the Arctic Ocean may be able to recover from drastic ice losses. Thus, contrary to the conventional point of view, an Arctic Ocean free of ice in one summer does not imply an Arctic Ocean free of ice in all subsequent summers. The seeming inexistence of such a tipping point is discussed by Serreze (2011). The basic physics behind the recovery is that most of the excess heat received by the ocean during an ice-free summer is lost to the atmosphere and then to space during the autumn and winter precisely because of the absence of an effective insulating layer between the ocean and the atmosphere.

In view of the above, the sea ice community and the global climate community expect the measurements of the sea ice thickness to continue and to become more and more accurate. And while we wait for a continuous, total and reliable satellite information, submarine missions remain essential.

## 2 Theory and measurements of sea ice thickness

### 2.1 The ice thickness distribution

The ice thickness (or, for this matter, ice draft) distribution of a region  $R$ , which can be a limited area or a section of a one-dimensional transect, is completely defined by the function  $g(h)$  such that  $g(h)dh$  gives the probability of finding in  $R$  ice with thickness in the interval  $(h, h+dh)$ . Since  $g(h)$  is interpreted as a probability density, one tends to normalize it to unity:

$$\int_0^{\infty} g(h)dh = 1.$$

The experimental determination of  $g$  begins with a set of  $S$  ice thickness observations (ideally with  $S$  very large) in the region  $R$  which are subsequently distributed over bins of size  $\Delta h$  in order to construct a histogram of measurements. Let  $G_n$  be the frequency distribution of the measurements over the set of  $N$  bins. In other words,  $G_n$ , with  $n=1, \dots, N$ , gives the number of measurements for which the thickness is between  $(n-1)\Delta h$  and  $n\Delta h$ . The new function

$$g_n \equiv \frac{G_n}{S\Delta h}$$

which is such that

$$\sum_{n=1}^N g_n \Delta h = 1$$

is a normalized frequency distribution that, in the limit  $S \rightarrow \infty$  and  $\Delta h \rightarrow 0$ , coincides with  $g(h)$ . It is the function  $g_n$ , very often called (wrongly) Probability Density Function (PDF), that is usually taken as representing the ice thickness distribution. It is normally presented as a histogram, of which the reader will find several examples in Chapters 5 and 6.

In the study of underice profiles it is common to work with draft, which is the directly measured quantity, instead of thickness. The conversion of draft into thickness is explained in Section 2.8. Except when the contrary is explicitly stated, all statistical quantities and histograms shown are for ice draft. We normally use bins with  $\Delta h=10\text{cm}$ .

For a sufficiently large number of thickness (or draft) measurements, the average is a reliable quantity to characterize the ice thickness (or draft) in  $R$  if one wants to summarize the information in one single number. However, the use of the mode as a statistical parameter requires some caution because the mode depends on the size of the bins, which is arbitrary. In ice draft observations by submarines the mode often coincides with the draft of the undeformed ice. This may not be the case, however, in regions where there is considerable ridging.

The histograms that represent ice thickness distributions tend to exhibit an approximately exponential form for large values of the thickness  $h$ . Thus, for  $h$  beyond a certain threshold  $h_1$ , the function  $g(h)$  behaves as

$$g(h) \approx e^{-\beta h} \approx e^{-h/\alpha}.$$

The (positive) parameters  $\alpha$  (with dimensions of length) or  $\beta$  (with dimensions of inverse length) describe the decline of the distribution for large values of the draft. The higher the value of  $\beta$  (the lower the value of  $\alpha$ ), the faster the distribution declines, signifying a comparatively small portion of highly deformed ice (in other words, a comparatively small number of pressure ridges). The choice of  $h_1$  is somewhat arbitrary. The calculations of  $\alpha$  and  $\beta$  performed by the author are based on  $h_1 = \text{mode}(h) + 1m$ , where  $\text{mode}(h)$  is the highest frequency non-zero value of  $h$ .

In view of this exponential behaviour of the tail of  $g(h)$  it is also common to display histograms in a semi-logarithmic scale, a procedure we will follow in Chapters 5 and 6.

## 2.2 The pressure ridge distribution

Pressure ridge depths (or heights, when observed from above), shapes and spacings are an important part of the sea ice thickness distribution. The value of submarine observations lies precisely on the possibility of identifying and studying this sort of small scale features.

They are formed when two ice floes collide if the forces that they exert on each other are sufficiently intense to fracture the ice sheet and create a number of blocks that will either submerge (forming the keel of the ridge) or pile on top of each other above the water level (forming its sail). In principle one could determine the statistical distribution of the number and size of the resulting ice blocks and, ultimately, the size and shape of the ridge, once the mechanical properties of the ice (which depend on its age) are known. In practice, the problem is impossible to solve exactly because of the complexity of the rheology of the sea ice and the impossibility of knowing the exact initial conditions (essentially the thickness and velocity of the floes before the collision) and the exact external forcing (namely the wind and ocean stresses) during the formation of the ridge.

In view of these difficulties, we rely on statistical methods to describe the pressure ridges found in a certain area or observed along a particular line such as the track of a submarine. The complete statistical description of a set of pressure ridges must include the distribution of the number of ridges per unit length of track (which we shall also call ridge density or ridge frequency) or, equivalently, the ridge spacing distribution, the ridge orientation distribution, the maximum keel depth distribution and the keel slope distribution. Other quantities that, in principle, could also be studied statistically are the shape of the keels, the size of the blocks that form the ridges, the type of ice used to build the ridges, the state of erosion of the keels, the ratio between the amount of ice and the amount of water in the keels, and the ratio between the maximum draft of the keel and the maximum height of the sail, prove too difficult, not to say impossible, to measure with the currently available sonars. On the other hand, ridge orientation cannot be retrieved from single beam measurements and the shape of the keels, namely the slopes, assuming an approximate triangular section, prove too unreliable. Thus, we are left with the ridge density and keel depth distributions.

Counting the number of independent ridges in a transect from a single-beam sonar record such as the one shown in Figure 3-1 is not a trivial exercise. The process begins with the identification of all local maxima above a certain threshold. This threshold is normally taken as the average draft of the undeformed ice surrounding the ridges,  $d_{ui}$ , of the order of 1.5m for first-year ice and 2.5m for multi-year ice. Then, one needs to decide whether two (or more) consecutive draft maxima belong to the same ridge or if they are the tips of independent ridges. For this we follow the criterion formulated by Wadhams (1981) according to which two consecutive maxima define two independent ridges if the maximum draft of the shallowest of the two keels (relative to the average draft of the undeformed ice) is at least twice the minimum draft of the trough between them (relative to the average draft of the undeformed ice). While the total number of independent keels turns out to be highly dependent on the value of  $d_{ui}$ , this is not the case for the number of keels with a draft above 6m, which shows little sensitivity to small changes in that value.

The density (number of ridges per unit track length) of keels deeper than 15m is very well described by a Poisson distribution, as the author concluded from the analysis of draft records obtained during submarine cruises in 2004 and 2007. The Poisson distribution is a consequence of the position of each deep keel being totally independent of the positions of all other deep keels, and deep keels being very rare events, hence the probability of finding two of them next to each other being negligible. Thus, if  $\mu$  is the mean number of deep keels per unit length over a certain transect, the probability of finding  $n$  ridges in the unit length is given by

$$P(n) = \frac{e^{-\mu}}{n!} \mu^n$$

It is well-known that in this case the keel spacings must obey a negative exponential distribution, as first suggested by Mock *et al.* (1972):

$$P(x)dx = \mu e^{-\mu x} dx,$$

This is, however, difficult to see in actual histograms as their shape is strongly dependent on the choice of the bin size. On the contrary, the Poisson distribution is almost perfectly reproduced by the data, as we shall see in Chapter 6.

The assumptions that form the basis of the Poisson distribution do not hold for shallow keels. Because they are not so rare, it is conceivable that two such keels could be found next to each other. And yet, for number of reasons, they cannot exist arbitrarily close to each other, which spoils the hypothesis of independence. The probability of having a ridge spacing equal to zero has to be zero, which is incompatible with the form of  $P(x)$  above. There are at least two reasons for this. One of them has to be with the finite width of the beam, which cannot distinguish two ridges that are separated by distances smaller than the footprint of the sonar (or whatever device is used to profile the ice). The other has to do with the proper definition of ridge according to the criterion proposed by Wadhams. The slope of the ridges is far from being vertical (in fact, it makes an angle of about 20-30° with the horizontal) and as such two ridges to be distinguishable, i.e., considered independent features, have to have a minimum horizontal distance. As such, the distribution of ridge spacings has to start at zero, then grow quickly and decay slowly to zero. This is intuitively how we expect it to be.

Two of the many distributions that have this sort of behaviour are the two-parameter lognormal

$$f_{\mu,\sigma}(x) = \frac{1}{\sigma x \sqrt{2\pi}} \exp\left(-\frac{(\log x - \mu)^2}{2\sigma^2}\right)$$

and the the three-parameter lognormal

$$f_{\mu,\sigma,\theta}(x) = \frac{1}{\sigma(x-\theta)\sqrt{2\pi}} \exp\left(-\frac{(\log(x-\theta) - \mu)^2}{2\sigma^2}\right).$$

The most suitable values of the parameters  $\mu$  and  $\sigma$  are found from the first and second moments of the actually observed ridge spacing histograms,  $\langle x \rangle$  and  $\langle x^2 \rangle$ , which are related to the former by

$$\langle x \rangle = \exp\left(\mu + \frac{\sigma^2}{2}\right); \quad \langle x^2 \rangle = \exp(2\mu + 2\sigma^2)$$

These relations can be inverted to give

$$\mu = \frac{1}{2} \log \frac{\langle x \rangle^2}{\langle x^2 \rangle}$$

$$\sigma^2 = \log \frac{\langle x^2 \rangle}{\langle x \rangle^2}$$

The lognormal fit to the observed ridge spacing distribution has been extensively used by Wadhams in his analyses of ice draft data collected during several UK submarine cruises (e.g. Wadhams and Horne, 1980; Wadhams, 1981, 1983). Much more recently, the lognormality of the ridge spacing was rediscovered by Rabenstein *et al.* (2010), this time in the study of pressure ridges from ice profiles obtained from above with electromagnetic induction methods (see Section 2.6). However, in his research on the pressure ridge statistics of the last two Royal Navy submarine cruises, the author of the present report only occasionally found an acceptable agreement between the observed ridge spacing distribution and a lognormal distribution.

We can also construct histograms for the distribution of the depths of the keels. For a very large number of keels we are allowed to choose narrow bins, each with a significant population, and the distribution becomes approximately continuous. Thus, it makes sense to talk about the number of keels with depth between  $h$  and  $h+dh$ , which we denote by  $n(h)dh$ .

Using a very narrow beam sonar and elementary statistical tools, Wadhams and Davy (1986) found that for  $h$  above a certain threshold  $h_0$  the distribution is very well described by an exponential function:

$$n(h)dh = B e^{-bh} dh.$$

The constants  $B$  and  $b$  are determined as a function of the total number of ridges

$$N = \int_{h_0}^{\infty} n(h)dh$$

and the mean depth of the keels in the same stretch

$$\bar{h} = \frac{\int_{h_0}^{\infty} h n(h) dh}{N}$$

It is then straightforward to derive the adequate form of the distribution:

$$n(h) = \frac{N}{\bar{h} - h_0} \exp\left(-\frac{h - h_0}{\bar{h} - h_0}\right)$$

The author believes that no one has ever shown from first principles that the ridge spacing and the keel depth should follow lognormal and exponential distributions, respectively. Thus, for the time being, they should be treated as empirical laws.

### 2.3 The lead distribution

Leads are another common feature of ice covered seas and play an important role in the heat budget of the Arctic Ocean. In fact, because sea ice is not a great heat conductor, most of the heat exchanged between the ocean and the atmosphere during the winter is done through leads. This is a first good reason to study frequency and width of leads. A second reason is more of operational nature: for a submarine navigation under thick sea ice it is useful to know the likelihood of quickly finding a lead in case of urgent need of surfacing.

From sonar profiles of the bottom surface of the ice (or laser profiles of its top surface) we can, in principle, derive statistical quantities such as the number of leads per unit length of submarine (or aircraft) track or, equivalently, the spacing between consecutive leads, and the width distribution. While this looks feasible, in practice there are severe obstacles that, in the author's view, prevent the extraction of reliable results, at least from submarine profiles.

The identification of leads is essentially the identification of segments of open water (or very thin ice). This, as we shall see in Sections 3.1 and 3.4, is quite a tricky operation for both analogue and digital submarine records. Different analysts come up with different strategies and end up with very different numbers of «leads». Of course it is also likely that they will end up with different mean drafts. This was evident when two analysts of the Polar Oceans Physics group studied the same profiles and selected a different set of points to define the water level.

In view of these difficulties, the author thinks that the attempt to find lead statistics is not worthwhile. Not everybody agrees. Wadhams (e.g. 1992) considered underice profiles from several submarine cruises and suggested empirical laws for lead spacing and lead width distributions.

An alternative, more robust approach is to study the fraction of thin ice (draft below 0.5 or 1m, for example) which, at very high latitudes and in the middle of the winter, can only signify an existing or refrozen lead. Such studies have been done in the past (e.g. Wadhams and Horne, 1980).

### 2.4 Submarine measurements

Basin-wide measurements of sea ice thickness in the Arctic Ocean began in 1958 when the *Nautilus* reached the North Pole for the first time. Since then, US submarines, equipped with upward-looking sonars, primarily for operational purposes, have collected a vast amount of sea ice draft data in their frequent voyages to the Arctic, mostly to the so-called SCICEX box, which roughly coincides with the portion of the Arctic Ocean outside international waters (but including the region north of Alaska). Most of these data sets are available through the National Snow and Ice Data Center archive (NSIDC, 2006) and have been extensively analysed by Rothrock *et al.* (1999, 2008).

In the early 1970s British submarines, using similar sonar technology, started cruising in the Arctic Ocean. In 15 voyages between 1971 and 2007 they have taken ice thickness data around the North Pole and in the European sector of the Arctic, namely in Fram Strait and the waters north of Greenland, which are rarely visited by US boats. Results from earlier cruises have been published in several papers (e.g. Williams *et al.*, 1975; Wadhams, 1981; Wadhams and Davis, 2001) and are partly reproduced in Chapter 4 of this report. Wadhams (1990) provides the first evidence of the thinning of the sea ice north of Greenland. Later, Wadhams and Davis (2000) and, independently, Rothrock *et al.* (1999) observed a significant overall thinning of the Arctic sea ice by comparing results from cruises in the mid-1970s and the mid-1990s.

Data from the last two Royal Navy submarine cruises, in the winters of 2004 and 2007, have been processed by the Polar Oceans Physics Group of the University of Cambridge. A summary of the main results can be found in (Wadhams *et al.*, 2011) and the as yet unpublished full analysis of the data composes Chapters 5 and 6 of the present report. Ice draft data collected by HMS *Tireless* during the March 2007 cruise acquire special relevance because they were taken in several regions of the Arctic with very different ice regimes, some of which would later become ice-free during the exceptional summer of 2007. The observations indicate, for instance, that, unlike the rest of the Arctic, there was no decline in ice thickness between 2004 and 2007 in the regions north of Greenland and Ellesmere Island, which are known to have the thickest ice in the Arctic.

Since 1994 British submarines cruising in the Arctic have been equipped with two types of single-beam upward-looking sonars known as Admiralty Pattern 780 and Admiralty Pattern 2077 (henceforth AP780 and AP2077, respectively). Before 1994 only the AP780 (or one of its earlier versions, such as Admiralty Pattern 776) was in operation. In 2007 an upward-looking multibeam sonar (manufactured by Kongsberg Maritime) was mounted for the first time on a submarine and used to generate the first three-dimensional images of the underside of the sea ice in the central Arctic Ocean.

AT780 is an analogue device that records the full return pulse on an electrically sensitive paper roll running at constant speed. The darkness of the trace increases with the intensity of the echo and its vertical position in the paper is a function of the arrival time. As there is a range of arrival times for each emitted ping (in theory one for each wave reflected at each point of the insonified area in the bottom surface of the ice), the record consists of a dark band, as in the roll section shown in Figure 3-1. Though the entire return signal is recorded, it is common to retain only the first arrival, which corresponds to the top boundary of the dark band, for instance the red line in the processed roll section shown in Figure 3-4. This standard procedure leads to more reliable results than to averaging over the entire return pulse, and ensures compatibility with many digital systems where

only the first return is recorded. Details of the techniques used to process this type of data can be found in Wadhams (1981) and in Section 3.1 of this report.

In an ideal sonar with an infinitely narrow beam and with continuously emitted pings, this red line would coincide exactly with the real bottom surface of the ice. In real life such identification is not possible and we are forced to distinguish the real draft from the observed draft. In many circumstances the two may have very different values. This is a severe problem in the case of the AP780, for which the beamwidth is not given in the documentation provided by the Royal Navy but has been quoted as less than 5° by Wadhams (1990) and as 3° by Wadhams (private communication). This issue, which is essentially a resolution error, is addressed in Section 3.2 of this report.

For a very brief description of the AP2077 sonar system and associated measurement errors see Section 3.4.

The aim of the present report is to summarize the observations made with single beam upward-looking sonars mounted on British submarines between 1976 and 1996, most of which have been published in the specialized literature by P. Wadhams and several of his collaborators, and to give a full, detailed account of the results obtained during the last two Royal Navy cruises, in the winters of 2004 and 2007.

## 2.5 Satellite altimetry measurements

In recent years several groups began applying satellite altimetry to the study of the large-scale sea ice thickness distribution in the Arctic (e.g. Forsberg and Skourup, 2005; Forsberg *et al.*, 2007; Kwok *et al.*, 2007; Zwally *et al.*, 2008; Farrell *et al.*, 2009). Laxon *et al.* (2003) used radar altimetry data from the European Space Agency (ESA) satellites ERS-1 and ERS-2 in order to explore the correlation between ice thickness and the length of the ice season. More recently, the same group analysed radar altimetry data from ESA's Envisat obtained between the winters of 2002/2003 and 2007/2008 (Giles *et al.*, 2008). They found a significant reduction in sea ice thickness in the region south of 81°30'N (the northern limit of Envisat's coverage) after the record minimum ice extent of September 2007 but no particular trend (in the winter season) between 2003 and 2007.

The launch in January 2003 of NASA's ICESat, which was equipped with the high accuracy Geoscience Laser Altimeter System (GLAS), allowed the first determinations of the central Arctic sea ice thickness from freeboard retrievals. In a thorough analysis of 10 ICESat campaigns between 2003 and 2008, Kwok *et al.* (2009) derived the evolution of the Arctic sea ice thickness during this five-year period, and were able to separate the contribution of first- and multi-year ice. They concluded that, while there was no observable trend in the thickness of first-year ice (which at the end of the winter typically reaches a thickness of 1.5-2m) in recent years, there was a strong decline in the basin-wide average winter thickness of multi-year ice, from 3.5m in 2005 to 2.9m in 2008. They also calculated that the combined average winter ice thickness in the Arctic was reduced by approximately 25% in three years, from 3.25m in the winter of 2005 to 2.45m in the winter of 2008 and showed that this decline was essentially due to the disappearance of multi-year ice which, in the winter of 2008, was responsible for only one third of the total volume of ice in the Arctic Ocean.

These findings are corroborated by an independent analysis of ICESat data by the Centre for Polar Observation and Modelling of the University College London (Farrell *et al.*, 2009). They found that from 2003 to 2008 sea ice in the Arctic Ocean got thinner at the average rate of about 15cm/year in the winter and 17cm/year in the autumn. Note, however, that the decline was not monotonic, as shown, for instance, by the fact that the average thickness in the winter of 2004 was lower than that of the following winter. Of particular curiosity is the substantial drop in ice thickness in the winter of 2008, with respect to the winter of 2007, in agreement with the above mentioned work of Giles *et al.* (2008).

Other than the complications inherent to the determination of distances of the order of tens of centimetres from a platform about 600 km above the surface of the Earth, the retrieval of the sea ice thickness from ICESat observations must take into account that what is actually measured is the elevation above the water line of the ice plus the snow that normally lies on top of it. The latter represents an additional problem because large-scale measurements or estimates of the depth of the snow on sea ice, and possible variations in recent times, are remarkably difficult.

In spite of these obstacles, Kwok *et al.* (2009) showed that there was satisfactory agreement between ICESat retrievals of ice thickness during the 2005 autumn campaign and nearly coincident measurements of the same quantity by a US submarine. By making the most of this rare opportunity, they validated the techniques used to process the altimetry data and made the estimates of the depth of the snow layer acceptable.

Figure 2-1 shows the Arctic Ocean sea ice thickness in March 2007 derived by Kwok and collaborators from satellite observations. Dark blue for ice less than 1m thick, light blue for thickness 1-2m, turquoise for 2-3m, yellow for 3-4m, orange for 4-5m and red for ice thicker than 5m. We see that most of the ice is less than 2m thick but there is still a substantial amount of ice thicker than 3m (necessarily deformed multi-year ice) pushed against Greenland and the Queen Elizabeth Islands. no attempt was made to assign values of ice thickness for the Barents Sea, Kara Sea, Baffin Bay and channels of the Canadian Archipelago.

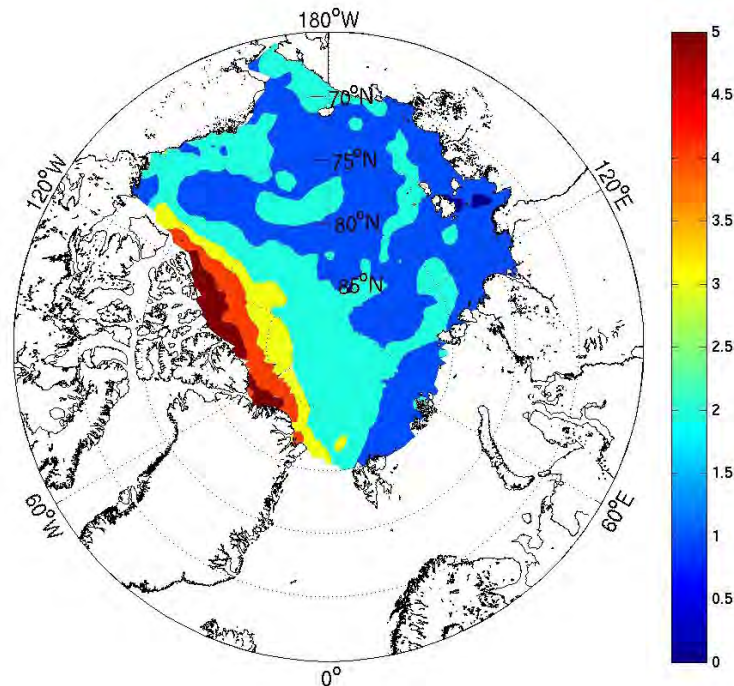


Figure 2-1. Sea ice thickness distribution in March 2007 from ICESat measurements.

ICESat was decommissioned in August 2010 and NASA plans to launch ICESat 2 in early 2016. In the meantime, ESA's CryoSat II was put in orbit in April 2010. Carrying on board the most sophisticated altimeter ever manufactured, it is expected to map accurately the Arctic sea ice thickness and to detect any small trends over the coming years. At the time of writing only preliminary analyses have been released (<http://www.esa.int>) while the process of calibration and validation of acquired data continues.

A component of the SIDARUS project is precisely the development of algorithms capable of retrieving ice thickness from CryoSat altimetry data.

## 2.6 Electromagnetic sounding

The possibility of measuring the thickness of an ice floe by electromagnetic sounding is based on the fact that the electric conductivity of the sea ice is negligible with respect to that of the underneath sea water. A transmitter coil generates an electromagnetic field which propagates downwards through air and sea ice. Inside the water the field quickly attenuates but it also induces electric currents which, in turn, create a secondary field to be detected by a receiver coil. From the intensity and phase of the received field we can infer the vertical distance between the coils and the water. Once the height of the system above the ice (normally measured with a laser altimeter) is subtracted from the latter we obtain the thickness of the sea ice (plus the snow that may lay on top of it).

The system developed at the Alfred Wegener Institute (AWI) in Bremerhaven, Germany, is known to have a high accuracy over flat ice (about 10cm) but difficulties in finding the thickness of unconsolidated ridges. In fact, because the conductive water percolates through the blocks that compose the keel of a ridge, its depth is underestimated, often by 50% of the real draft. Consequently, mean ice drafts of segments of highly ridged ice obtained with this technique have to be used in moderation. On the other hand, the modal ice thickness which, as mentioned above, tends to coincide with the thickness of the undeformed ice, appears to be a reliable parameter, especially suitable to compare results of different years.

The AWI group began measurements of sea ice thickness by ground-based electromagnetic sounding in 1991. Ten years later the same group opened the era of airborne electromagnetic induction measurements by flying a helicopter with the apparatus suspended at heights of 10-20m above the surface of the ice. The system became then known as *the bird*. In 2009 it was for the first time suspended to a fixed wing aircraft. There has been a total of 27 airborne campaigns between 2001 and 2011.

Helicopter surveys found a significant drop in the late summer ice thickness in the Transpolar drift, from a mean and a mode of approximately 2.3 and 2.0m, respectively, in 2001, to 1.3 and 0.9m in 2007 (Rabenstein *et al.*, 2010). However, some caution is needed in the interpretation of this result as the flights took place in different areas. In any case, it reveals a much faster decline than the one that occurred between 1991 and 2001. The latter, according to ground electromagnetic surveys, was of the order of 20%, from 3.1 to 2.4m in mean and from 2.5 to 2.0m in modal ice thickness (Haas *et al.*, 2008).

In April 2009 the AWI group enjoyed another successful campaign with 2400km of data collected during nine aircraft flights in different regions of the Arctic (Haas *et al.*, 2010). Of these, we shall briefly consider the 150km flight across Fram Strait, at an approximately constant latitude of 81°N, and a nearly 600km-long flight northwards from Alert, reaching almost to 88°N. In the first of these, the team observed a mean ice thickness of 2.8m for the W part of the strait and 1.9m for its E part. The modal ice thicknesses were 1.6 and 2.5m for first- and second-year ice, respectively, for the western part of the strait, and 2.2m for second-year ice in its E part. For the second flight, their analysis produced averages (modes) of 5.7m (4.4m), 5.3m (3.2m), 4.3m (3.1m), 3.7m (2.7m) and 3.4m (2.7m) for sections of about 100km with centres at latitudes 83°14', 84°31', 85°30', 86°27', 87°46'N, respectively, and longitudes not far from 65°W. In another flight, on the vicinity of the N coast of Ellesmere Island, the average ice draft was about 6m, the highest recorded during the whole survey.

The authors compared these results with previous ones and concluded that there were not big changes since 2007, especially for old ice. In the region of the North Pole (roughly 87°-88°N), for example, the modal ice thickness increased from 2.4m in 2007 to 2.8m in 2009. In the Lincoln Sea the modal draft of 4.3m in 2009 was substantially higher than the 3.3m observed in 2008, in agreement with the hypothesis of a fast recovery from the low values of 2008 that followed the remarkable summer of 2007.

They returned to the Arctic with their flying machines in 2010 and 2011 but the results of their observations are as yet to be published. However, a preliminary analysis was presented to the SIDARUS consortium in December 2011 (Schwegmann, 2011). Flights in the spring of 2011 are not

directly comparable to the ones in the spring 2009 because of non-coincident tracks. The modal draft at the end of the winter of 2011 in the Lincoln Sea was estimated in 3.0m. In the summer of 2011 more than 2500km of (mostly first-year) ice profiles were obtained during 16 flights in the central Arctic Ocean, in areas not far from the ones that were visited by the same group in 2007. The first indications are that the overall modal ice draft had the same value as in 2007 (0.9m).

## 2.7 Other methods of ice thickness determination

Old fashioned **drilling** is by far the most accurate method to determine the ice thickness of an ice floe and it is still in use when the region of interest has a manageable size, in the validation of other more sophisticated techniques or in the calibration of new instruments. Drilling was routinely used, for instance, in the extensive Arctic programmes of the Soviet Union that began in the early 1930s (Romanov, 2004).

**Moorings** equipped with upward-looking sonars based on technology arguably similar to that of the AT780 were first employed in the measurement of sea ice draft in the Beaufort Sea in the late 1970s and early 1980s. A second generation of sonars, then coupled to acoustic Doppler current profilers to measure ice velocities, was deployed in the same area of the Canadian Arctic in the early 1990s. Among their main specifications, described in Melling *et al.* (1995), we quote a nominal beamwidth (defined as the angular width of the main lobe of the beam at -3 dB) of approximately 2° and a depth of operation of about 70 m. Since 1991 long sea ice thickness time-series (of more than one year) have been obtained with these instruments in several points of the Beaufort Sea, allowing, for instance, the identification of trends in ice thickness in that part of the Arctic (Melling *et al.*, 2005).

The same type of technology has also been used in the European sector of the Arctic. In the late 1980s a year-long ice draft time-series was obtained at about 75°N on the vicinity of the east coast of Greenland. The first deployments of moored upward-looking sonars in Fram Strait took place in 1988 but it was only in 1990 that the continuous recording of the draft of the ice exiting the Arctic Ocean through Fram Strait began. The moorings, operated by the Norwegian Polar Institute, are located on the 79°N parallel at positions that change from year to year. The technical characteristics of the instruments used to monitor the motion and the thickness of the ice in Fram Strait can be found in Vinje *et al.* (1998). The nominal beamwidth of the sonar is again around 2° but they operate at an approximate depth of 50 m.

Airborne **laser profilometry** in the Arctic Ocean has been used since the early 1970s to study the frequency and height distributions of pressure ridge sails and the spatial distribution of surface roughness (Wadhams, 2000). As the technology advanced, it became possible to obtain good estimates of the ice thickness itself through reasonably accurate measurements of the ice freeboard. Hvidegaard and Forsberg (2002) developed methods to determine sea ice thickness using a combination of airborne laser altimetry and an accurate geoid model. These methods have been applied in several aircraft surveys, namely in May 2004 in the region north of Greenland (Skourup and Forsberg, 2006).

**Ice mass balance buoys**, first developed by the Cold Regions Research and Engineering Laboratory in Hanover, New Hampshire, and later also manufactured by the Scottish Association of Marine Science in Oban, Scotland, are relatively inexpensive and efficient devices to observe how the thickness of an ice floe and the depth of its snow cover vary throughout the season and, in some cases, throughout a number of years. Equipped with a set of thermistor strings that extend from the atmosphere down to the ocean through the snow and ice layers, they measure continuously the temperature in each of these four media. What makes these buoys special is the possibility of measuring separately the surface melting and the bottom ablation. As a bonus, one can also get information about the ice velocity field.

It was based on data collected by ice mass balance buoys that Perovich *et al.* (2008) concluded that one of the main causes of the small ice cover of the summer of 2007 was an anomalously high melt from below in the Beaufort Sea (approximately 2m, or six times the average of the previous years). The high influx of warm water from the Pacific in that year (Woodgate *et al.*, 2010) enhanced the bottom melt directly and indirectly. In fact, it triggered the appearance of areas of open water at the beginning of the summer, which led to a large amount of solar radiation being absorbed by the ocean which, in turn, induced further melting.

## 2.8 Conversion of draft and freeboard into thickness

From isostatic equilibrium, which in most cases is a convincing assumption, the conversion of observed ice draft ( $d$ ) into ice thickness ( $h_i$ ) is, in theory, quite straightforward:

$$h_i = \frac{\rho_w}{\rho_i} d - \frac{\rho_s}{\rho_i} h_s$$

where  $\rho_w$ ,  $\rho_i$  and  $\rho_s$  are the densities of sea water, sea ice and snow, and  $h_s$  is the depth of the snow layer on top of the sea ice. In a similar way, the ice thickness is related to the elevation  $e$  above the water line, which is the sum of the sea ice freeboard  $f$  and the snow depth, by

$$h_i = \frac{\rho_w}{\rho_w - \rho_i} e - \frac{\rho_w - \rho_s}{\rho_w - \rho_i} h_s$$

In some applications, like ICESat measurements, one is forced to work with  $e$  instead of  $f$  because the laser pulse is reflected at the snow/air interface.

The water density is traditionally taken as  $1024 \text{ kg/m}^3$ . This is, for instance, the value used by Hvidegaard *et al.* (2006), Spreen *et al.* (2009), and Kwok *et al.* (2009). However, Gascard and Bourgain of the University of Paris VI observed near surface salinities between 1020 and  $1027 \text{ kg/m}^3$  in diverse locations of the Arctic Ocean during the EU DAMOCLES project.

Observed values of sea ice density range from  $720$  to  $940 \text{ kg/m}^3$  with a sort of world average of  $910 \text{ kg/m}^3$  (Timco and Weeks, 2010). These authors distinguish between density of the ice below the water line, with values of  $900$  to  $940 \text{ kg/m}^3$  for both first- and multi-year ice, and above the water line, with values of  $720$  to  $910 \text{ kg/m}^3$  for multi-year ice and  $840$  to  $910 \text{ kg/m}^3$  for first-year ice. Considering all information available,  $910 \text{ kg/m}^3$  and  $920 \text{ kg/m}^3$  look like good bets for the bulk

densities of multi-year ice and first-year ice, respectively. These figures are in line, for instance, with detailed measurements in the early 1970s by Ackley *et al.* (1974) and Hibler *et al.* (1972). However, other authors recommend slightly different values. Kwok and Cunningham (2008) use  $925 \text{ kg/m}^3$  (for both ice types) in their extraction of ice thicknesses from ICESat freeboards and mention that the same value had been quoted by Weeks and Lee (1958) and Schwarz and Weeks (1977). Yi and Zwally, who also processed ICESat data independently of Kwok and co-workers, use  $915 \text{ kg/m}^3$ . And finally, Spreen *et al.* (2009) go for  $887 \text{ kg/m}^3$  for multi-year ice and  $910 \text{ kg/m}^3$  for first-year ice.

The situation with the snow density is even more complex in part because of a strong seasonal variability. Freshly fallen snow can have densities between  $50$  and  $200 \text{ kg/m}^3$ , depending on the temperature, but typically in the range  $50$ - $90 \text{ kg/m}^3$ . For their retrievals of ice thickness from freeboard measurements, Kwok and Cunningham (2008) start with the value of  $200 \text{ kg/m}^3$  for September, followed by a non-linear increase to  $330 \text{ kg/m}^3$  in March and remaining approximately constant until the beginning of the summer (which is, incidentally, the value used by Spreen *et al.* (2009)). Then during the summer there is a slight increase and the highest values, of the order of  $350 \text{ kg/m}^3$ , are found in July, for whatever snow is left. This seasonal evolution is similar to the one proposed earlier by Warren *et al.* (1999) who, instead, start from a value of  $250 \text{ kg/m}^3$  for September but warn that a wide range of values ( $100$ - $325 \text{ kg/m}^3$ ) is possible in this month. For a recent review of densities of snow and sea ice the reader is referred to the paper by Forsström *et al.* (2011).

But perhaps the largest uncertainties (at least in laser altimetry) are those of the snow depth. Between 2002 and 2010 the large-scale distribution of the snow depth over sea ice was monitored daily by the AMSR-E instrument onboard NASA's EOS Aqua satellite. The technique for retrieving snow depth from passive microwave imagery is described by Markus and Cavalieri (1998). According to the authors of the algorithm, the extraction of snow depth is complicated by the presence of multi-year ice, which has a radiometric signature similar to that of snow over first-year ice. Therefore, the algorithm only retrieves snow depth in the seasonal sea ice zones and in regions where the ice concentration is higher than 20% and the concentration of multi-year ice below 20% (Cavalieri and Comiso, 2004). Perhaps because of these problems, snow fields obtained from passive microwave are seldom used to generate sea ice thicknesses from satellite freeboard measurements.

One of the most used sources of information on snow depth over sea ice is the so-called Warren Climatology (Warren *et al.*, 1999). However, authors such as R. Kwok and J. Zwally do not adopt it for two main reasons. In first place, it is based in measurements performed between 1954 and 1991 and it is not obvious that it is still valid today (it is well-known that there have been changes in precipitation patterns at low latitudes and that may also be the case at high latitudes). And second because the observations were made over multi-year ice and, as we know, that type of ice is no longer the dominant one in the Arctic Ocean.

Kwok and Cunningham (2008) prefer to start from a certain snow depth distribution at the time of minimum sea ice cover (mid-September), which, in fact, they borrow from the Warren Climatology, and then calculate the snow accumulation over the year from the ECMWF snow fall data. This is a quite elaborate procedure that has to take into account several effects, namely the opening of leads.

Most of the snow fall in the Arctic Ocean occurs in the period September-December during autumn and early winter storms. By October/November, the traditional time of the year for an ICESat

campaign, Kwok *et al.* (2009) estimate the spatial average of the snow depth over sea ice in the Arctic Ocean as 24cm, increasing to 30cm at the end of the winter. The amount of snow over multi-year ice (26cm and 34cm in the fall and late winter, respectively) is typically higher than over first-year ice (12cm and 22cm, respectively).

Putting together all this information, we are led to the approximate expression for the sea ice thickness as a function of the elevation and the snow depth

$$h_i = 9.39e - 6.46h_s$$

If one does not want to go into too many complications regarding seasonal and spatial variations, this equation seems to be a good bet (at least for the winter). It is used, for instance, by Kurtz *et al.* (2009). It is clear that the two terms on the RHS give contributions of the same order of magnitude, which means that the amount of snow plays a crucial role in the extraction of the sea ice thickness from altimetry measurements.

On the contrary, in submarine measurements the snow depth can be safely neglected because it only introduces a minor correction to the case of no snow. This has been hailed as one of the greatest advantages of submarines over satellites for accurately measuring sea ice thickness. For submarines it is quite safe to use

$$h_i = 1.12d$$

### 3 Draft measurements with single-beam sonars

The usefulness of ice draft measurements by submarines cruising in the Arctic, originally intended for operational purposes, one suspects, was soon recognized by US and UK scientists of great value for scientific research. For decades, more exactly until the first satellites were placed in near-polar orbits, they offered the only mean of surveying the large scale properties of the Arctic Ocean sea ice cover. In addition, it was also early understood that changes in sea ice, namely in sea ice thickness, could be interpreted as a reliable sign of more general climatic changes.

#### 3.1 Analysis of Admiralty Pattern 780 sonar records

Examples of records of the bottom topography of the sea ice obtained with an upward-looking AP780 single-beam echo-sounder mounted in a submarine are shown in Figure 3-1 Figure 3-2. These 5.4km profiles were taken in April 1991 in the Arctic Ocean from depths of 95m and 83m, respectively, when the boat was cruising at a speed of 10 kts, in the regions of (84°10'N, 0°) and (85°40'N, 23°E), respectively. The horizontal axis represents time, with white minute marks visible in the dark horizontal strip at the bottom of the figure showing that the duration of these records was 17.5 minutes. The thickness of this line indicates the vertical range at which the sonar is operating, in both cases 80m, the most common sonar range encountered during the analysis of the records. Other possible values are 40m or, rarely, 200m. The vertical axis is the ice draft, growing upwards, originally in pixels but easily converted to metres once the sonar range and the paper scale are known. Notice that the images are actually upside down, with depth increasing upwards, and that the vertical and horizontal scales (once time is converted to along-track position in the horizontal axis) are very different.

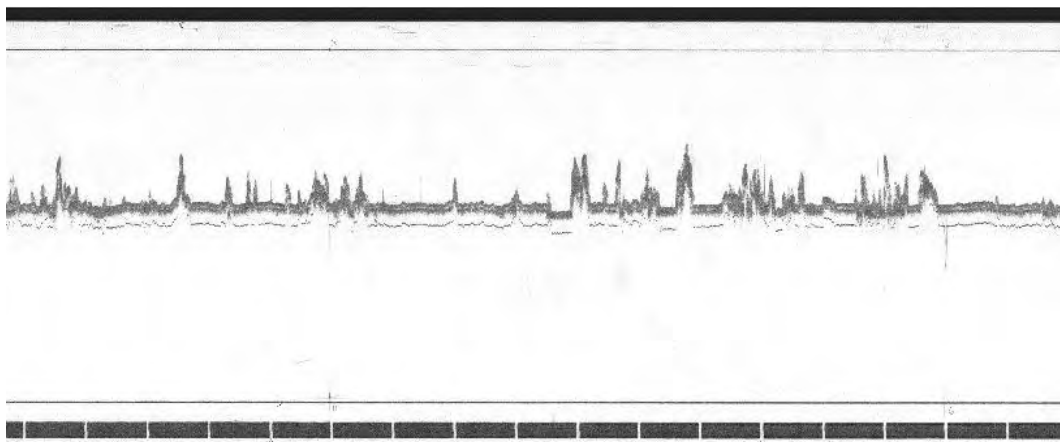


Figure 3-1. First example of a record of the bottom topography of the sea ice obtained with an AP780 sonar.

Such a digital image, called a *roll section* because it is the digitized version of a section of the full paper roll, has 3600x1500 pixels. Each pixel of the (black and white) image has a darkness range between 0 (black) and 255 (white).

Each roll section is processed separately with a Matlab routine written by B. Denby and N. Hughes (then at the Scott Polar Research Institute in Cambridge), and further developed by J. Rodrigues. This program creates a file with the values of the ice draft for each roll section. These files are later combined to produce the ice draft and associated statistics for each of the 50km section into which the transect of the submarine is traditionally divided.

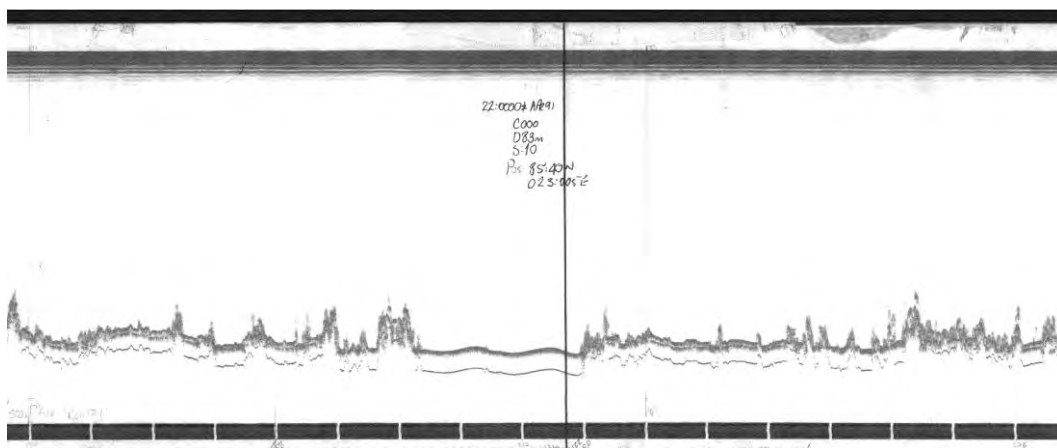


Figure 3-2. Second example of a record of the bottom topography of the sea ice obtained with an AP780 sonar.

The data analyst starts by assigning a time to some points of the roll section (normally two, one at each end of the record, but more if the time scale varies within the record). Explicit indications of time exist regularly in the form of handwritten annotations in the paper roll itself (as in Figure 3-2). Once these points are marked, a simple linear interpolation associates a time to each pixel of the record.

Then, he or she proceeds to select the valid portions of the record. Those with insufficient quality or in which the submarine is changing depth are discarded (some analysts also reject records obtained during the change of course). In some cases entire roll sections or even sets of adjacent roll sections are discarded.

Next, the program determines the profile of the underside of the ice, the red line in Figure 3-4Figure 3-5. This is done by finding, for each value of  $x$ , the first pixel of the record, starting from the top of the figure, with a darkness below a certain preset threshold. By running  $x$  through all 3600 values of the length of the roll section we generate the bottom surface of the ice. If there are dark marks between the top of the image and the true ice record (such as a manual annotation) the user must define a “top offset” (the green line in Figure 3-5), in such a way that no unwanted dark areas exist between this line and the record.

While in most situations this procedure is straightforward and to a large extent independent of the chosen threshold of darkness, problems in the precise identification of the bottom surface of

the ice may arise in cases where the scanned image is of bad quality. This happens, for instance, when the image is very light or very dark, when certain portions of the image are lighter than others, or when, instead of a sharp transition from the white background to the dark record, there is a band of grey pixels of variable darkness. In these cases the value of the ice draft may depend on the choice of the threshold of darkness and the responsible analyst has to go through a sequence of trials in order to find the optimal threshold. In fact, if the darkness threshold is too high, the red line may appear slightly above the top of the dark record, leading to an artificial increase of the average draft. More exactly, a high threshold is likely to overestimate the thickness of the undeformed ice but perform well with deep keels. On the other hand, if the chosen threshold is too low, the red line may appear inside the dark record and the resulting ice draft may be underestimated. A low threshold will possibly underestimate the deep keels (where a sharp transition from white to black is less likely) but do well with the undeformed ice (which normally corresponds to darker pixels). If possible, we use the same threshold within a roll, although different rolls may be processed with different thresholds because the darkness of the paper trace is affected by the depth of the boat, the state of the stylus and even the age of the chart roll.

The next step is the determination of the water level in each roll section. This is likely to be the largest source of error in the evaluation of the ice draft because the open water signature is not unambiguous and some (naturally subjective) criteria must be adopted. Here are the criteria used in our analysis.

The analyst starts by seeking portions of the trace which are comparatively thin and dark, structureless, and either flat (as for about half a minute in the centre of the record in Figure 3-1) or gently undulating (as for about three minutes in the centre of the record in Figure 3-2). In the latter case the approximately sinusoidal shape of the curve is due to the periodic motion of the submarine in the vertical direction. Often a secondary return due to signal reflection from the submarine's hull is visible. This feature, a thin line below the main echo, is especially prominent when the echo-sounder passes under open water and, to a less extent, under undeformed ice.

However, the distinction between open water and thin undeformed ice is sometimes unclear because the signature of the latter may also be a single dark line, flat or undulating. Indeed, one can legitimately expect that the areas of thin ice (essentially refrozen leads) will outnumber the areas of open water in the winter Arctic sea ice cover. Thus, when available, the analyst will make use of other data sources (such as video images) to remove the ambiguities.

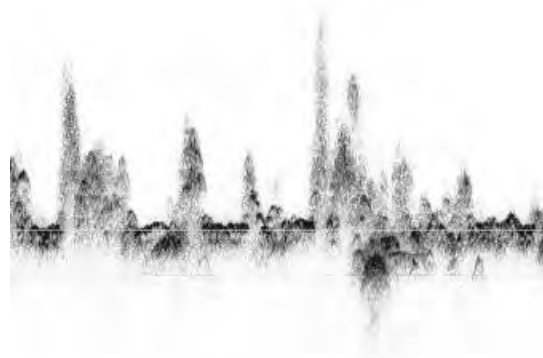


*Figure 3-3. Example of a dark hyperbolic shaped feature used to identify the water level.*

In the absence of these continuous areas that can be identified with open water (or, possibly, thin ice) with some degree of confidence, other indicators must be used. The most common ones are isolated, normally very dark features of hyperbolic shape such as the one shown in Figure 3-3). They are generated by the echo-sounder when the sound wave reflects from a narrow crack or lead in the sea ice (Wadhams, priv. comm.). The characteristic shape and the contrast with the rest of the record are often enough to safely mark the water level at the top of such a feature.

If none of the water marks described above can be found in the record, the user may identify the water level with the absolute minimum of the record or, in some cases, with the absolute and one or more relative minima. This procedure must be used with caution because the minimum ice draft may not necessarily be zero. However, if the record spans a long enough time interval, one may assume with confidence that the minimum ice draft corresponds to open water due to the high likelihood of having a lead or a polynya above the path of the submarine (even in the winter). When forced to use the minima to find the water level, we limit ourselves to the absolute minimum of the roll section or, at most, to the latter and one other local minimum.

If a certain roll section does not have clear water marks and the minimum doesn't seem to correspond to open water (either because it is significantly higher than the minima in the following or preceding sections or because it appears to be in an area of ridged ice), we have to define the water level from water marks in adjacent roll sections.

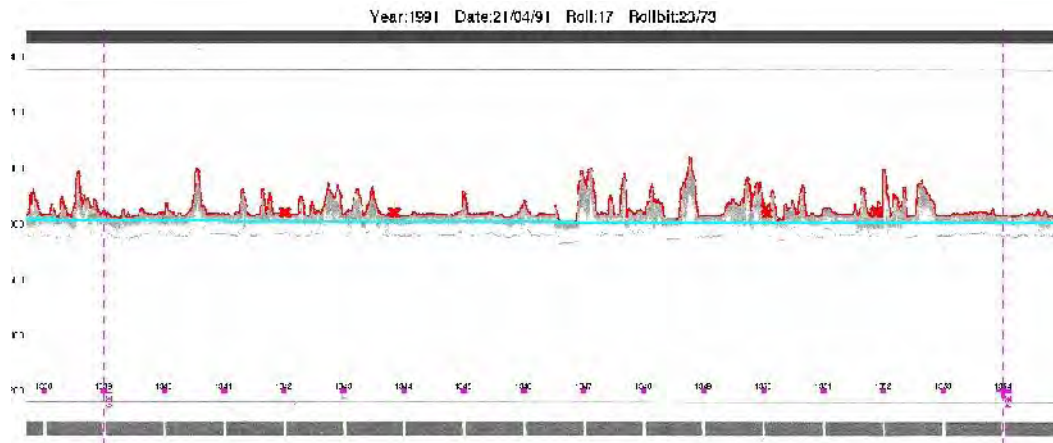


Figure 3-4. The roll section shown in Figure 3-1 after processing is complete.

Once all points that correspond to water are identified, the continuous water level is found by linear interpolation between neighbouring water marks. Continuity between consecutive images must be ensured. Because the vertical motion of the submarine is essentially periodic (as shown, for instance, by the waving pattern in the central part of the record depicted in Figure 3-2), the use of a straight line for the water level will not affect the average draft, though it may introduce small (hopefully negligible) local errors.

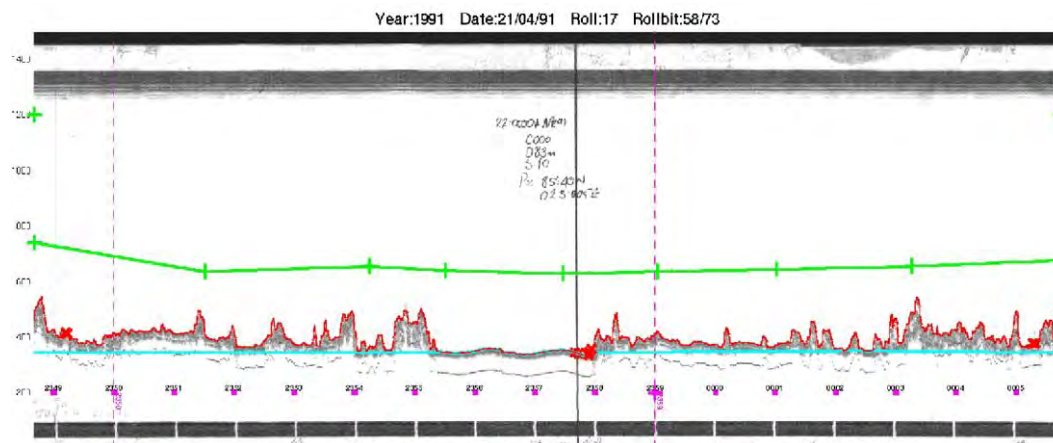


Figure 3-5. The roll section shown in Figure 3-2 after processing is complete.

With the water level set, the draft is simply the difference between the level of the bottom surface of the ice and the water level. Figure 3-6 shows the graph of ice draft versus time corresponding to the roll section of Figure 3-1.

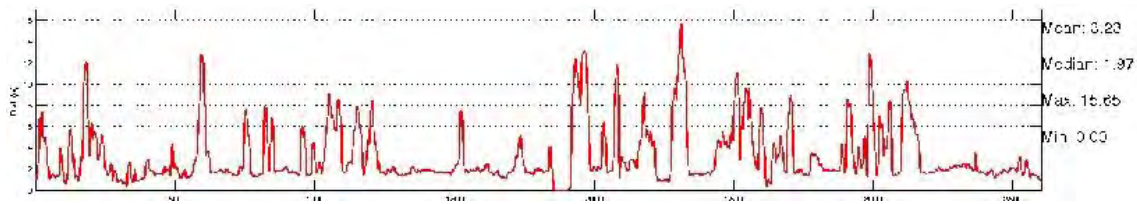


Figure 3-6. Draft of the roll section shown in Figure 3-1.

We proceed in this way to find the draft for every roll section, creating in the process a complete set of files with draft versus time. These files are merged in order to create the full draft file for the complete transect of the submarine, which is subsequently divided into sections of 50km (it has been shown that is a long enough length to generate robust statistical results but sufficiently short to contain different ice regimes). For each section we determine the usual statistical quantities (mean, median and maximum) for the ice draft, as well as the frequency (often called probability) distributions. We also study the ridge and lead distributions.

A navigation file containing the values of the latitude, longitude, course, speed and depth of the submarine is produced for each roll section. Such information is obtained from the logs (or navigation data tapes) that were provided together with the paper rolls. When the detailed route of the submarine was not provided separately (as in the 1991 cruise), we have to rely on the annotations of position, time and maneuvering data written on the rolls by the sonar operator.

## 3.2 Beamwidth effects

The finite width of the sonar beam introduces a bias in the measurement of the ice draft. When the undersurface of the ice is not horizontal, the most common situation in the Arctic Ocean, the observed draft, taken as the locus of first returns from the sonar, is higher than the real draft. Such beamwidth effects, as we shall call them, have been considered in the past. For UK submarines, Wadhams (1990) estimates that the corrections due to a small beamwidth (less than 5°) are of the order of 1–2% and gives a procedure to deal with wider beams (Wadhams, 1981). For US submarines, the bias introduced by a finite footprint was calculated by Rothrock and Wensnahan (2007) who, based on previous work by Vinje *et al.* (1998), arrived at the value of  $44 \pm 9$  cm.

However, after performing analytic calculations for simple geometric profiles and numerical calculations for real profiles obtained with accurate multibeam sonars, the author of this report is convinced that the bias due to the finite beamwidth of the sonars mounted on UK submarines is much higher than that quoted above. The discrepancies between the real and the observed drafts depend on several factors which include, other than the beamwidth and the depth of the submarine, which are perhaps the most obvious ones, the value of the real draft and the topography (or roughness) of the underside of the ice (namely the number and shape of pressure ridges on the transect) which, in turn, depend on the location and time of the survey. As such, we argue that the subtraction of (or the multiplication by) a single overall number to extract the real draft from the observed one is an oversimplified procedure from where large errors may result.

We now briefly describe how to obtain estimates for the errors that result from the finite footprint of the sonar. For the details of the calculations the interested reader is referred to (Rodrigues, 2010).

The first thing we need is a sufficiently long real underice profile. However, because no instrument has an infinite resolution, we couldn't find one, and had to content ourselves with a good approximation. For that we chose a profile obtained with a modern multibeam sonar.

In 2004 the Autosub-II autonomous underwater vehicle (AUV), built and operated by the National Oceanographic Centre in Southampton, and equipped with an upward-looking SIMRAD EM-2000 swath multibeam sonar, collected more than 450km of under-ice topographic data in the region of the Northeast Water Polynya (Wadhams, 2006). In view of the very small width of each of the beams in the swath (at most  $1.5^\circ$  in the along-track direction), the low depth of operation of the AUV (less than 40m), and the consequent small footprint (about 1m, much smaller than the one of the sonar of submarine at typical depths), it is safe to assume that the central beam reproduces faithfully the real profile of the bottom surface of the ice directly above the sonar, except possibly for the fact that the mean distance between pings is of the order of 2.5m. However, because this number is still smaller than the typical size of the footprint of the single-beam sonar, it makes sense to compute the corrections in this situation in order to find adequate methods of performing corrections in a general case. So, what we call real profile is the one obtained from the centre-beam record by linear interpolation at constant spacings of 25cm. The reader will accept that this poses no problem. In fact, we could have worked instead with a computer generated profile with characteristics (number of ridges, geometry of ridges, fractions of ice type, and so on) similar to those of real sea ice.

We then simulate the measurement of the same profile by a wide beam sonar for several values of the beamwidth and the sonar depth in order to estimate the effects of these two variables on  $\langle \Delta d \rangle$ , the difference between the mean draft of the simulated profile and the mean draft of the real profile. Next, we try to quantify the influence of the topography of the bottom surface of the ice. Amongst the plethora of parameters commonly used to characterise the roughness of a surface our preference goes to the average of the directional derivative of the draft along the track of the submarine, a positive quantity that we shall denote by  $\langle d' \rangle$  which, according to a robust conjecture, has similar values for the real and the simulated profiles.

In order to get a maximum range of average roughnesses, we defined a set of about 40 sections of the real profile, each 1km-long, with diverse terrains (from flat ice to the most ridged ice encountered during the mission). For each section we calculated the average draft and roughness for the real and simulated profiles for several values of the beamwidth and sonar depth. The results indicate that the growth of  $\langle \Delta d \rangle$  with  $\langle d' \rangle$  is approximately linear, especially for small footprints. We can then find the equations of the best linear fits to the graphs of  $\langle \Delta d \rangle$  versus  $\langle d' \rangle$ . With this technique we derived empirical relations between  $\langle \Delta d \rangle$  and beamwidth, depth and roughness of the terrain which we then apply to profiles obtained by sonars mounted in submarines.

They were first applied to 1200km of ice draft data collected by the British submarine HMS *Tireless* in the region north of Greenland during a mission in the Arctic Ocean in the winter of 2004 (see Chapter 5). For this particular transect the mean bias of the observed draft was 47cm (with a standard deviation of 15cm) for a beamwidth of  $3^\circ$  and 95cm (with a standard deviation of 28cm) for a beamwidth of  $6^\circ$ . Because the magnitude of the error varies significantly with the depth of the

submarine, the beamwidth of the sonar and the topography of the underside of the ice, it has to be calculated for each individual transect. For the 50km-long sections of the 2004 voyage the observed drafts were estimated to be 7-20% and 15-35% higher than the real drafts for beamwidths of 3° and 6°, respectively.

To make things worse, these are minimum values, with the actual differences between the observed draft and the real draft expected to be slightly higher. This has to do with the fact that the simulated draft does not exactly coincide with the observed draft, though the differences are expected to be small (see (Rodrigues, 2010) for more on this).

The good news is that the modal draft is unlikely to be affected by this bias. In fact, the bias exists because the first return, which defines the profile in AP780 and AP2077 records, may not be coming from the point directly above the sonar. However, this is not the case under flat ice which is, in almost all cases, the most common type of ice. It is also easy to explain why the maximum draft (or the maximum depth of a ridge) is not affected by this type of corrections.

Unsurprisingly, due to its finite footprint, the upward-looking sonar is likely to be unable to resolve some systems of ridges into individual ridges. Therefore, the number of independent ridges that can be identified in a certain record is usually smaller than the actual number of independent ridges. We carried out similar analyses for several other sections of the AUV missions and found that in all cases the number of observed ridges is smaller than the real number of ridges but we were not able to find a consistent relation between these numbers as a function of the beamwidth and the depth of the sonar. The number of deep keels (draft higher than 15m) and their depth and spacing statistics are very likely to be independent of the characteristics of the sonar because it is very improbable to find two independent deep keels inside the footprint of the sonar.

In view of the size of these errors, we argue that beamwidth corrections must always be taken into account when measuring sea ice draft from below.

### **3.3 Other errors and uncertainties**

### **3.4 Analysis of Admiralty Pattern 2077 sonar records**

The second type of sonar, the AP2077, operates in a quite different way. Results from measurements made by this sonar were provided by the Royal Navy to the Polar Oceans Physics Group of the University of Cambridge in the form of encoded files with time, position of the submarine (which comes directly from its inertial navigation system), sonar depth and calculated ice draft and ice thickness for each ping.

11	10	03	2007	07	36	05	-4.52278	75.77139	132.87	1.60	1.42
12	10	03	2007	07	36	06	-4.52274	75.77144	132.83	1.59	1.45
13	10	03	2007	07	36	07	-4.52270	75.77149	132.83	1.35	1.23
14	10	03	2007	07	36	08	-4.52266	75.77154	132.59	1.91	1.72
15	10	03	2007	07	36	09	-4.52262	75.77159	132.52	2.12	1.91
16	10	03	2007	07	36	09	-4.52262	75.77159	132.81	1.80	1.62
17	10	03	2007	07	36	10	-4.52258	75.77165	132.69	2.03	1.83
18	10	03	2007	07	36	11	-4.52254	75.77170	132.02	1.66	1.50
19	10	03	2007	07	36	12	-4.52250	75.77175	132.63	2.04	1.83
20	10	03	2007	07	36	13	-4.52246	75.77180	132.32	2.43	2.19
21	10	03	2007	07	36	14	-4.52242	75.77185	132.43	2.31	2.08
22	10	03	2007	07	36	15	-4.52238	75.77190	132.25	2.51	2.26
23	10	03	2007	07	36	16	-4.52234	75.77195	132.45	2.05	1.85
24	10	03	2007	07	36	17	-4.52230	75.77200	132.60	1.90	1.71
25	10	03	2007	07	36	18	-4.52226	75.77205	132.02	1.83	1.60
26	10	03	2007	07	36	19	-4.52222	75.77210	132.92	1.59	1.39
27	10	03	2007	07	36	19	-4.52222	75.77210	132.87	1.60	1.42
28	10	03	2007	07	36	20	-4.52219	75.77215	132.89	1.35	1.22
29	10	03	2007	07	36	21	-4.52215	75.77220	133.05	1.19	1.06
30	10	03	2007	07	36	22	-4.52211	75.77225	133.34	0.98	0.83

Figure 3-7. Example of an AT2077 record.

Not much information is available about the specifications of this type of sonar. The beamwidth, for instance, is unknown but thought to be less than that of AP780. We know, however, that this is a digital device that only records the first return. Thus, if  $t$  is the travel time of the pulse between the moment it is generated by the transmitter unit and the moment the first return arrives at the receiver unit,  $H$  is the sonar depth and  $c$  is the speed of sound in the water, the ice draft is simply given by

$$d = H - \frac{ct}{2}$$

(assuming that variations of  $c$  with depth are negligible), as illustrated in Figure 3-8. Hence, with such a sonar we should be able to obtain a high-quality continuous profile of the underside of the ice and determine with great accuracy the ice draft as a function of time or along-track distance without the need for much post-processing by the user, other than the standard removal of notoriously bad return signals. Unfortunately, things are not so straightforward.

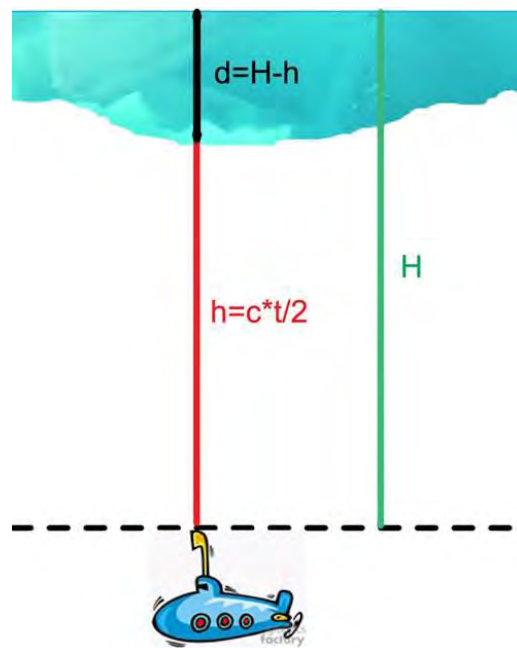


Figure 3-8. Basic principle of sonar operation.

The most severe problem is that the determination of the ice draft relies on the knowledge of the sound speed profile, which, being a function of the temperature and salinity, is subjected to seasonal and regional variations as high as a few metres per second (e.g. Rothrock and Wensnahan, 2007). On top of this, global warming is having an impact on ocean temperatures both directly due to an increase in heat transfer from the atmosphere to the ocean and indirectly through modifications in ocean circulation patterns. For example, the increase in recent years of the influx of warm water from the Atlantic (e.g. Gerdes *et al.*, 2003) and the Pacific (e.g. Shimada and Kamoshida, 2008) into the Arctic Ocean will influence the sound speed profile.

In general, ice draft determinations with upward-looking sonars are not accompanied by in-situ determinations of the sound speed profile. Instead, it is reasonable to assume that the values of the speed of sound used to calculate the draft are taken from climatological data bases which are arguably incomplete due to obvious difficulties in measuring oceanographic parameters in the Arctic Ocean and keeping track of their variation over time. As the actual speed of sound is likely to be different from the one found in the tables, we are bound to have an uncertainty  $\delta d$  in the draft associated with the uncertainty  $\delta c$  in the speed of sound. The order of magnitude of this draft uncertainty can be easily estimated by noting that a change in the speed of sound from  $c_0$  to  $c_0 + \delta c$  leads to an approximate change  $\delta d$  in the observed draft of

$$\delta d \approx -H \frac{\delta c}{c_0}.$$

It follows from this equation that an error of, say, 6m/s in the speed of sound (roughly 0.4% of its value at the ocean surface when  $T=0^\circ\text{C}$  and  $S=35$ ) leads to an error of approximately 42cm in the draft for a sonar depth of 100m. Because  $\partial c/\partial T \sim 4.6$  m/s, such a variation in the speed of sound can

be due to a variation in temperature of just over 1°C. We conclude that uncertainties in the speed of sound generate uncertainties in the measured ice draft which are far from negligible.

The author was provided by Gascard and Bourgain of the University of Paris VI with a wealth of recent CTD measurements in several locations of the Arctic Ocean shown in Figure 3-9. The speed of sound is obtained from the values of the salinity, temperature and depth with an empirical formula. The results are shown for Fram Strait in Figure 3-10, for the area N of Greenland and Ellesmere Island in Figure 3-11, and for the N Beaufort Sea in Figure 3-12.

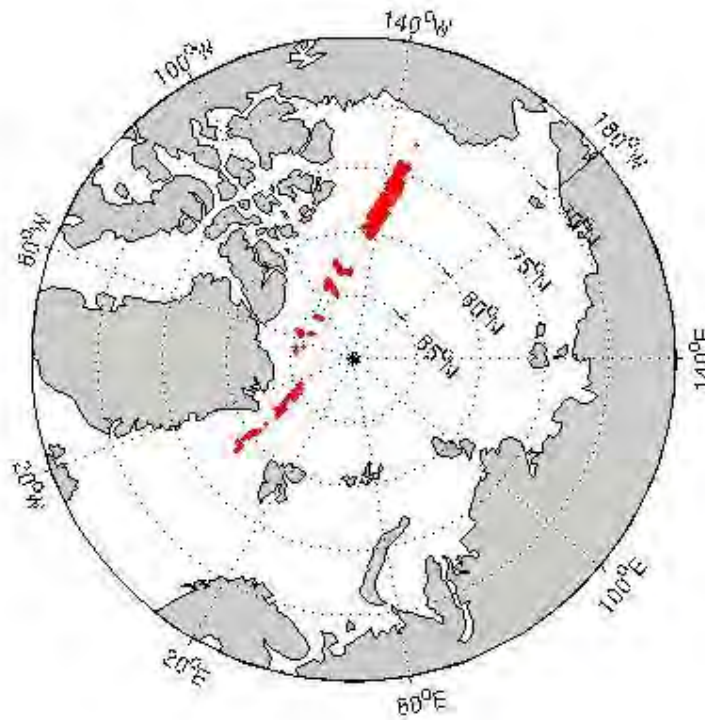


Figure 3-9. Locations of recent CTD measurements used in the determination of the speed of sound.

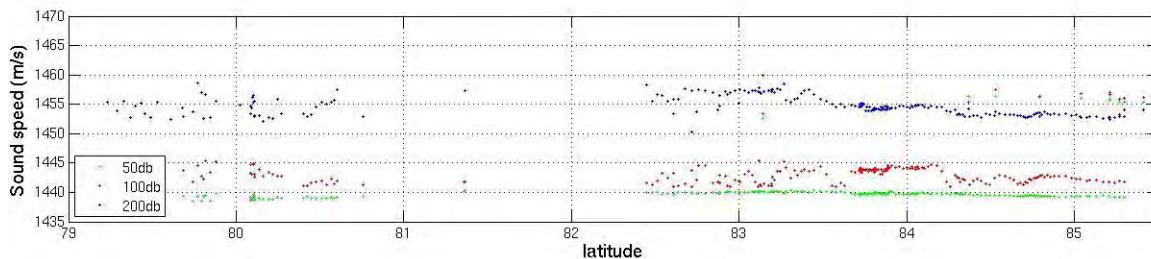


Figure 3-10. Speed of sound measurements in Fram Strait.

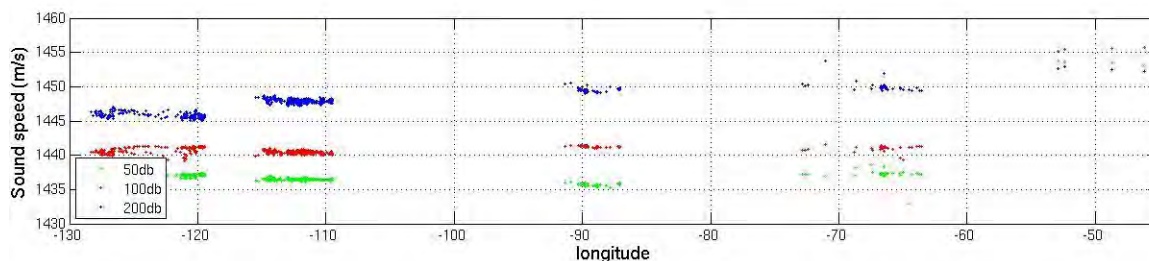


Figure 3-11. Speed of sound measurements N of Greenland and Ellesmere Island.

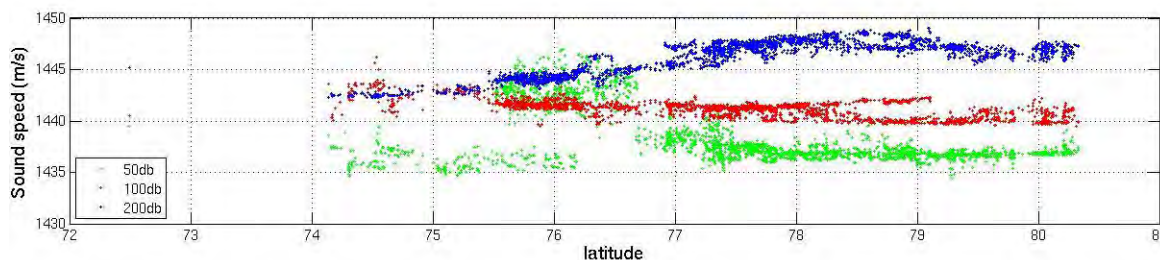


Figure 3-12. Speed of sound measurements in the N Beaufort Sea.

Each of these three plots has measurements at 50db (roughly  $z=40m$ ), 100db (roughly  $z=90m$ ) and 200db (roughly  $z=190m$ ) in green, red and blue, respectively. For instance, if we consider depths of the order of 100m we observe that the speed of sound ranges from about 1440m/s at the N end of the Beaufort Sea sector and N of Ellesmere Island to 1445m/s at the S end of the Beaufort Sea sector and some points in Fram Strait.

We do not know which value of the speed of sound was used to calculate the draft of the ice (last column of the file shown in Figure 3-7).

It is due to the lack of information on the speed of sound and on the beamwidth that the results from the AP2077 have been less favoured than those obtained with the AP780. On the other hand, the longer series of cruises in which AP780 was used is an advantage to identify possible trends in Arctic sea ice thickness.

A comparison between the data obtained with each sonar during the April 2004 cruise indicated that ice drafts from AP2077 were, on average, 14% lower than those obtained from AT780 paper rolls, a difference which is possibly a consequence of the suspected smaller beamwidth of the AP2077, though this is by no means the only possibility. AP2077 data were not processed for the March 2007 cruise as the device malfunctioned during most of the voyage.

### 3.5 Multibeam sonars

In 2007 a Kongsberg EM3002 upward-looking multibeam sonar fitted to the Royal Navy submarine HMS *Tireless* was used to produce the first detailed maps of the bottom topography of the Arctic Ocean sea ice. Each ping of the EM3002 is formed by 254 very narrow beams spanning a wide angle. Coverage (across-track distance between extreme beams at surface) can reach 200m though at typical submarine depths it rarely exceeds 140m. Topographic features such as pressure ridges and leads appear distinctively in the computer generated images of the underside of the ice, an example of which is shown in Figure 3-13. Multibeam data are thus particularly suitable for the determination of the number of ridges or leads per unit length of the submarine track, keel depth of ridges, width of leads, and in the study of the shape and orientation of pressure ridges.

There are good reasons to assume that the maps of the bottom surface of the ice generated with such a multibeam sonar are very accurate, and that the profile obtained with the centre-beam is identical, or almost identical, to the real profile of the ice directly above the sonar. However, the retrieval of the exact values of the ice draft is likely to be affected by some of the problems mentioned earlier, notably those associated with uncertainties in the sound speed profile.

At the time of writing the Polar Oceans Physics group of the University of Cambridge is still processing the multibeam data collected during the 2007 voyage of the *Tireless*. From the initial evaluation it appears that most of the data are of bad quality, the exception being those for the area covered by and around the so-called DAMOCLES Survey, N of Greenland (see Chapter 6 for details). Preliminary analyses reveal excessively large differences between the values of the ice draft obtained with the single-beam sonars and with the multibeam sonar for the same tracks. The causes of such an unpleasant situation are not yet known but sound speed effects may well be responsible for it.

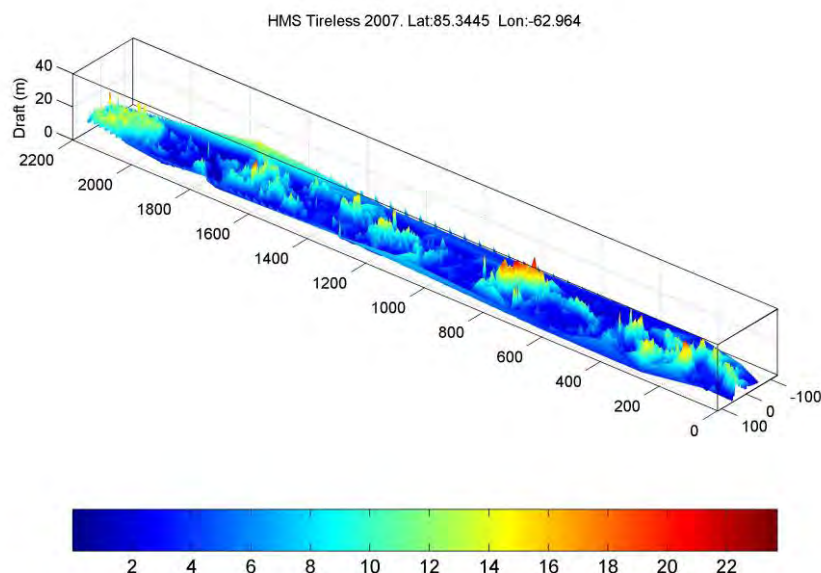


Figure 3-13. Computer generated image of the underside of the ice from multibeam data.

## 4 Previous Royal Navy cruises

On 3 March 1971, HMS *Dreadnought* became the first British submarine to reach the North Pole. Since then, Royal Navy submarines have been cruising the Arctic Ocean regularly, collecting ice draft data (above all for operational reasons) that are then sent to the University of Cambridge where they are analysed and archived by the Polar Oceans Physics Group, whose scientists were often invited to join the cruises.

Table 4-1 contains the full list of Arctic voyages made by UK submarines where sea ice draft data was collected. Data are mostly in the form of analogue paper rolls, which is the normal output of the AP780, but also in digital form for the most recent cruises, where the AP2077 was in use.

Year	Month	Sonar System	Processed
1971	August	776	Yes
1976	October/November	MS45, SS	Yes
1979	April/May	780	Yes
1985	June/July	780	Yes
1987	May	780, SS	Yes
1988	April/May	780, SS	No
1989	April/May	780, SS	No
1990	April	780, SS	No
1990	May	780, SS	No
1991	April	780, SS	Partially
1992	April/May	780, SS	No
1994	April	780, SS, 2077	No
1996	August/September	780, SS, 2077	Yes
2004	April	780, SS, 2077	Yes
2007	March	780, SS, 2077, Multibeam	Partially

Table 4-1. UK submarine cruises to Fram Strait and the Arctic Ocean.

To this table we will add the April 1976 cruise of the American submarine USS *Gurnard* whose data collected in the region N of Alaska were processed by P. Wadhams, at the time at the Scott Polar Research Institute of the University of Cambridge.

### 4.1 The 1976 Gurnard Cruise

Between 7 and 10 April 1976 the submarine USS *Gurnard*, equipped with a high frequency upward-looking echo-sounder of very narrow beam (believed to be less than 3° wide), surveyed the area around the AIDJEX (Arctic Ice Dynamics Joint Experiment) ice camp located N of Alaska at approximate position (72°40'N, 144°W). The survey, whose 1400km-long track is shown in Figure 4-1, can be divided into three legs: (1) OPQ, heading N, start at position (70°36'N, 144°13'W), end at position (75°30'N, 144°20'W); (2) QR, heading approximately SSE, end at position (72°43'N, 138°15'W); and (3) RPS, heading W, end at position (72°43'N, 154°15'W). Point P in Figure 4-1 marks the position of the ice camp.

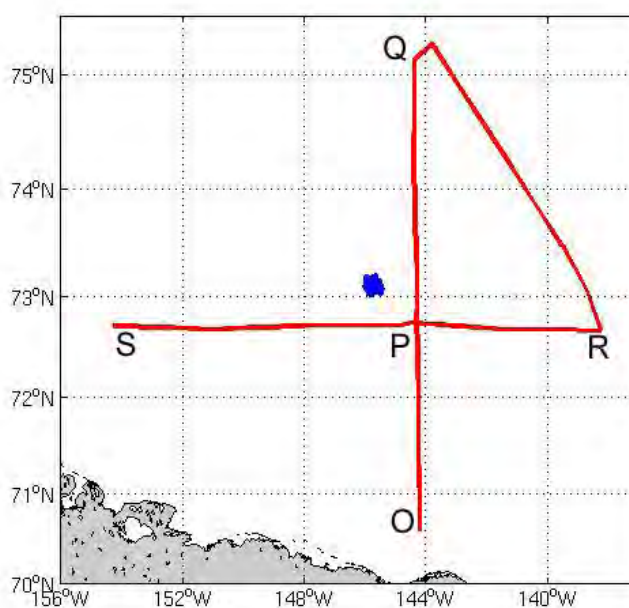


Figure 4-1. Track of the 1976 Gurnard cruise in the Beaufort Sea (in red). The track of the 2007 Tireless cruise around the SEDNA ice camp is also marked (in blue).

Wadhams and Horne (1980) analysed the recorded ice profiles and found a mean ice draft of 3.81m (CONF). According to the authors of the paper, the distribution of the different types of ice was as follows: thin ice (0-0.5m), 0.9%; thin ice (0-1.0m), 3.4%; young ice (0.5-2.0m), 10%; level ice (2.0-5.0m), 71%; ridged ice (5.0m or more), 19%.

The full track was divided into 27 sections of approximate length 50km whose centroid location, length and mean draft are shown in Table 4-2.

Section	Centroid		Length	Draft		
	Lat (N)	Lon (W)		Mean	Max	Mode
1	71°04'	144°13'	53	5.09	23.13	---

2	71°31'	144°14'	51	4.22	28.83	---
3	71°58'	144°14'	50	3.77	21.64	---
4	72°25'	144°15'	51	4.14	19.60	3.1
5	72°52'	144°18'	52	3.92	22.65	2.7
6	73°20'	144°18'	52	3.45	22.65	2.7
7	73°48'	144°20'	52	3.19	20.54	2.0
8	74°17'	144°23'	53	3.37	20.73	2.4
9	74°44'	144°22'	51	3.61	20.09	2.0
10	75°08'	144°22'	51	3.47	16.86	2.7
11	75°16'	143°47'	51	3.40	22.59	2.7
12	74°52'	142°48'	52	3.74	23.65	2.7
13	74°16'	141°20'	52	3.70	20.97	2.7
14	73°52'	140°25'	52	3.78	24.93	2.7
15	73°29'	139°32'	52	3.51	23.38	2.7
16	73°04'	138°44'	53	3.38	18.96	2.7
17	72°40'	138°15'	52	3.89	24.84	2.7
18	72°41'	139°50'	53	3.87	18.35	2.0
19	72°41'	141°26'	53	3.62	26.73	2.7
20	72°43'	142°56'	50	3.69	20.36	2.7
21	72°45'	144°27'	50	3.47	19.99	2.0
22	72°43'	146°24'	53	3.53	19.66	2.7
23	72°43'	147°59'	53	4.14	24.48	3.1
24	72°42'	149°32'	52	3.63	22.01	3.1
25	72°41'	151°03'	50	4.17	22.07	3.1
26	72°42'	152°39'	53	4.50	29.23	3.1
27	72°43'	154°15'	53	4.61	29.14	

Table 4-2. Centroid, length (in km) and average draft (in metres) of each section of the 1976 Gurnard cruise in the Beaufort Sea.

Mean drafts above 5m were only observed in Section 1, which was also the one with the highest fraction (40%) of ridged ice. The centroid of this section was located just 50 nautical miles N of the Alaskan coast, an area of active pressure ridge formation due to drifting ice piling up along and near the coast. In all other sections the ice distribution was, in general, quite uniform. In about half of the sections the mean draft was between 3.5 and 4.0m. The lowest mean draft observed was 3.19m, just N of the centre of the survey.

## 4.2 The 1976 Sovereign Cruise

In October 1976 the nuclear submarine HMS *Sovereign* acquired 3750km of sea ice draft data in the European sector of the Arctic Ocean. Its approximate track, together with the colour-coded mean draft of each of its division into 100km sections, can be seen in Figure 4-2.

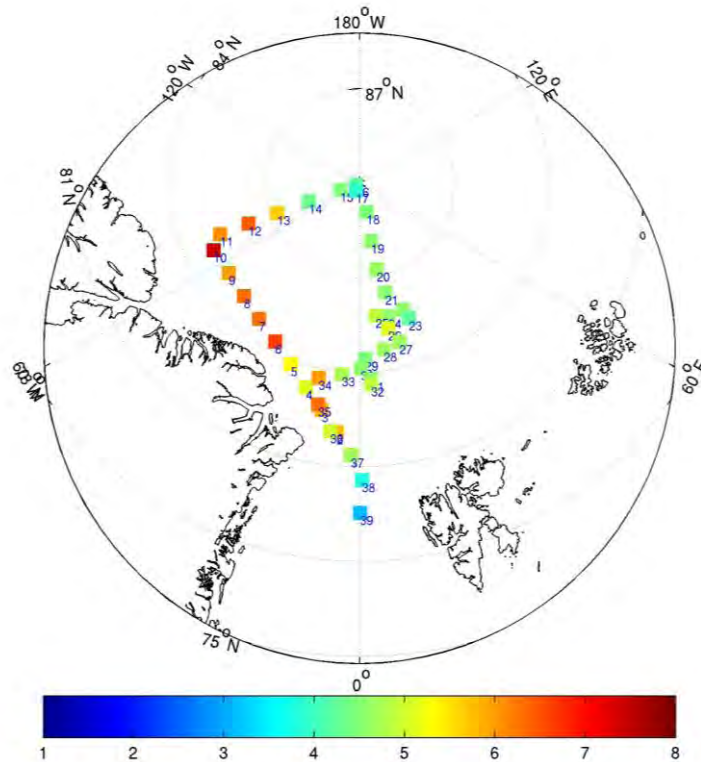


Figure 4-2. Mean draft (in metres) for each section of the 1976 Sovereign cruise.

The first leg of the cruise, from position (81°N, 0°W) at the N entrance of Fram Strait, to position (84°50'N, 70°W) N of Ellesmere Island, covers the heavily ridged ice zone off the N coast of Greenland. The second leg, to the North Pole, ended on 23 October at 0720 GMT. From the Pole the *Sovereign* returned southwards along the 11°E meridian until it reached 85°N. Then the boat diverted to run several zigzag tracks across the Arctic mid-Oceanic Ridge for hydrographic purposes. Then from a position close to the centroid of section 4 to a position close to the centroid of section 37 (see figure above) it reproduced its outward track a few kilometres to the south.

The analysis of the acquired ice draft data was performed by Wadhams (1981). Other than mean and modal sea ice drafts for each of the sections, the author generated probability density functions of ice draft and elevation, studied the level ice distribution, found empirical laws governing the distribution of pressure ridge and lead spacings, the distribution of the depths of ridge keels and the distribution of lead widths. Details of the procedures to measure sea ice draft, analyse the data collected and the main results can be found in (Wadhams, 1981). Here we limit ourselves to reproduce the results for the mean ice draft and for the distribution of ice types, see Table 4-3.

Section	Centroid		Length	Mean draft	Percentage of ice			
	Lat (N)	Lon			<0.5m	0.5-2.0m	2.0-5.0m	>5.0m
1	81°22'	1°36'W	80	5.84	3.2	9	42	45
2	82°03'	5°08'W	89	5.77	10.0	10	40	40
3	82°41'	9°26'W	92	5.78	9.4	10	39	42

4	83°18'	14°39'W	104	5.07	13.4	13	38	35
5	83°51'	20°46'W	90	5.38	10.1	11	44	36
6	84°18'	27°59'W	84	6.66	3.3	6	43	47
7	84°39'	36°23'W	88	6.32	3.6	4	47	46
8	84°52'	45°41'W	62	6.31	2.1	6	46	46
9	84°58'	55°35'W	74	6.05	3.7	5	48	44
10	84°55'	65°19'W	43	7.49	2.5	4	38	55
11	85°18'	69°59'W	95	6.14	2.6	5	51	42
12	86°16'	69°59'W	100	6.41	5.1	5	49	40
13	87°14'	70°01'W	100	5.72	8.3	9	46	37
14	88°18'	70°00'W	101	4.38	4.3	9	62	25
15	89°22'	70°00'W	101	4.44	1.0	16	55	28
16	89°53'	65°00'W	100	4.25	2.5	15	56	26
17	89°44'	21°43'W	101	3.94	6.4	15	56	23
18	89°03'	14°13'E	100	4.41	2.6	9	61	27
19	88°07'	11°35'E	101	4.60	2.4	9	59	30
20	87°12'	11°14'E	100	4.64	2.0	10	59	29
21	86°26'	13°18'E	101	4.60	1.3	9	62	28
22	85°44'	18°58'E	100	4.50	4.2	11	60	25
23	85°26'	20°17'E	103	4.23	3.1	14	58	25
24	85°40'	12°21'E	100	4.59	2.6	11	58	29
25	85°45'	7°02'E	99	4.94	2.6	10	56	31
26	85°17'	11°21'E	101	5.06	2.1	10	55	33
27	84°47'	14°08'E	99	4.65	2.3	13	59	26
28	84°39'	8°21'E	104	4.67	0.5	10	59	31
29	84°26'	1°57'E	102	4.46	2.1	11	59	28
30	84°07'	0°37'E	102	4.51	1.3	9	62	28
31	83°46'	3°25'E	98	4.55	3.3	12	56	28
32	83°36'	3°19'E	100	4.86	6.3	9	52	33
33	83°54'	5°16'W	102	4.80	9.6	17	44	30
34	83°41'	11°50'W	95	5.97	2.6	11	43	43
35	82°50'	10°35'W	102	6.35	2.1	14	41	43
36	82°04'	6°40'W	101	5.02	11.2	20	37	32
37	81°21'	1°49'W	101	4.63	4.7	17	49	29
38	80°34'	0°35'E	99	3.77	16.3	16	45	22
39	79°31'	0°09'E	136	3.07	10.1	21	55	14

Table 4-3. Ice draft statistics for the 1976 Sovereign cruise.

Next, we divide the cruise into regions, as shown in Table 4-4. Such a division will later prove useful to compare measurements of different cruises.

Region	Lat (N) limits	Longitude limits	Length	Sections	Mean draft
Central Fram Strait I	81°00' - 81°43'	0°00' - 3°12'W	80	1	5.84
Northeast Greenland I	81°43' - 83°36'	3°12'W - 17°30'W	285	2-4	5.52
North Greenland	83°36' - 84°59'	17°30'W - 70°00'W	441	5-10	6.26
Going N at 70°W	84°50' - 88°54'	69°58'W - 70°01'W	396	11-14	5.65

<b>North Pole</b>	88°54' - 90°00'	---	302	15-17	4.21
<b>Transpolar Drift</b>	84°02' - 89°32'	0°10'E – 22°31'E	1312	18-30	4.61
<b>Northeast Greenland II</b>	82°25' - 84°06'	12°18'W – 5°47'E	497	31-35	5.30
<b>Central Fram Strait II</b>	80°10' - 82°25'	8°51'W – 0°52'E	301	36-38	4.48
<b>South Fram Strait</b>	78°53' - 80°10'	0°52'E - 0°00'	136	39	3.07

Table 4-4. Regions covered by the 1976 Sovereign cruise, their boundaries, length (in km), sections involved and mean draft (in metres).

It is worth noting that the Sovereign was equipped with a very wide beam (17°) upward-looking sonar which, in agreement with section 3.2, requires a strong beamwidth correction. The procedure used to take this bias into account was described in the same paper by Wadhams (1981). The values of the ice draft quoted in Table 4-3 and Table 4-4 are supposed to be the beamwidth corrected ones.

### 4.3 The 1979 Sovereign Cruise

In a two-week period between 22 April and 4 May 1979 the *Sovereign* conducted a thorough survey of Fram Strait and its approaches before proceeding to the Arctic Basin, providing a significant contribution to our knowledge of the ice conditions in the area. It produced the first synoptic measurements of the ice thickness distribution in the region at a time when no airborne technique had yet been developed to sound sea ice. Its convoluted track permitted a dense grid of ice draft distributions to be constructed from its upward-looking echo sounder profiles, sufficient to generate contours of mean ice draft (Wadhams, 1983).

The track was divided into 50km sections and mean drafts and other characteristics of the ice cover were determined. Table 4-5 shows the mean ice drafts for each section, identified by the approximate position of its centroid, for latitudes above 80°N.

Section	Latitude (N)	Longitude	Mean draft
1	80°00'	5°E	2.09
2	80°45'	4°E	2.42
3	80°45'	7°W	5.09
4	81°00'	7°W	4.24
5	81°15'	2°E	3.96
6	81°25'	6°W	3.66
7	81°40'	0°	3.94
8	82°00'	4°W	3.78
9	82°15'	3°W	4.25
10	82°20'	0°	4.08
11	82°50'	0°	4.97
12	82°55'	0°	5.20
13	83°00'	1°W	5.37

<b>14</b>	83°00'	2°E	3.69
<b>15</b>	83°20'	3°W	5.96
<b>16</b>	83°30'	2°E	4.19
<b>17</b>	83°40'	1°W	3.85

Table 4-5. Basic ice draft statistics for the 1979 cruise in Fram Strait.

In order to later compare these observations with those of other cruises, we present a summary of the results in Table 4-6.

Latitude (N)	Longitude	Mean draft (m)
80-82°	4-7°W	4.19
80-82°	0-5°E	3.10
80-82°	all	3.65
82-84°	3°W-2°E	4.62

Table 4-6. Basic ice draft statistics for the 1979 cruise in Fram Strait.

The map in Figure 4-3, which we borrowed from (Wadhams, 1983), shows all ice draft values obtained during this cruise and the approximate contours constructed from the observations.

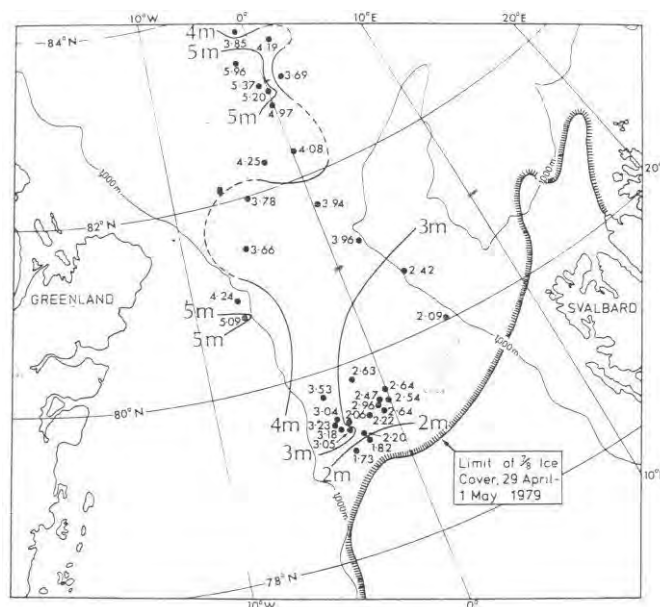


Figure 4-3. Mean ice drafts from 50km sections obtained during the 1979 cruise (from (Wadhams, 1983)).

#### 4.4 The 1985 Cruise

In June and July 1985 a British submarine returned to the Arctic and obtained sea ice draft profiles with a 45kHz sonar of narrow beam (less than 5°) in the Greenland Sea, Fram Strait and northwards into the Eurasian Basin of the Arctic Ocean. The draft record was not corrected for the effect of beamwidth as it was estimated (by Wadhams) that it would lead to a reduction of at most 1-2% to the mean ice drafts. Data points were interpolated to 1.5m intervals and the record was divided into 50km sections (Wadhams, 1989).

Figure 4-4 and Figure 4-5 show the mean draft of each 50km section plotted in the position of the centroid of the section. The second figure is a detailed representation of the measurements taken between latitudes 83°30'N and 84°30'N and longitudes 0 and 10°E.

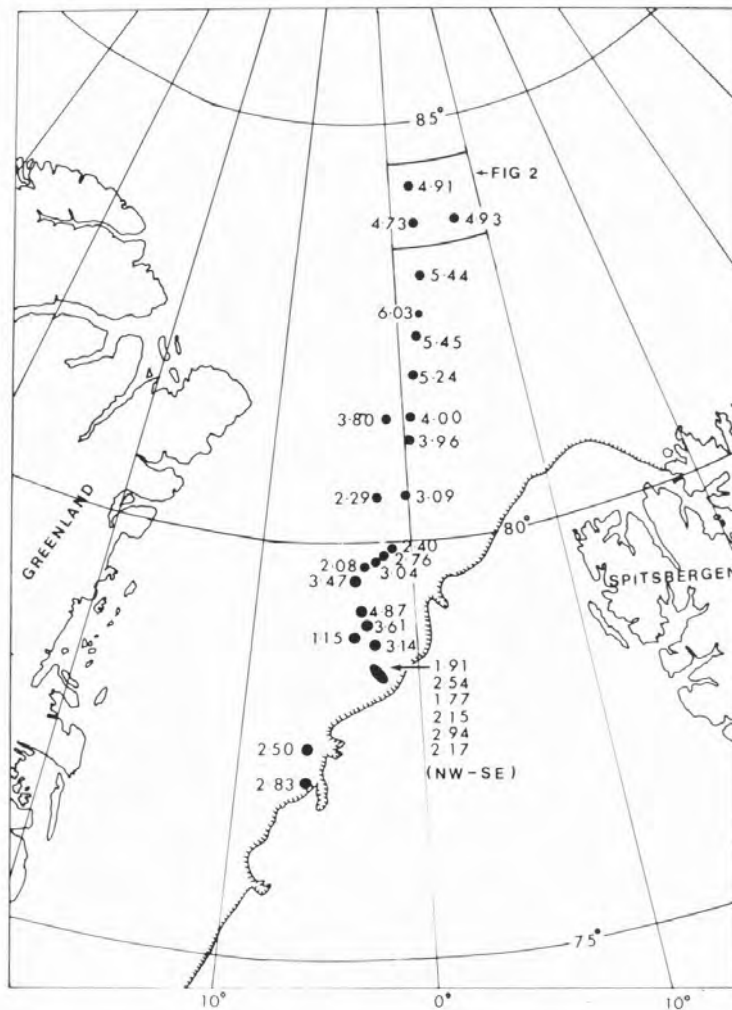


Figure 4-4. Mean ice drafts from 50-km track sections obtained during the 1985 cruise (from (Wadhams, 1989)). The top box at high latitude is expanded in the next figure.

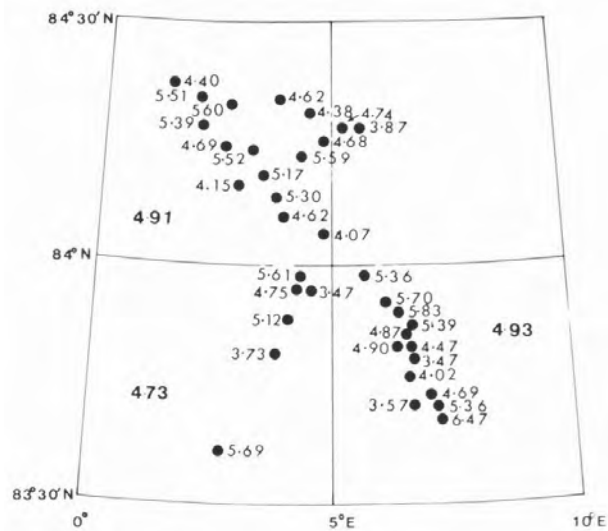


Figure 4-5. Mean ice drafts from 50-km track sections obtained during the 1985 cruise (from (Wadhams, 1989)).

Table 4-7 has the basic ice draft statistics for this cruise. Note that in the last three rows the mean draft is already an average over a large number of sections at those approximate coordinates.

Latitude (N)	Longitude	Mean draft (m)	Number of sections
80°30'	0°	3.09	1
80°30'	3°W	2.29	1
81°15'	0°	3.96	1
81°50'	0°	4.00	1
81°50'	2°W	3.80	1
82°00'	1°E	5.24	1
82°30'	2°E	5.45	1
82°45'	3°E	6.03	1
83°15'	3°E	5.44	1
83°45'	4°E	4.73	6
83°50'	7°E	4.93	13
84°15'	3°E	4.91	17

Table 4-7. Basic ice draft statistics for the 1985 cruise in Fram Strait.

For the area 80-82°N, 0-3°W (first five rows of Table 4-7) the mean draft is 3.43m. For the area 82-84°N, 1-7°E (rows 6-11 of the same table) it is 4.98m.

### 4.5 The 1987 Superb Cruise

Another cruise took place in May 1987 for which the exact track is not known but believed to be similar to the 1976 cruise in which case it would have been approximately as follows: northwards in Fram Strait not far from the prime meridian; thence a W turn towards NE and N Greenland; thence cruise N of Greenland at about 85°N, likely to be until 55°W (though possibly until 70°W if it is really similar to the 1976 cruise); thence to the pole, northwards, along the 55°W (possibly 70°W) meridian; and finally all the way down to Fram Strait along the prime meridian. The submarine was equipped with an upward-looking echo-sounder of the type AP780 with a beamwidth of less than 5°. The total length of the profile is reported to be 3400km in (Wadhams, 1992) and 6000km in (Wadhams, 1990). The latter paper compares the main results of this cruise with those of the October 1976 cruise and concludes that there was a significant thinning of the ice between the two cruises in the region N of Greenland. The former paper describes in more detail the sea ice thickness distribution observed during the cruise.

The approximate track of the *Superb* in Fram Strait is shown in Figure 4-6. Sea ice profiles were obtained in two distinct areas: between the latitudes 72°N and 75°N (which is of little interest to us because it cannot be compared with any other observations from other cruises), and between 76 and 82°N. In Table 4-8 we present the observed mean drafts in bins of 1° of latitude for some of the northern sectors of the latter region.

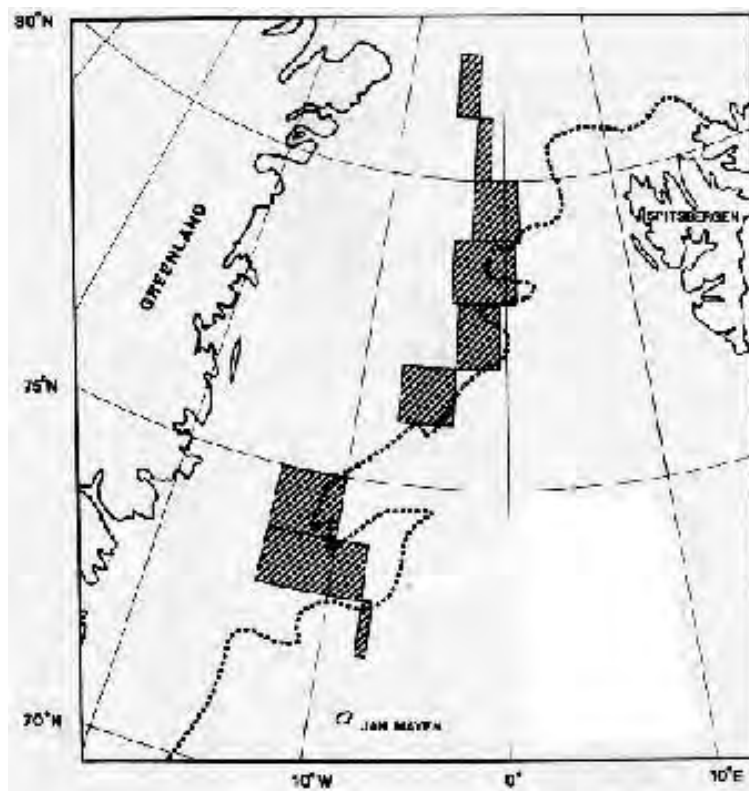


Figure 4-6. Regions where sonar data were collected in Fram Strait during the 1987 cruise. Dark boxes mark extreme E and W limits of submarine track within 1° latitude increments (from (Wadhams, 1992)).

Latitude (N)	Longitude	Mean draft (m)
--------------	-----------	----------------

78-79°	1°E-4°W	1.0
79-80°	1°E-2.5°W	2.0
80-81°	1°W-2.5°W	3.3
81-82°	2.5°W-4.5°W	3.8

Table 4-8. Mean drafts for latitude bins of 1° of latitude in the 1987 cruise in Fram Strait.

Table 4-9 shows the mean ice draft for five 50km sections in the northernmost sector of Fram Strait, between 80 and 82°N. The approximate positions of the centroids of the sections were taken from (Wadhams, 1992). The mean draft for these 250km of track was 3.62m and the deepest keel found had a draft of 23.55m.

Latitude (N)	Longitude	Mean draft (m)
80°10'	1°30'W	3.32
80°40'	2°20'W	3.33
81°05'	2°40'W	3.99
81°25'	3°00'W	3.95
81°50'	4°00'W	3.53

Table 4-9. Mean drafts for 50km sections in the N part of Fram Strait during the 1987 cruise.

Wadhams (1992) found modal drafts of the order of 2.5m for the areas N of Greenland, presumably around 85°N, and for the transect between 85°N and the Pole. In another paper published two years earlier, Wadhams (1990) compared directly the ice thickness statistics of this cruise with those of the 1976 cruise along similar transects. We shall come back to this in Chapter 7. The same author made extensive studies of pressure ridge and lead distributions from the data collected during this voyage.

## 4.6 The 1991 *Tireless* Cruise

The full track of the first voyage of the *Tireless* to appear in our report is shown in Figure 4-7. It looks nice, doesn't it, with that visit to the Pole and that unique eastwards diversion to Franz Joseph Land? However, the reader must not get too enthusiastic with this long and potentially interesting track. In first place because we are only in possession of sonar data for the portion of the cruise in Fram Strait; second because the Royal Navy has not provided us with the detailed navigation logs; and finally because the analysis of the AP780 draft records is still incomplete and no results will be shown in the present issue of this report.

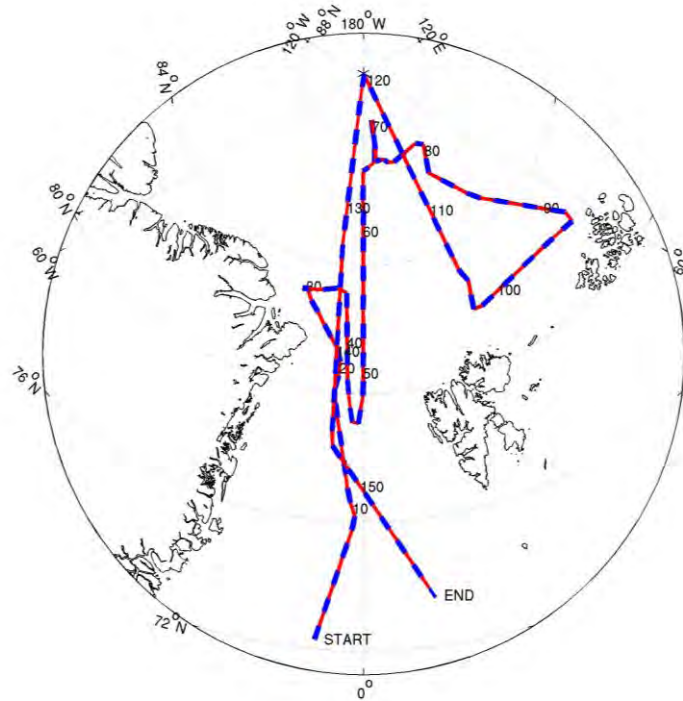


Figure 4-7. Track of the April 1991 cruise.

#### 4.7 The 1996 *Trafalgar* Cruise

The track of the *Trafalgar* during its journey to the North Pole and back in September 1996 is depicted in Figure 4-8.

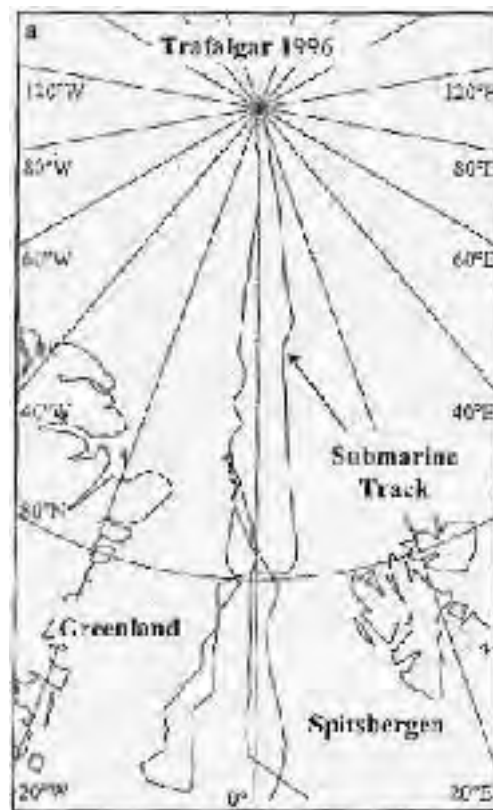


Figure 4-8. Track of the September 1996 cruise (from (Wadhams and Davis, 2001)).

Results of the analysis of the ice draft data collected during this cruise can be found in (Wadhams and Davis, 2001). They indicate that the thickness of the Arctic Ocean sea ice in 1996 was substantially lower than in 1976.

## 5 The 2004 *Tireless* Cruise

### 5.1 Description of the cruise

In April 2004 HMS *Tireless* carried out the route shown in Figure 5-1. Along-track single-beam upward-looking sonar data were recorded using an Admiralty Pattern 780 echo-sounder which operates at 48 kHz with transducers (fitted on bow, fin and stern) having a reported nominal beamwidth of 3°. This is the same system that had been used in previous Arctic voyages dating back to 1979. The boat was also equipped with the newer Admiralty Pattern 2077 system, an upward-looking sidescan sonar, an along-track oceanographic sensor package, an XBT launcher and an upward-looking video camera.

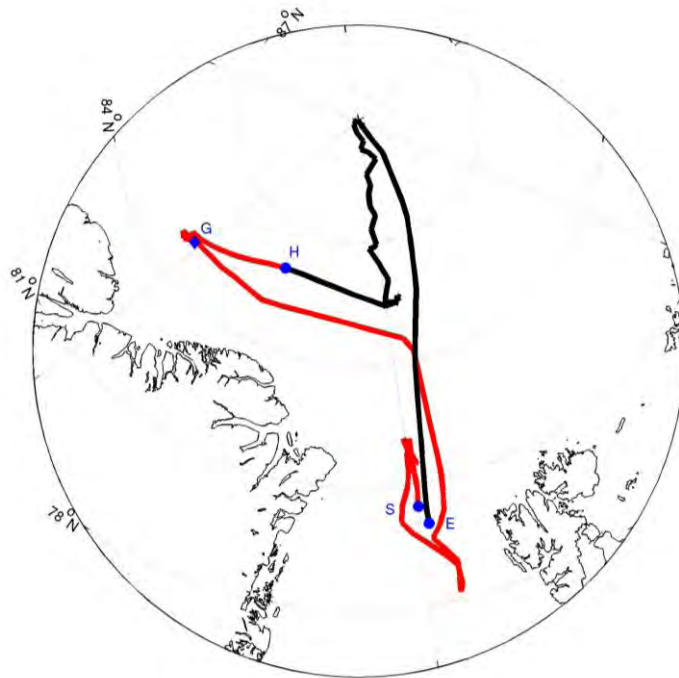


Figure 5-1. Track of the April 2004 cruise.

We start counting time, along-track distance and sections on 01 April at 00:00:38, when the submarine was at position (80°26'N, 0°30'E) at the edge of the ice-pack (the point marked with S in Figure 5-1). For seven days the boat followed an intricate trajectory near the N-S axis of Fram Strait, with a few changes of direction. It began with a leg in the S-N direction close to the prime meridian, in which it reached a maximum latitude of 82°14'N in section 8. This was followed by several shorter legs essentially in the N-S and S-N directions. When the boat was at 81°12'N it changed its heading from S to SSW and then, at 80°08'N, to SE. Shortly after the end of section 18, at 13:14 on 04 April,

approximate position (79°30'N, 0°10'E), the submarine left the ice pack. For about two days it cruised in ice-free waters, filling sections 19 to 29. We assume that the boat reentered the ice-pack on 06 April at 13:48, at position (80°48'N, 4°37'E), somewhere in the second half of section 30, though it may have already been in the marginal ice zone for some time.

Figure 5-2 depicts the track of the submarine in Fram Strait, together with the 15, 50, 75 and 95% ice concentration contours on 05 April 2004 obtained from AMSR-E data. The different colours of the track (red, orange and yellow) correspond to different regions of the strait, defined in Table 5-1 and Table 5-2.

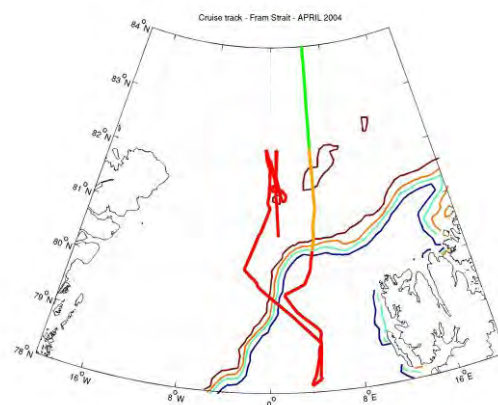


Figure 5-2. Track of the submarine in Fram Strait during the 2004 cruise.

Once under the ice-pack, the boat headed N along the 5°E meridian and crossed the 84°N parallel on 08 April at 00:59. About four and a half hours later, at the approximate latitude of 84°30'N, it started turning W to round NE Greenland. Thence it followed the usual route N of Greenland at around 85°N until it reached 65°W (point G in Figure 5-1).

Afterwards, in what we designate by GreenICE Survey, the *Tireless* ran a series of lines under the area which a month later was used for an ice camp experiment as part of the EU GreenICE project. This survey enabled the profiled ice to be studied by drilling, helicopter electromagnetic sounding and with an array of tiltmeter buoys (used to derive ice thickness from wave dispersion). It was also possible to compare submarine data with ENVISAT SAR imagery (Hughes and Wadhams, 2006). The GreenICE Survey is defined here as the set of ice draft observations made W of the 62°W meridian, between 19:34 on 10 April and 14:15 on 11 April. Its 247 km-long track is shown in Figure 5-3. In terms of 50km sections it includes the end of section 52, all of sections 53 to 56 and the initial part of section 57. In terms of AP780 paper rolls it starts at roll/roll section/pixel=07/30/2065 and it ends at 07/64/1726. The depth of the boat during the Survey was mostly around 130m, with short intervals at 80m.

After this survey the boat took a ENE course but soon the upward-looking sonars stopped recording ice drafts regularly. We processed AP780 data until the end of section 62, at 08:46 on 12 April, when the boat was at approximate position (86°00'N, 31°46'W), point H in Figure 5-1. From

that point until the end of the voyage there are only about 50km of acceptable AP780 data obtained in the vicinity of the North Pole on 18 and 19 April (sections 101 and 102). Thus, there is no AP780 data with sufficient quality in sections 63 to 100 and no data at all for the return journey from the Pole (black portion of the track in Figure 5-1).

Almost all statistics for the ice draft and pressure ridge distributions that we are about to present are based on AP780 measurements. The reader shall assume that this is the case unless otherwise stated. However, we processed AP2077 data for sections 1-18, 20-24, 26-63, 67, 70-72, 74-75, 78-79, 83 and 101-102, with the corresponding statistics shown in Section 5.5. There is no AP2077 data available for the homebound journey.

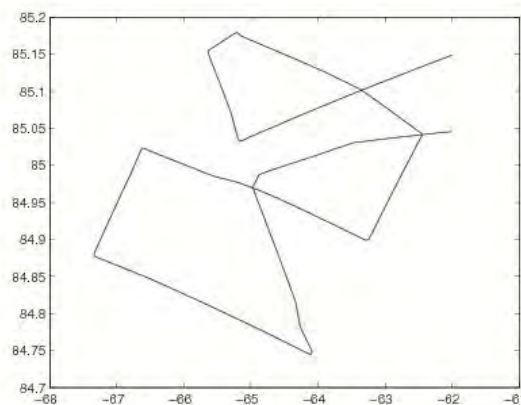


Figure 5-3. Track of the GreenICE Survey on 10-11 April 2004.

In Table 5-1 we show the time intervals in which the boat was cruising inside each of the seven regions, the numbers of the 50km-long sections that form the track inside each region and, in the last column, the corresponding portions of the AP780 rolls in the form roll/roll section/pixel. In Table 5-2 the reader can find the exact boundaries of these regions, the length of the track with valid data and the percentage of valid data in each of them.

Region	Start time	End Time	Sections	AP780 Rolls
<b>Central Fram Strait I</b>	01 Apr 00:01	04 Apr 13:14	01-18	01/09/1446 – 03/56/1696
<b>Central Fram Strait II</b>	06 Apr 11:04	07 Apr 04:53	30-33	04/25/2139 – 04/57/0693
<b>North Fram Strait</b>	07 Apr 04:53	08 Apr 01:15	34-37	04/57/0694 – 05/25/0531
<b>Northeast Greenland</b>	08 Apr 01:15	09 Apr 02:59	38-43	05/25/0532 – 05/70/0927
<b>North Greenland I</b>	09 Apr 02:59	11 Apr 16:50	44-57	05/70/0928 – 07/66/1851
<b>North Greenland II</b>	11 Apr 16:50	12 Apr 08:46	59-62	07/68/3597 – 08/20/2934
<b>North Pole</b>	18 Apr 14:37	19 Apr 18:27	101-102	08/32/0584 – 09/32/3600

Table 5-1. Regions covered by the 2004 cruise, their start and end times, sections involved and AP780 rolls used.

The region designated by Central Fram Strait is the portion of the strait comprised between the 80 and the 82°N parallels. Within this band of latitudes we must distinguish two disjoint areas, corresponding to the W (Central Fram Strait I, red in Figure 5-2) and E (Central Fram Strait II, orange in Figure 5-2) paths of the submarine. Such distinction is necessary because the ice conditions in these two regions may differ significantly, as shown, for example, by the position of the ice concentration contours depicted in Figure 5-2. North Fram Strait (green in Figure 5-2) is the part of the strait between 82°N and 84°N, where the trajectory of the boat was roughly a straight S-N segment at around 5°E.

Region	Lat (N) limits	Longitude limits	Length	% Valid data
Central Fram Strait I	79°37' - 82°14'	2°41'W – 1°48E	595	66.1
Central Fram Strait II	80°28' – 82°14'	4°23'E – 5°00'E	152	75.8
North Fram Strait	82°14' – 84°02'	4°58'E – 5°09'E	169	84.6
Northeast Greenland	84°02' – 85°08'	18°36'W – 5°10'E	248	82.7
North Greenland I	84°45' – 85°20'	18°37'W – 67°20'W	533	76.2
North Greenland II	85°26' – 86°00'	31°49'W – 54°13'W	177	88.4
North Pole	89°44' – 89°59'	180°W – 180°E	51	50.9

Table 5-2. Regions covered by the 2004 cruise, their boundaries, length of track with valid data (in km) and percentage of valid data.

Northeast Greenland is the part of the track around the NE corner of Greenland. By convention, it starts when the boat crosses the 84°N parallel and ends around (85°N, 18°30'W). The region named North Greenland I is the path along the 85°N parallel between 18°30'W and the location of the GreenICE camp. As we shall see, this is the portion of the 2004 route that coincides almost exactly with part of the 2007 track. After the GreenICE Survey the *Tireless* headed ENE. What we call North Greenland II is the stretch between points G and H in Figure 5-1. Finally, there are 51km of valid data near the North Pole, the seventh region of the list.

## 5.2 Ice draft distribution: general results

For each section of the full track with valid AP780 data we have calculated the average (observed and corrected for beamwidth effects according to the procedure outlined in Section 3.2), maximum, minimum and modal ice draft, as well as the full ice draft frequency distribution. When the modal draft is zero we have calculated the most frequent non-zero value of the ice draft, a quantity designated by mode\* (which represents the most likely ice draft when open water is not taken into account). Mode and mode\* were computed from histograms with bins of 10cm. The minimum ice draft in a section is almost always zero.

Table 5-3 and Table 5-4 display the basic statistics for each section of the cruise with valid data as well as their starting times, centroids and percentages of valid data. The mean, maximum and modal drafts shown were the observed ones (not beamwidth corrected).

Section	Start time				Centroid		Draft			$\alpha$	% valid data
	d	h	m	s	Lat (N)	Lon	Mean	Max	Mode		
1	1	0	0	38	80°55'	0°47'E	2.30	12.22	1.75	1.41	100
2	1	3	46	20	81°23'	0°40'E	2.66	19.69	1.65	2.43	85.8
3	1	10	0	6	81°50'	0°40'E	3.05	14.22	1.85*	1.80	93.0
4	1	14	38	19	82°07'	0°44'E	3.12	17.08	2.05	2.11	78.4
5	1	22	4	41	81°44'	0°37'E	3.12	17.72	2.05*	2.09	77.0
6	2	4	50	6	81°31'	0°35'E	2.79	14.88	2.15*	1.12	50.2
7	2	11	18	23	81°46'	0°25'E	2.94	17.75	2.15*	1.91	100
8	2	15	59	41	82°08'	0°22'W	3.27	19.22	2.25	1.99	81.0
9	2	21	24	42	81°53'	0°05'E	2.87	13.64	1.15	2.30	21.6
10	3	3	28	35	81°27'	1°10'E	2.56	16.33	2.05	1.69	60.8
11	3	8	49	23	81°31'	1°18'E	2.57	13.01	2.35*	1.22	73.6
12	3	14	19	55	81°52'	0°17'E	3.52	18.34	1.55	1.93	77.1
13	3	19	32	59	81°46'	0°05'W	3.08	8.94	2.35	2.76	34.1
14	3	21	46	3	81°19'	0°12'W	3.78	13.83	2.55*	2.11	35.6
15	4	0	14	5	80°55'	0°47'W	4.09	19.80	2.65	2.86	43.9
17	4	6	11	15	80°05'	2°14'W	3.83	19.98	2.25*	2.77	88.7
18	4	9	6	58	79°47'	0°46'W	2.34	13.96	1.85	1.52	89.6
30	6	11	3	41	80°43'	4°35'E	2.06	9.55	1.85	1.04	17.5
31	6	15	49	9	81°07'	4°53'E	1.73	7.77	1.65	0.81	100
32	6	19	27	29	81°35'	4°59'E	1.75	8.94	1.65	0.99	85.9
33	7	0	17	8	82°01'	4°58'E	2.15	9.40	1.75	1.24	100
34	7	4	53	14	82°29'	5°00'E	2.37	19.20	1.55*	1.95	90.7
35	7	10	21	12	82°55'	5°02'E	2.41	13.55	2.05	1.60	79.7
36	7	15	6	21	83°22'	5°05'E	2.73	13.10	2.45	1.68	99.7
37	7	19	24	19	83°49'	5°08'E	3.05	18.84	1.85	1.95	68.4

Table 5-3. Ice draft statistics for the 2004 cruise, sections 1-37 (Fram Strait). Draft and coefficient  $\alpha$  in metres.

Section	Start time				Centroid		Draft			$\alpha$	% valid data
	d	h	m	s	Lat (N)	Lon	Mean	Max	Mode		
38	8	1	15	23	84°14'	5°10'E	3.46	18.80	1.75	2.34	77.4
39	8	5	33	48	84°34'	3°10'E	3.71	15.69	1.85	2.06	94.2
40	8	9	29	33	84°45'	1°07'W	3.03	17.65	2.05	1.92	81.8
41	8	13	41	12	84°55'	6°02'W	2.87	14.16	2.15	1.52	82.0
42	8	17	15	38	85°02'	11°05'W	3.16	17.14	2.25	1.86	84.7
43	8	21	53	43	85°06'	15°45'W	3.49	17.70	2.25	2.42	75.8
44	9	2	58	33	85°08'	21°20'W	3.78	17.97	2.55	2.39	56.9
45	9	7	56	31	85°08'	26°26'W	3.43	20.82	2.25	3.14	67.3
46	9	12	55	32	85°05'	31°28'W	4.61	28.09	2.45	3.16	88.7

<b>47</b>	9	17	31	7	85°01'	36°51'W	4.12	21.24	1.75	2.53	68.3
<b>48</b>	9	22	9	46	85°05'	41°29'W	4.25	17.83	2.05	4.99	8.1
<b>49</b>	10	2	54	26	85°07'	46°45'W	5.13	22.80	3.15	2.75	76.1
<b>50</b>	10	7	34	27	85°05'	51°50'W	5.46	30.37	3.05	3.69	78.1
<b>51</b>	10	12	45	4	85°05'	57°03'W	5.38	25.82	2.95	3.84	100
<b>52</b>	10	17	28	14	85°02'	62°23'W	6.70	24.17	2.95	3.91	94.0
<b>53</b>	10	22	26	34	84°50'	64°44'W	5.38	28.82	3.25	2.92	96.3
<b>54</b>	11	2	2	10	84°56'	66°31'W	5.96	27.41	2.95	4.29	89.3
<b>55</b>	11	5	35	12	84°59'	63°25'W	6.23	27.36	2.85	3.58	97.2
<b>56</b>	11	9	9	7	85°07'	64°44'W	5.12	31.97	2.25	3.77	90.8
<b>57</b>	11	13	16	43	85°10'	61°33'W	5.61	24.19	2.55	3.30	55.6
<b>59</b>	11	20	20	37	85°29'	52°02'W	4.56	21.88	2.95	2.95	53.4
<b>60</b>	12	0	56	23	85°41'	46°30'W	4.91	24.94	2.85	3.47	100
<b>61</b>	12	3	34	50	85°52'	40°56'W	4.94	26.64	2.95	3.41	100
<b>62</b>	12	6	10	58	85°58'	34°54'W	4.87	28.87	2.55	4.22	100
<b>101</b>	18	14	37	2	89°56'	149°36'W	3.97	24.33	1.65*	2.73	85.3
<b>102</b>	18	21	5	37	89°58'	142°07'W	4.62	17.76	1.85	3.05	21.0

Table 5-4. Ice draft statistics for the 2004 cruise, sections 38-102 (Northeast Greenland, North Greenland and North Pole). Draft and coefficient  $\alpha$  in metres.

Figure 5-4 shows colour-coded (not beamwidth corrected) mean ice drafts for each section, with the centre of each square coinciding with the centroid of the section it represents.

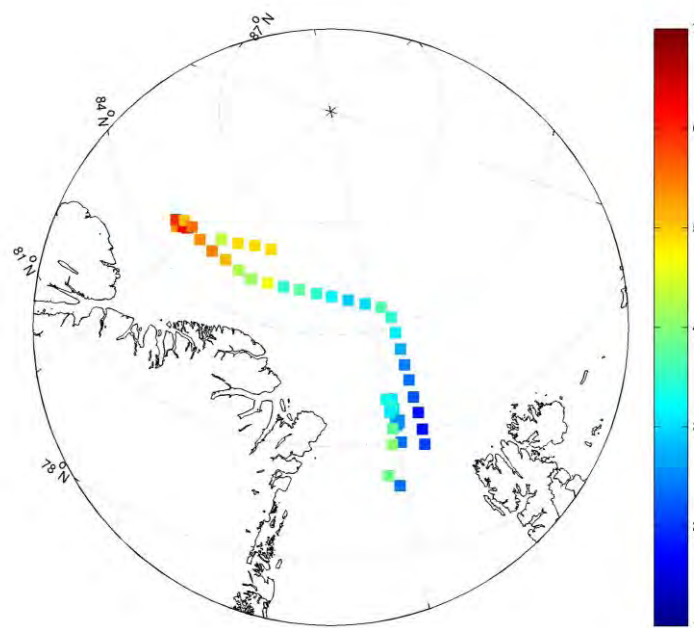


Figure 5-4. Mean ice draft (in metres) for each section of the 2004 cruise.

Table 5-5 and Table 5-6 contain the beamwidth corrected values of the mean draft for the sections with enough information on the depth of the submarine and with quality judged sufficient for a correction to be worthwhile. This is not the case, for instance, of the two sections in vicinity of the North Pole. At the time of writing the author has not yet been performed the corrections for the Fram Strait part of the cruise. As we cannot be sure about the exact beamwidth, corrections were done for two plausible values following the procedure described in Section 3.2. At the time of writing the author has not yet calculated the corrections for sections 1 to 37.

Section	Mean depth	Observed mean draft	$bw=3^\circ$			$bw=6^\circ$		
			$d_{real}$	$\Delta d$	$\Delta d/d_{real}$	$d_{real}$	$\Delta d$	$\Delta d/d_{real}$
1		2.30						
2		2.66						
3		3.05						
4		3.12						
5		3.12						
6		2.79						
7		2.94						
8		3.27						
9		2.87						
10		2.56						
11		2.57						
12		3.52						
13		3.08						
14		3.78						
15		4.09						
17		3.83						
18		2.34						
30		2.06						
31		1.73						
32		1.75						
33		2.15						
34		2.37						
35		2.41						
36		2.73						
37		3.05						

Table 5-5. Beamwidth corrections for the 2004 cruise, sections 1-37. Drafts and depths in metres,  $\Delta d/d_{real}$  as a percentage. Not yet calculated.

Section	Mean depth	Observed mean draft	$bw=3^\circ$			$bw=6^\circ$		
			$d_{real}$	$\Delta d$	$\Delta d/d_{real}$	$d_{real}$	$\Delta d$	$\Delta d/d_{real}$
38	174	3.46	3.02	0.43	14.3	2.57	0.89	34.4

39	160	3.71	3.30	0.41	12.4	2.87	0.84	29.4
40	167	3.03	2.65	0.38	14.2	2.26	0.77	33.8
41	180	2.87	2.46	0.41	16.9	2.03	0.84	41.5
42	180	3.16	2.73	0.43	15.7	2.29	0.87	38.1
43	215	3.49	3.03	0.45	14.9	2.60	0.88	34.0
44	202	3.78	3.28	0.50	15.4	2.78	1.00	36.0
45	175	3.43	3.02	0.41	13.6	2.60	0.84	32.1
46	180	4.61	4.08	0.53	12.9	3.54	1.07	30.2
47	175	4.12	3.60	0.52	14.5	3.06	1.06	34.8
48	230	4.25	3.30	0.96	29.0	2.39	1.86	77.7
49	186	5.13	4.30	0.83	19.3	3.45	1.68	48.6
50	166	5.46	4.88	0.58	11.9	4.27	1.19	27.9
51	130	5.38	5.00	0.37	7.45	4.58	0.79	17.2
52	124	6.70	6.26	0.43	6.91	5.78	0.92	15.9
53	130	5.38	5.06	0.33	6.43	4.69	0.69	14.7
54	130	5.96	5.57	0.39	7.07	5.13	0.84	16.3
55	130	6.23	5.84	0.39	6.69	5.40	0.83	15.4
56	126	5.12	4.73	0.39	8.32	4.29	0.84	19.5
57	131	5.61	5.16	0.45	8.67	4.66	0.95	20.4
59	173	4.56	4.01	0.37	9.15	3.64	0.74	20.3
60	230	4.91	4.40	0.51	11.6	3.92	0.99	25.3
61	230	4.94	4.41	0.54	12.2	3.90	1.04	26.7
62	230	4.87	4.19	0.68	16.2	3.55	1.32	37.2
101	---	3.97	---	---	---	---	---	---
102	---	4.62	---	---	---	---	---	---

Table 5-6. Beamwidth corrections for the 2004 cruise, sections 38-102. Drafts and depths in metres,  $\Delta d/d$  real as a percentage.

### 5.3 Pressure ridge distribution: general results

In this section we present the pressure ridge statistics for each section of the cruise with valid data. It consists of the number of ridges found in the 50km section, the number of ridges per km (taking into account the length of valid data only), the mean draft of the keels, the number of ridge spacings considered (this is not necessarily equal to the number of ridges minus one because there may be regions of no data inside the section), the mean ridge spacing and the modal ridge spacing. The latter is only computed if there are at least five spacings, and even in this case it cannot be considered a reliable parameter because it strongly depends on the choice for the bin size. In our statistics we use bin sizes of 20m for 5m keels, 100m for 9m keels and 50m for 15m keels.

Section	Number of ridges	Ridge frequency	Mean draft	Ridge spacing		
				Number	Mean	Mode
1	76	1.52	6.76	75	661	30
2	124	2.89	7.21	120	319	10
3	200	4.30	7.35	197	227	110

4	172	4.39	7.64	169	229	50
5	139	3.61	7.51	133	270	50
6	106	4.23	6.77	104	232	50
7	254	5.08	7.14	253	195	50
8	193	4.77	7.26	188	201	50
9	45	4.17	7.37	42	231	90
10	75	2.47	6.97	70	380	30
11	82	2.23	6.80	78	394	90
12	220	5.71	7.38	217	172	70
13	58	3.40	6.77	57	296	50
14	53	2.98	7.44	52	308	170
15	85	3.87	8.45	83	258	110
17	193	4.35	8.08	191	230	90
18	69	1.54	6.58	66	534	130
30	15	1.72	6.63	14	324	150
31	21	0.42	5.78	20	2352	30
32	24	0.56	6.05	22	1233	10
33	90	1.80	6.18	89	540	110
34	111	2.45	7.05	109	374	70
35	85	2.13	6.94	83	464	130
36	149	2.99	6.83	148	335	30
37	130	3.80	7.52	126	254	90

Table 5-7. 5m keel spacing statistics for the 2004 cruise, sections 1-37. Ridge frequency in  $\text{km}^{-1}$ , mean draft, mean and modal spacings in metres.

Section	Number of ridges	Ridge frequency	Mean draft	Ridge spacing		
				Number	Mean	Mode
38	164	4.24	7.50	162	234	70
39	239	5.07	7.57	237	194	50
40	146	3.57	7.37	144	279	70
41	159	3.88	7.16	157	258	50
42	147	3.47	7.15	145	286	70
43	129	3.40	7.83	127	290	50
44	115	4.04	8.51	110	233	90
45	130	3.87	7.83	126	255	90
46	220	4.96	8.76	215	193	110
47	170	4.98	8.81	164	196	70
48	20	4.92	8.02	18	151	10
49	228	5.99	9.03	224	165	90
50	247	6.33	9.26	242	158	90
51	272	5.44	9.79	271	184	110
52	298	6.34	10.90	295	158	110
53	260	5.40	9.50	259	183	70
54	250	5.60	10.51	248	177	150

55	271	5.58	10.38	269	179	90
56	269	5.92	9.71	266	167	110
57	181	6.51	10.36	180	154	90
59	132	4.63	9.46	127	196	50
60	206	4.12	9.26	205	242	110
61	204	4.08	9.42	203	246	150
62	234	4.68	9.87	233	214	90
101	268	6.28	8.48	264	157	50
102	47	5.68	9.00	44	175	70

Table 5-8. 5m keel spacing statistics for the 2004 cruise, sections 38-102. Ridge frequency in  $\text{km}^{-1}$ , mean draft, mean and modal ridge spacing in metres.

Section	Number of ridges	Ridge frequency	Mean draft	Ridge spacing		
				Number	Mean	Mode
1	9	0.18	10.21	8	3544	250
2	16	0.37	12.35	14	1196	150
3	41	0.88	10.49	38	1079	150
4	39	0.99	10.97	36	989	50
5	26	0.68	11.59	23	708	150
6	9	0.36	10.15	8	2501	50
7	33	0.66	10.95	32	1398	150
8	19	0.47	11.24	16	915	150
9	10	0.93	11.03	7	803	350
10	10	0.33	11.07	7	609	150
11	5	0.14	10.66	3	5274	---
12	31	0.80	10.78	28	813	150
13	0	0	---	0	---	---
14	12	0.67	11.03	11	1269	250
15	25	1.14	12.51	23	749	50
17	52	1.17	11.86	50	813	150
18	5	0.11	10.79	3	1076	---
30	1	0.11	9.55	0	---	---
31	0	0	---	0	---	---
32	0	0	---	0	---	---
33	2	0.04	9.22	1	7421	---
34	12	0.26	11.29	10	1505	50
35	10	0.25	10.77	8	3384	50
36	14	0.28	10.49	13	3806	50
37	28	0.82	11.04	24	676	150

Table 5-9. 9m keel spacing statistics for the 2004 cruise, sections 1-37. Ridge frequency in  $\text{km}^{-1}$ , mean draft, mean and modal ridge spacing in metres.

Section	Number of ridges	Ridge frequency	Mean draft	Ridge spacing
---------	------------------	-----------------	------------	---------------

				Number	Mean	Mode
38	32	0.83	10.64	30	1046	150
39	51	1.08	11.07	49	827	250
40	27	0.66	10.94	25	1464	150
41	22	0.54	10.39	20	1577	950
42	23	0.54	10.81	21	1471	250
43	23	0.61	12.35	21	1215	150
44	44	1.55	11.74	39	558	50
45	26	0.77	12.28	22	1204	50
46	84	1.89	12.00	80	480	150
47	68	1.99	11.91	62	419	250
48	5	1.23	12.38	3	712	---
49	101	2.65	12.07	97	376	150
50	111	2.84	12.29	106	354	150
51	129	2.58	13.02	128	386	250
52	179	3.81	13.52	176	253	150
53	120	2.49	12.44	119	387	150
54	130	2.91	13.77	128	328	150
55	140	2.88	13.52	138	342	150
56	122	2.69	12.99	119	371	150
57	101	3.63	12.93	100	274	150
59	63	2.21	12.29	59	409	150
60	73	1.46	13.51	72	672	150
61	82	1.64	13.26	81	603	250
62	100	2.00	13.81	99	500	150
101	93	2.18	11.63	89	429	250
102	18	2.18	12.66	15	396	50

Table 5-10. 9m keel spacing statistics for the 2004 cruise, sections 38-102. Ridge frequency in  $\text{km}^{-1}$ , mean draft, mean and modal ridge spacing in metres.

Section	Number of ridges	Ridge frequency	Mean draft	Ridge spacing		
				Number	Mean	Mode
1	0	0	---	0	---	---
2	4	0.09	17.62	2	376	---
3	0	0	---	0	---	---
4	3	0.08	16.32	1	1179	---
5	2	0.05	17.06	1	306	---
6	0	0	---	0	---	---
7	3	0.06	16.87	2	7620	---
8	1	0.02	19.22	0	---	---
9	0	0	---	0	---	---
10	1	0.03	16.33	0	---	---
11	0	0	---	0	---	---

12	2	0.05	17.54	1	8546	---
13	0	0	---	0	---	---
14	0	0	---	0	---	---
15	5	0.23	17.44	3	3132	---
17	7	0.16	17.76	6	4807	275
18	0	0	---	0	---	---
30	0	0	---	0	---	---
31	0	0	---	0	---	---
32	0	0	---	0	---	---
33	0	0	---	0	---	---
34	1	0.02	19.20	0	---	---
35	0	0	---	0	---	---
36	0	0	---	0	---	---
37	1	0.03	18.84	0	---	---

Table 5-11. 15m keel spacing statistics for the 2004 cruise, sections 1-37. Ridge frequency in  $\text{km}^{-1}$ , mean draft, mean and modal ridge spacing in metres.

Section	Number of ridges	Ridge frequency	Mean draft	Ridge spacing		
				Number	Mean	Mode
38	2	0.05	18.67	1	1467	---
39	1	0.02	15.69	0	---	---
40	2	0.05	16.75	1	7176	---
41	0	0	---	0	---	---
42	1	0.02	17.14	0	---	---
43	5	0.13	16.53	3	1202	---
44	8	0.28	16.03	4	1082	---
45	4	0.12	19.00	1	86	---
46	10	0.23	18.84	8	2529	275
47	10	0.29	17.57	6	1022	125
48	2	0.49	16.87	1	410	---
49	15	0.39	18.59	12	1732	75
50	20	0.51	19.08	15	1108	125
51	27	0.54	19.30	26	1876	525
52	47	1.00	18.43	44	906	425
53	21	0.44	18.13	20	2188	3125
54	41	0.92	19.05	39	833	175
55	42	0.86	18.74	40	1140	125
56	27	0.59	18.94	24	1563	225
57	23	0.83	17.83	22	1226	125
59	8	0.28	19.22	5	1107	25
60	22	0.44	18.08	21	2261	125
61	25	0.50	17.94	24	2035	325
62	35	0.70	18.40	34	1234	175

<b>101</b>	9	0.21	17.81	7	3594	75
<b>102</b>	4	0.48	16.59	1	349	---

Table 5-12. 15m keel spacing statistics for the 2004 cruise, sections 38-102. Ridge frequency in  $\text{km}^{-1}$ , mean draft, mean and modal ridge spacing in metres.

## 5.4 Regional analysis

In this section we describe the main characteristics of the ice thickness distribution in each of the seven regions traversed by the *Tireless*. A summary of the statistics, before and after beamwidth corrections, is presented in Table 5-13. The coefficient  $\beta$  was calculated from the observed (uncorrected) draft frequency distribution. No corrections were performed for the region of the North Pole and at the time of writing the corrections for Fram Strait have not yet been done. All plots and maps show observed (uncorrected) values for the draft and the number of ridges.

Region	Mean	Mean ( $bw=3^\circ$ )	Mean ( $bw=6^\circ$ )	Mode	Maximum	$\beta$
<b>Central Fram Strait I</b>	3.00			2.15*	19.98	0.45
<b>Central Fram Strait II</b>	1.89			1.65	9.55	0.96
<b>North Fram Strait</b>	2.62			1.85	19.20	0.55
<b>Northeast Greenland</b>	3.29	2.87	2.44	2.05	18.80	0.48
<b>North Greenland I</b>	5.24	4.77	4.27	2.75	31.97	0.29
<b>North Greenland II</b>	4.82	4.28	3.76	2.75	28.87	0.28
<b>North Pole</b>	4.08	---	---	1.65	24.33	0.38

Table 5-13. Ice draft statistics, before and after beamwidth corrections, for the regions of the 2004 cruise. Draft in metres, coefficient  $\beta$  in  $\text{metres}^{-1}$ .

Table 5-14 has the number of ridges (N) and the number of ridges per km (of valid data) for each of the seven regions.

Region	5m		9m		15m	
	N	N/km	N	N/km	N	N/km
<b>Central Fram Strait I</b>	2144	3.60	285	0.57	28	0.05
<b>Central Fram Strait II</b>	150	0.99	3	0.02	0	0
<b>North Fram Strait</b>	475	2.81	64	0.38	2	0.01
<b>Northeast Greenland</b>	984	3.97	178	0.72	11	0.04
<b>North Greenland I</b>	2929	5.49	1359	2.55	297	0.56
<b>North Greenland II</b>	775	4.34	317	1.78	89	0.50
<b>North Pole</b>	314	6.16	110	2.16	13	0.26

Table 5-14. Numbers of keels deeper than 5, 9 and 15m for the regions of the 2004 cruise.

### 5.4.1 Fram Strait

The plot in Figure 5-5 displays the mean and modal drafts of each section in Fram Strait and can be used to illustrate the different ice regimes in the different parts of the strait. The map in Figure 5-6 shows the mean ice draft of each section and the ice concentration contours as in Figure 5-2.

Let us start with sections 17 and 18, which form the southern part of the strait, where the latitudes range from 79°37'N to 80°17'N and the longitudes are in the interval 2°41'W-0°12'E. These two sections are the only part of the track (at these comparatively low latitudes) in ice-covered waters. The average ice draft of the 89km of valid data was 3.08m and the modal draft was zero because the submarine was not far from the ice edge. The modal draft excluding open water was 1.85m. There is a significant difference in mean and maximum drafts between sections 17 and 18. While section 17 has the second highest average draft in Fram Strait, section 18 has the second lowest. One of the causes of this disparity is likely to be the fact that section 18 is partially in the marginal ice zone, whereas section 17 lies entirely inside the 95% ice concentration contour. However, in section 17 we find slightly more open water, but also more thick ice, than in section 18. In section 17 there is a considerable fraction of ice with draft over 4m (and a non-negligible percentage of ice with draft higher than 6m); on the contrary, in section 18 almost all the ice has a draft below 4m.

Let us now consider the central W part of the strait, or sections 1 to 15 (it does not coincide with what we designated by Central Fram Strait I in the tables because the latter includes sections 17 and 18), with a range of latitudes of 80°43'N-82°14'N and longitudes between 1°22'W and 1°48'E. Section 1 contains a large amount of open water and little thick ice and is thus the one with the lowest average draft in this region. Unfortunately, the sonar range was set to 200m in this section, which generated low resolution records and large uncertainties in the calculated draft.

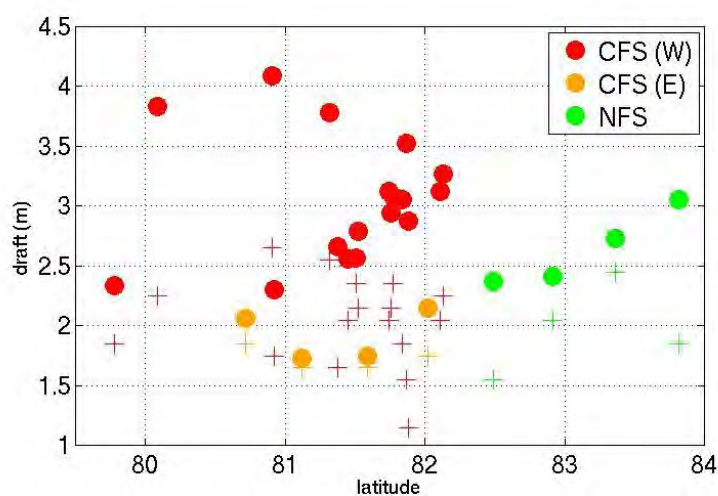


Figure 5-5. Mean (circles) and modal (crosses) ice drafts for each section of the 2004 cruise in Fram Strait.

The average drafts in sections 2-11 and 13 are always between 2.5 and 3.3m, with a slight increase with latitude. They form the dense set of red circles in the centre of the plot shown in Figure 5-5. The modal draft tends to be between 2.0 and 2.5m, though in a few cases it is lower than 2m. Section 12 has a comparatively low modal draft (one of the lowest in Fram Strait) but a large amount of thick ice and ridging, resulting in a high average draft. Sections 14 and 15, two of the westernmost legs of this part of the track, have the highest mean and modal drafts of the central W part of the strait. In fact, the highest mean and modal drafts in Fram Strait are 4.09 and 2.65m, respectively, in section 15 (though we have to bear in mind that this section has less than 50% of valid data). Section 14, which has the third highest mean draft and the second highest modal draft in the whole strait, has only 18km of valid data. The results for sections 14 and 15 are of low confidence because of the small amount of valid data, bad quality of the records and coarse resolution. The difference in mean drafts between sections 1 and 15, which are centred at the same latitude, can be due to a difference in longitude but can also be a consequence of the low quality of the corresponding paper rolls. Altogether, the mean, modal, modal without open water and maximum drafts for sections 1-15 are 2.99, 0, 2.15 and 19.80m.

The ice thickness distribution in the E stretch of the track in Fram Strait, sections 30 to 33, is quite different from its W counterpart. In each of these four sections the mean ice draft is lower than in any of the sections of the W track (all orange circles in Figure 5-5 lie below the red ones). The histograms that represent the draft probability distributions for each section and for this portion of the track as a whole are very narrow, indicating an absence of thick ice and, consequently, similar values for the average and modal drafts.

Finally, let us look at the results for North Fram Strait, sections 34 to 37. The mean draft, higher than the mean draft in the W but lower than the one in the E Fram Strait, appears to increase moderately and monotonically with latitude. The modal draft, on the contrary, is higher than in the central and southern parts of the strait.

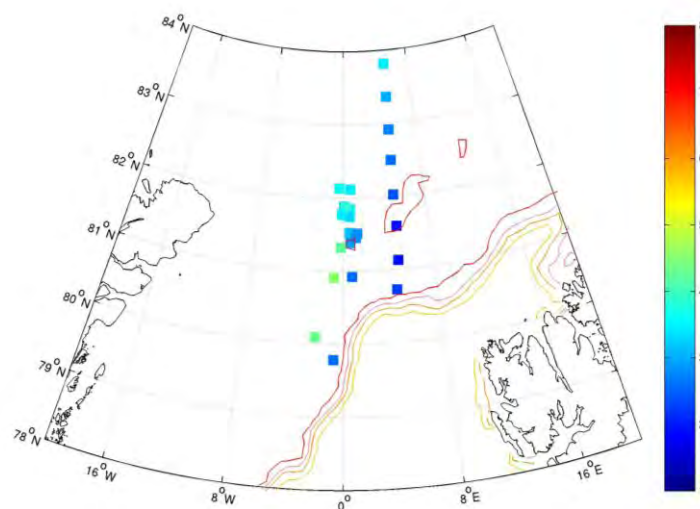


Figure 5-6. Mean ice draft (in metres) for each section of the 2004 cruise in Fram Strait.

Histograms with full draft probability distributions for the Central W, Central E and N Fram Strait are depicted in Figure 5-7, Figure 5-8 and Figure 5-9, respectively.

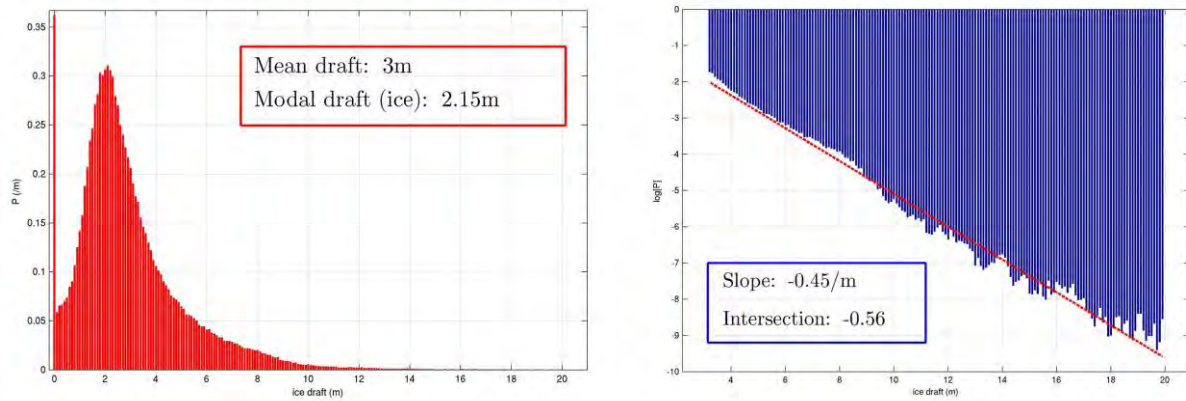


Figure 5-7. Ice draft histograms for Central Fram Strait W (sections 1-18) in linear (L) and semi-logarithmic (R) scales.

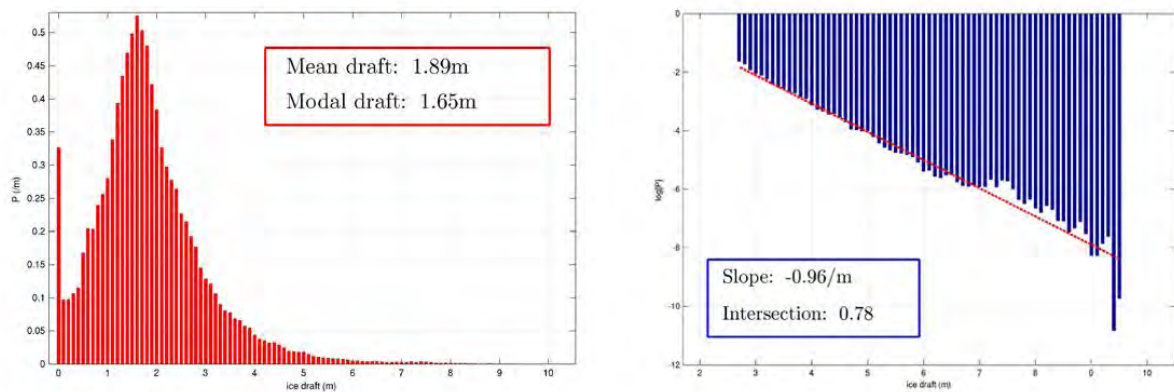


Figure 5-8. Ice draft histograms for Central Fram Strait E (sections 30-33) in linear (L) and semi-logarithmic (R) scales

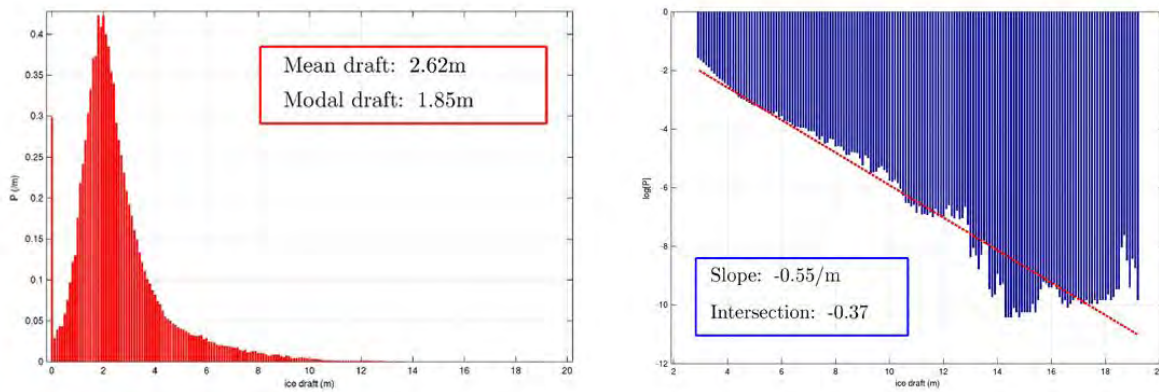


Figure 5-9. Ice draft histograms for North Fram Strait (sections 34-37) in linear (L) and semi-logarithmic (R) scales.

The ridge frequency for each section of the track in Fram Strait is shown in the form of a plot in Figure 5-10 and in the form of maps in Figure 5-11 and Figure 5-12. We consider separately number of ridges per km with keels deeper than 5, 9 and 15m. These plots and maps, together with the results of Table 5-14, clearly indicate that the number of ridges per unit length is, unsurprisingly, much higher in the W part of the strait than in its E part. Deep ridges are essentially absent in the E part and a rarity in the N part.

A histogram with the distribution of the keel depths in the W part of Fram Strait (sections 1 to 18) is shown in Figure 5-13. One notices the exponential shape of the distribution.

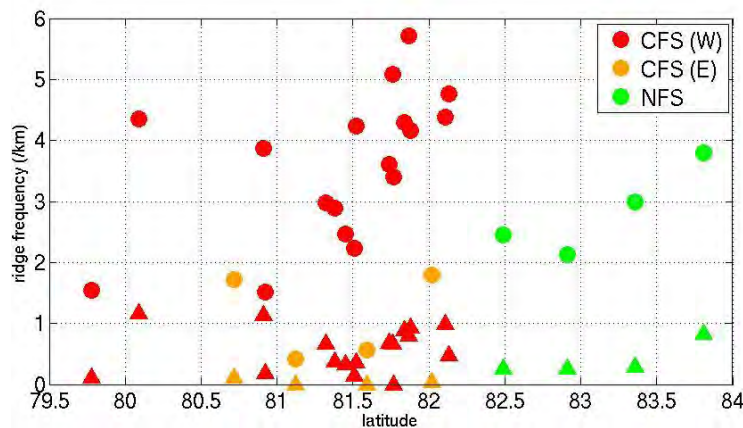


Figure 5-10. 5m (circles) and 9m (triangles) ridge keel frequency in each section of the 2004 cruise in Fram Strait.

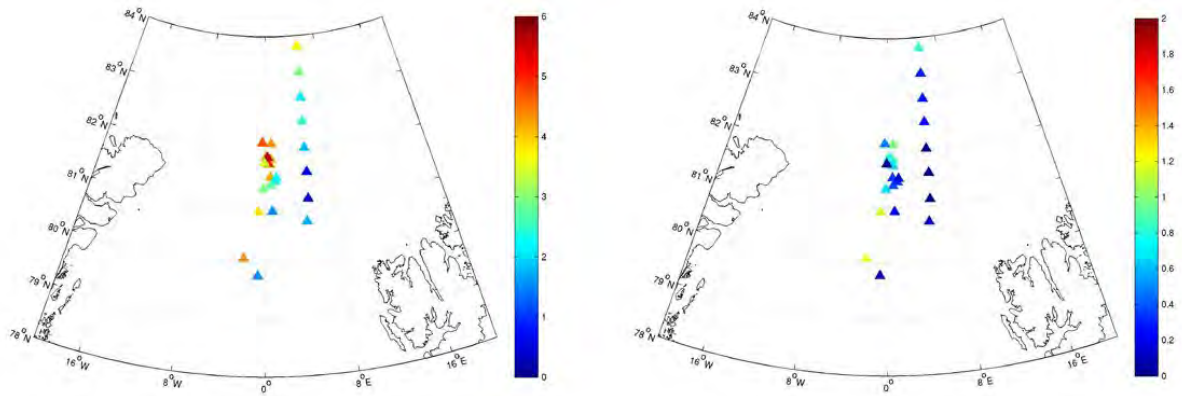


Figure 5-11. Mean number of ridges per km for each section of the 2004 in Fram Strait. Left for 5m keels, right for 9m keels .

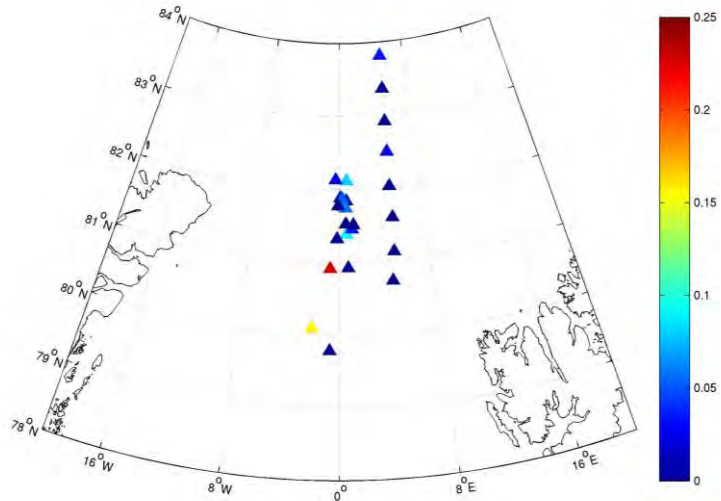


Figure 5-12. Mean number of 15m keels per km for each section of the 2004 in Fram Strait.

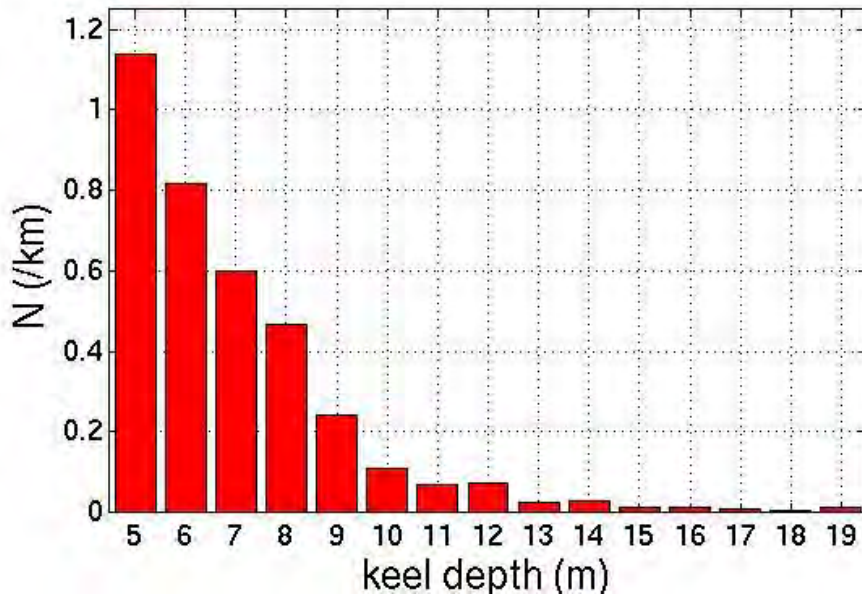


Figure 5-13. Keel depth distribution histogram for sections 1-18.

### 5.4.2 Northeast Greenland and North Greenland

The plot in Figure 5-14 shows the mean and modal drafts for each section of the cruise in the areas designated by Northeast Greenland and North Greenland, including the GreenICE Survey. Circles and crosses represent mean and modal values, respectively, a convention we shall use throughout this and the next chapter. In red we have the six sections in the region that we called Northeast Greenland, in blue the 14 sections in the area North of Greenland, in the vicinity of the 85°N parallel, and in green the four sections of the transect between 85 and 86°N.

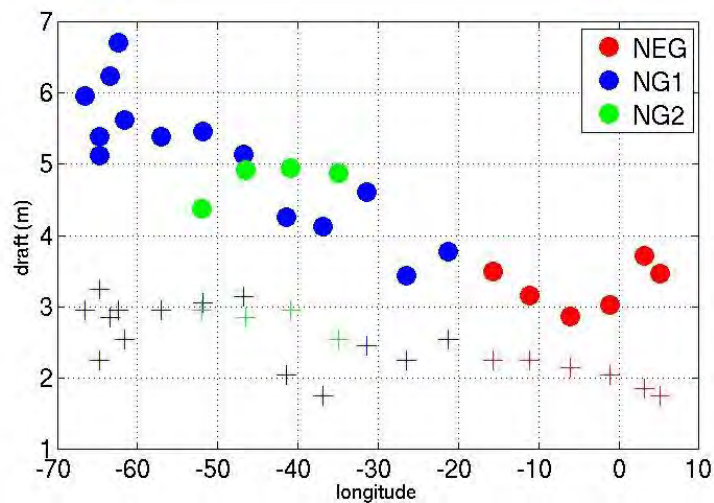


Figure 5-14. Mean (circles) and modal (crosses) ice drafts for each section of the 2004 cruise in Northeast and North Greenland.

The map in Figure 5-15 shows the colour coded mean drafts of each section in this part of the *Tireless* transect. The dense set of squares at the westernmost part of the track corresponds to the GreenICE Survey.

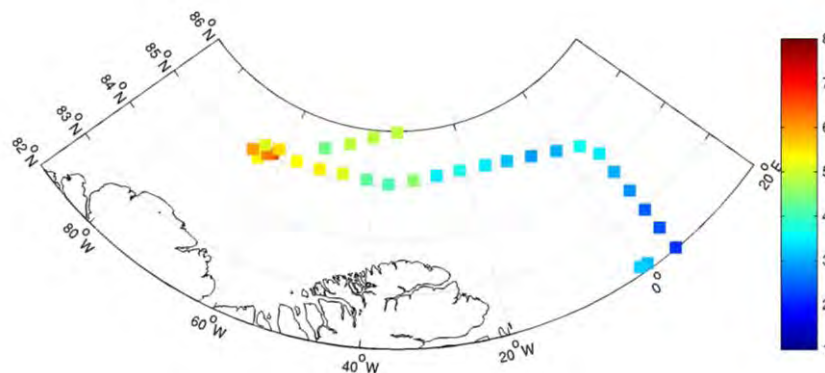


Figure 5-15. Mean ice draft (in metres) for each section of the 2004 cruise in Northeast Greenland and North Greenland.

Northeast Greenland is, for our purposes, the portion of the track covered by sections 38-43. The quality of the corresponding AP780 records is comparatively good, with a high percentage of valid data, and the results can be accepted with confidence. The overall modal ice draft of 2.05m (which corresponds to a modal thickness around 2.3m) is just above what could be expected for first-year ice at the end of the winter. It is perhaps indicative of a second-year ice dominated ice cover but this is not the only possible interpretation. The plot in Figure 5-14 suggests that there is a slight increasing trend in the modal draft with latitude but no particular pattern in the distribution of the mean draft among the six sections.

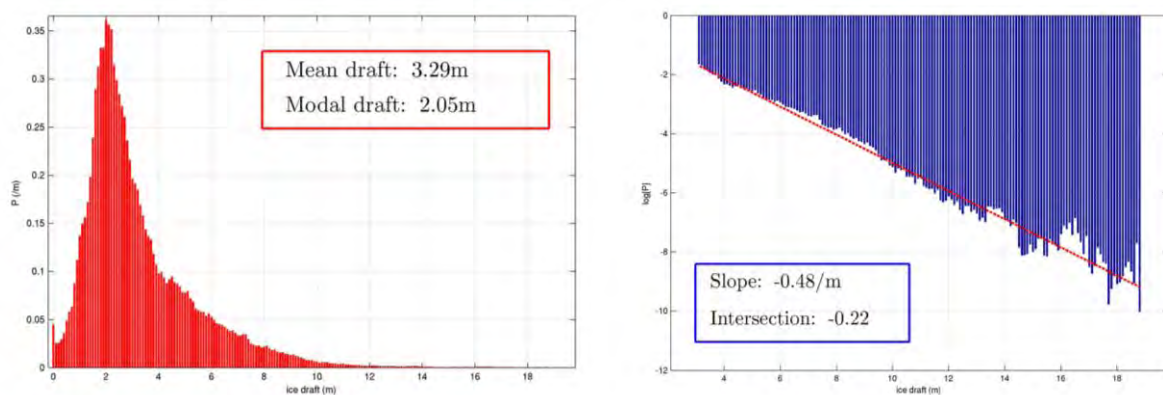


Figure 5-16. Ice draft histograms for Northeast Greenland (sections 38-43) in linear (L) and semi-logarithmic (R) scales.

The set of sections 44-57 at approximately constant latitude 85°N constitutes what we call North Greenland I. Of these, the last part of 52, the whole 53-56 and the first part of section 57 constitute the GreenICE Survey, which we analyse separately in the next section of this report. Note the low percentage of good data in sections 44, 45, 47 and, especially, 48. In all other sections we had records of good quality.

A mean ice draft of 5.24m (less 50 and 100cm, approximately, when beamwidth corrections are applied for 3- and 6°-wide beams, respectively), makes this segment the one under the thickest and most deformed ice (in fact, it is the one where one finds the largest number of pressure ridges) of the whole cruise. There is a westwards increase of mean ice draft which reaches the highest values in the GreenICE Survey, represented by the six blue circles on the top left of the plot in Figure 5-14. The modal ice draft increase from 2-2.5m in sections 44-48 to about 3m in sections 49-57.

The histograms in Figure 5-17 describe graphically the full ice draft distribution (they include the sections of the GreenICE Survey). The reader notes the sharp unimodal distribution and the exponential shape of the tail of the distribution.

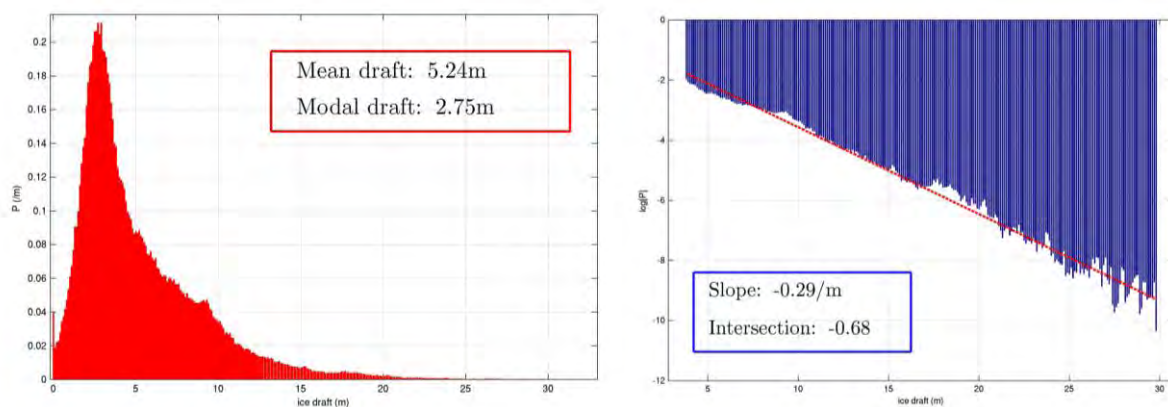


Figure 5-17. Ice draft histograms for North Greenland (sections 44-57) in linear (L) and semi-logarithmic (R) scales.

There is no data for the end of section 57 and for the whole section 58. Then there is good quality data for about half of section 59 and for the full sections 60, 61 and 62. These last four constitute the region designated by North Greenland II. We observe that the mean ice draft and the number of ridges are lower than in North Greenland I. This is in good agreement with the well established fact that ridging is more effective closer to the N shores of Greenland and Ellesmere Island than at higher latitudes. There is no clearly discernible trend with latitude or longitude in this part of the transect.

The histogram in Figure 5-18 exhibits a clear secondary peak at about 7.5m which is difficult to explain.

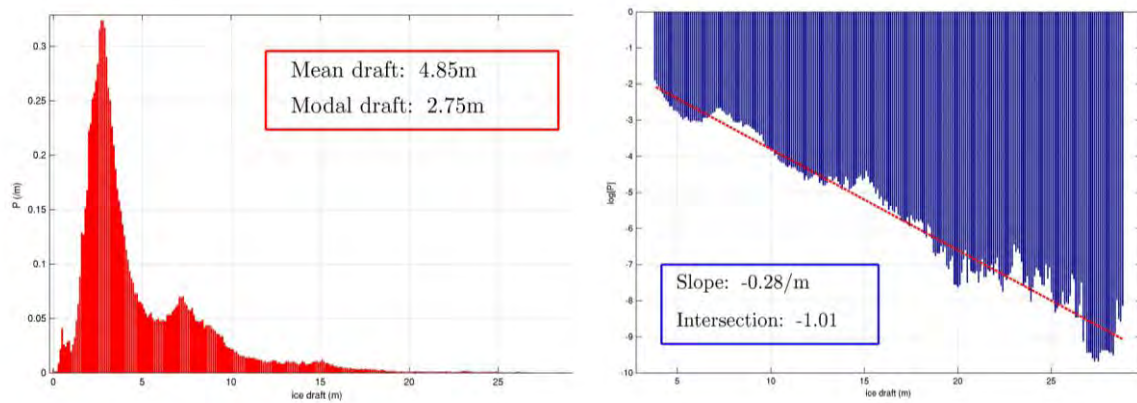


Figure 5-18. Ice draft histograms for North Greenland (sections 59-62) in linear (L) and semi-logarithmic (R) scales.

The plot in Figure 5-19 and the maps in Figure 5-20 illustrate the pressure ridge distribution for Northeast Greenland and North Greenland I and II.

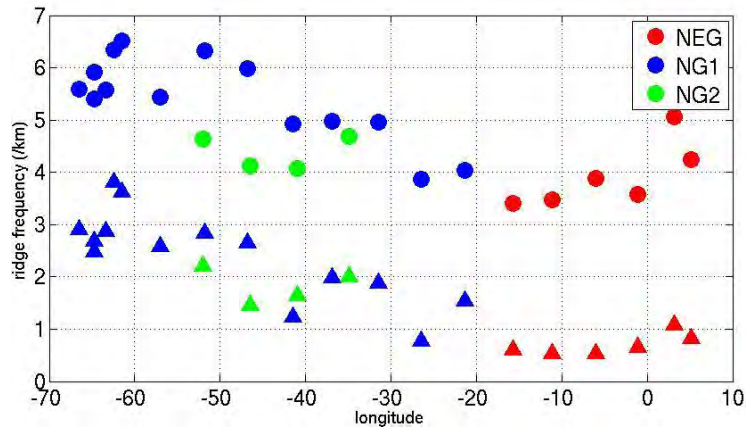


Figure 5-19. 5m (circles) and 9m (triangles) ridge keel frequency in each section of the 2004 cruise in Northeast Greenland and North Greenland.

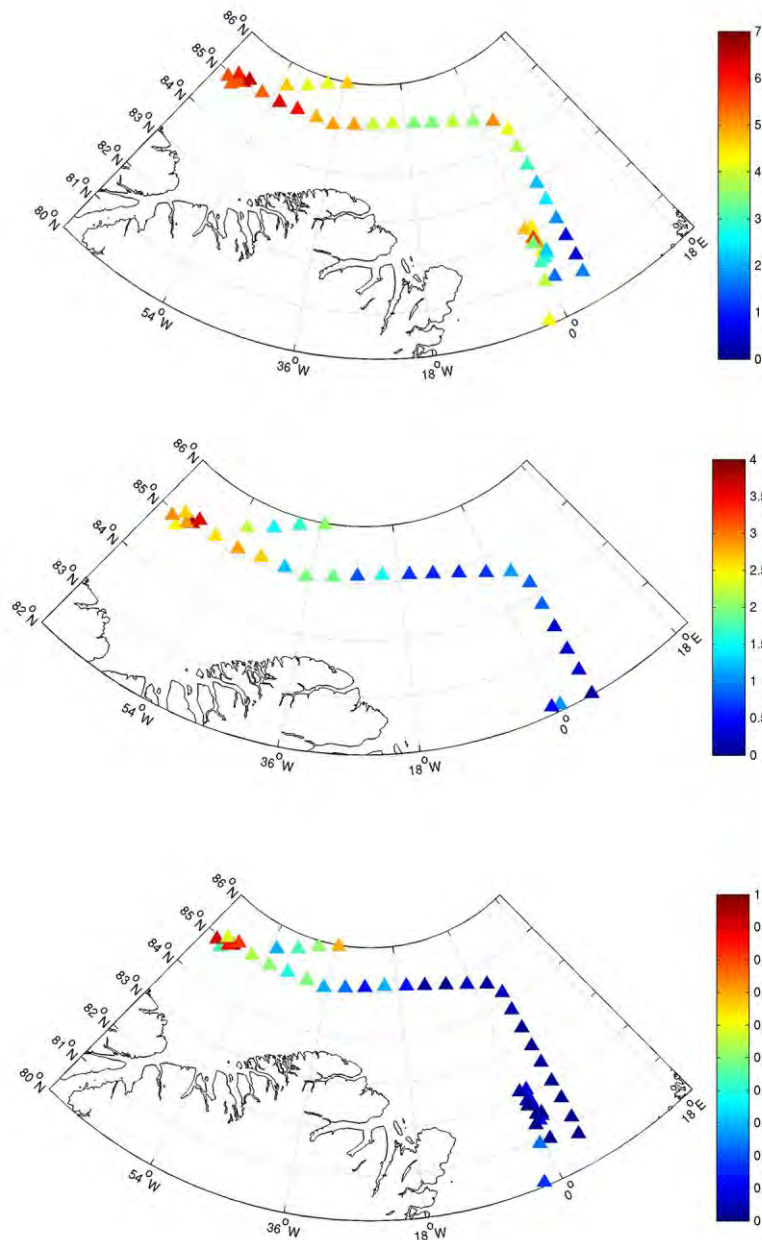


Figure 5-20. Mean number of ridges per km for each section of the 2004 in Northeast Greenland and North Greenland. Top for 5m keels, middle for 9m keels and bottom for 15m keels.

The histogram in Figure 5-21 represents the observed ridge spacing distribution for keels deeper than 9m in bins of 25m (in violet), and its best lognormal fit (in yellow). The reader thinks, correctly, that the agreement is far from convincing, and yet the author has tried hard. He experimented with several bin sizes, several thresholds for the keel draft, and several values of  $\mu$  and  $\sigma$  but couldn't get anything much better than shown. The same occurred for other segments of the track.

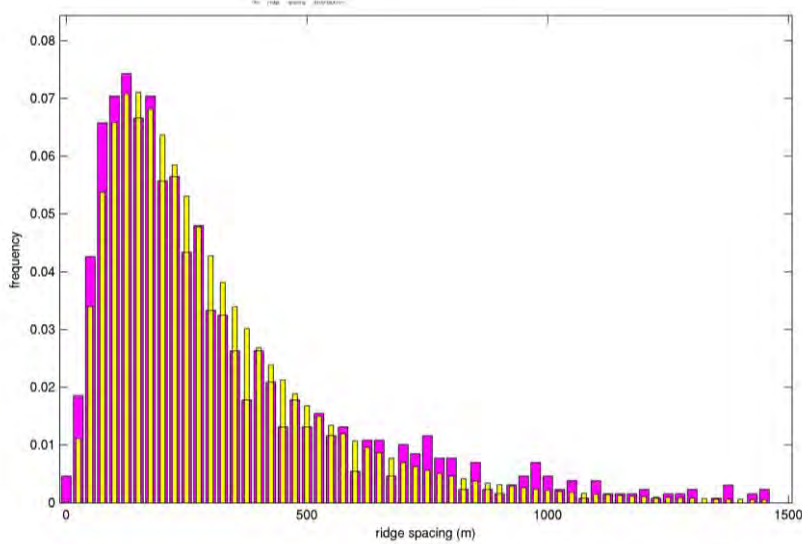


Figure 5-21. Ridge spacing distribution for keels deeper than 9m in North Greenland (sections 44-57). In violet the observed values, in yellow the best lognormal fit, both normalized to unity.

On the other hand, the Poisson fit to the distribution of the frequency of deep keels is remarkably good throughout the whole transect. Perhaps there is nothing special about it. If the deep ridges are randomly and independently distributed and we counted them correctly, they had to satisfy, automatically, a Poisson distribution. Figure 5-22 shows an example for the segment designated by North Greenland II. It contained 89 deep ridges in 179km of valid data. The Poisson fit with  $\mu=0.50$  is very reasonable.

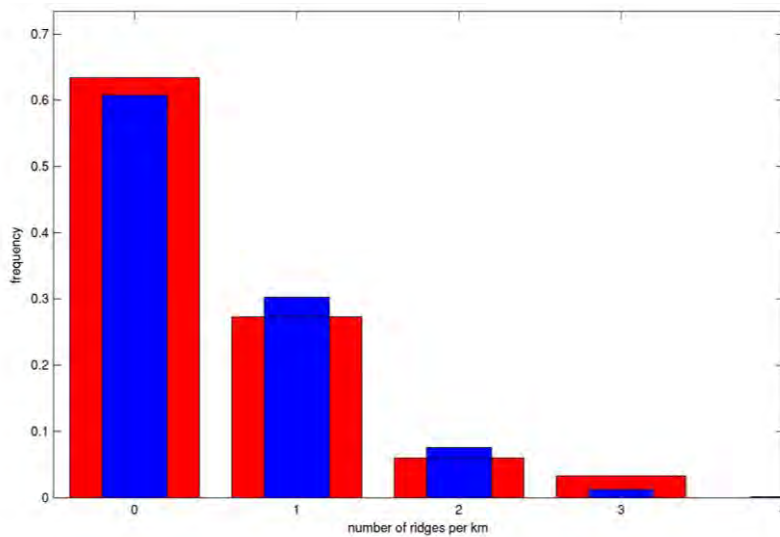


Figure 5-22. Distribution of the number of ridges deeper than 15m per km in North Greenland II (sections 59-62). In red the observed values, in blue the Poisson fit, both normalized to unity.

### 5.4.3 The GreenICE Survey

The track of the GreenICE Survey can be found in Section 5.1. From the 247km of ice draft records, we used 231km (93.5%) for our statistical analysis and rejected the rest because of its low quality. The mean (not corrected for beamwidth effects), modal and maximum ice drafts were 5.77m, 2.75m and 31.97m, respectively. After removing the bias due to the beamwidth, the mean draft decreases by about 40cm for a 3° beam and by about 85cm for a 6° beam. We note that the beamwidth corrections tend to be smaller in these sections than in the rest of the cruise because of the lower depth of the submarine.

The GreenICE Survey took place in one the areas of the Arctic Ocean with the thickest ice cover. It includes the four sections with highest mean draft of the whole voyage, the two sections with the highest frequency of keels deeper than 5m and the four sections with the highest frequency of keels deeper than 9m. It is here that we found the highest number of deep keels (draft above 15m) and the deepest keel of the whole journey (almost 32m deep). The modal draft of around 3m is characteristic of undeformed multi-year ice.

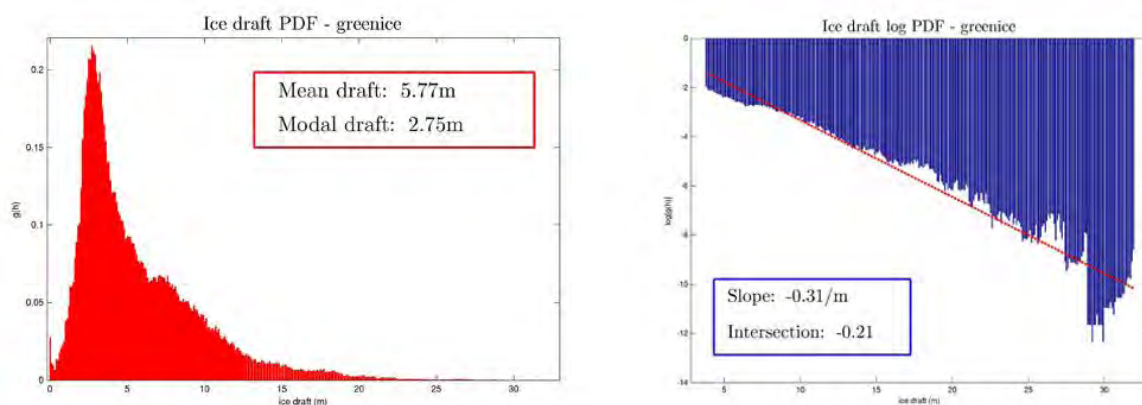


Table 5-15. Ice draft histograms for the GreenICE Survey in linear (L) and semi-logarithmic (R) scales.

### 5.4.4 North Pole

Unfortunately, the quality of the records for the region of the North Pole (in our case points within 15 nautical miles of the Pole), is not good. Out of the 100km or so collected, we selected 51km of reasonable data but still there is a low level of confidence in the results obtained. For this reason, beamwidth corrections were considered unnecessary.

The mean ice draft of just over 4m looks unrealistically high, certainly much higher than the estimates based on satellite altimetry. This appears to be the result of a large amount of deformed ice, as shown by the histograms below. On the contrary, the modal draft of 1.65m is quite sensible for the end of the winter.

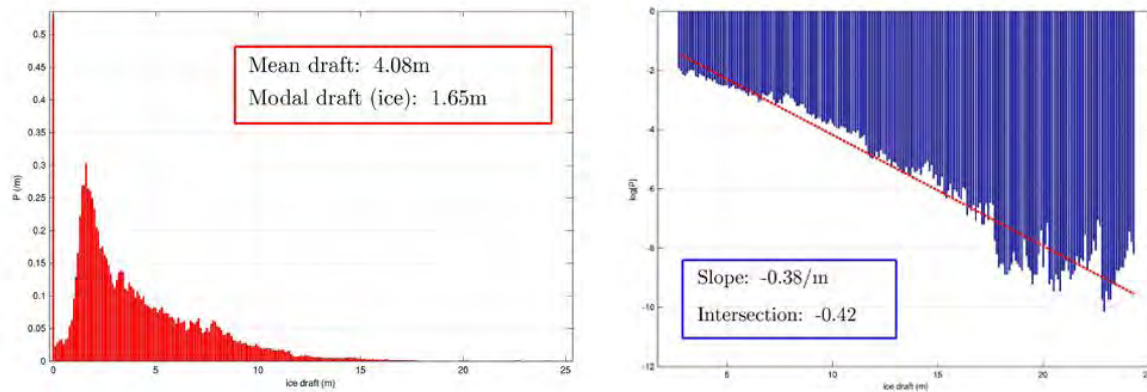


Figure 5-23. Ice draft histograms for the North Pole in linear (L) and semi-logarithmic (R) scales.

### 5.5 AP2077 results

Table 5-16 and Table 5-17 show the results of the draft measurements with the AP2077 sonar and a comparison with the corresponding measurements made with AP780. Overall, the draft obtained with AP780 are 14% higher than those obtained with AP2077. One is tempted to attribute that difference to the beamwidth but that is really not possible because the differences between the measurements of the two sensors are sometimes positive and sometimes negative.

Sec.	Start time				Centroid		Draft			$\alpha$	% Valid data	780 vs 2077	
	d	h	m	s	Lat	Lon	Mean	Max	Mode			D(780)-D(2077)	$\Delta D/D(2077)$
1	1	0	0	38	80°55'	00°47'E	2.26	27.73	1.15	1.83	81.2	0.04	1.7
2	1	3	46	20	81°23'	00°40'E	2.74	28.85	2.05	1.93	96.5	-0.08	-2.8
3	1	10	0	6	81°50'	00°40'E	3.97	15.64	2.25	2.04	100	-0.94	-23.6
4	1	14	38	19	82°07'	00°44'E	3.15	16.93	1.55	2.14	100	-0.04	-1.1
5	1	22	4	41	81°44'	00°37'E	2.71	22.47	1.35	2.17	96.2	0.37	13.9
6	2	4	50	6	81°31'	00°35'E	3.50	20.29	0.15	2.81	96.1	-0.77	-22.0
7	2	11	18	23	81°46'	00°25'E	4.12	19.13	2.65	2.56	93.1	-1.23	-29.9
8	2	15	59	41	82°08'	00°22'W	3.20	27.65	1.65	2.38	95.2	0.07	2.0
9	2	21	24	42	81°53'	00°05'E	2.77	30.87	1.05	2.24	88.9	0.10	3.8
10	3	3	28	35	81°27'	01°10'E	1.70	15.08	0.25	1.96	73.9	0.86	50.6
11	3	8	49	23	81°31'	01°18'E	2.13	14.69	0.65	2.04	92.6	0.41	19.1
12	3	14	19	55	81°52'	00°17'E	3.62	27.40	1.65	2.31	96.9	-0.10	-2.6
13	3	19	32	59	81°46'	00°05'W	2.49	36.17	1.15	3.70	94.9	0.59	23.7
14	3	21	46	3	81°19'	00°12'W	1.74	26.33	0.75	2.49	83.4	2.04	117.8
15	4	0	14	5	80°55'	00°47'W	2.74	28.02	1.35	3.69	80.4	1.35	49.2
16					80°29'	01°53'W	2.91	33.18	1.85	4.86	88.6	---	---
17	4	6	11	15	80°05'	02°14'W	3.40	35.51	0	3.22	97.3	0.43	12.8

18	4	9	6	58	79°47'	00°46'W	1.84	28.35	1.35	1.69	87.7	0.50	27.3
20					79°11'	02°51'E	1.37	30.97	0.15	7.80	88.8	---	---
21					78°51'	04°18'E	0.90	35.45	0.15	9.47	89.6	---	---
22					78°23'	04°24'E	0.44	25.89	0.25	-5.94	94.5	---	---
23					78°11'	04°01'E	0.93	27.15	0.15	0.62	54.4	---	---
24					78°31'	04°12'E	0.88	9.46	1.05	0.14	100	---	---
26					79°16'	03°19'E	0.58	8.83	0.15	1.25	92.7	---	---
27					79°37'	01°49'E	0.75	26.80	0.15	4.75	95.8	---	---
28					79°52'	03°00'E	0.46	5.48	0.15	0.68	73.3	---	---
29					80°14'	04°07'E	0.38	14.80	0	0.63	75.2	---	---
30	6	11	3	41	80°43'	04°35'E	1.37	9.81	0.85	1.36	94.6	0.69	50.8
31	6	15	49	9	81°07'	04°53'E	2.43	35.55	0.85	4.93	98.4	-0.72	-29.7
32	6	19	27	29	81°35'	04°59'E	1.90	16.86	1.15	1.78	97.9	-0.17	-8.9
33	7	0	17	8	82°01'	04°58'E	2.40	10.81	0.85	1.94	20.9	-0.31	-12.8
34	7	4	53	14	82°29'	05°00'E	3.48	19.08	2.05	2.11	71.9	-1.11	-31.9
35	7	10	21	12	82°55'	05°02'E	3.19	17.79	2.05	1.84	99.7	-0.82	-25.6
36	7	15	6	21	83°22'	05°05'E	2.33	17.25	1.35	2.11	97.3	0.40	17.4
37	7	19	24	19	83°49'	05°08'E	3.04	21.90	1.85	2.65	100	0.01	0.5

Table 5-16. Ice draft statistics in the 2004 cruise from AP2077 records for sections 1-37. Draft, coefficient  $\alpha$  and  $\Delta D$  in metres.  $\Delta D/D(2077)$  as a percentage.

Sec.	Start time				Centroid		Draft			$\alpha$	% Valid data	780 vs 2077	
	d	h	m	s	Lat	Lon	Mean	Max	Mode			D(780)- D(2077)	$\Delta D/D(2077)$
38	8	1	15	23	84°14'	05°10'E	3.21	19.22	1.45	2.64	100	0.25	7.8
39	8	5	33	48	84°34'	03°10'E	3.69	26.10	1.95	2.54	97.0	0.02	0.6
40	8	9	29	33	84°45'	01°07'W	3.17	21.20	1.95	2.22	92.0	-0.14	-4.4
41	8	13	41	12	84°55'	06°02'W	3.30	16.60	2.15	2.07	90.8	-0.43	-13.0
42	8	17	15	38	85°02'	11°05'W	2.80	19.59	1.45	2.58	100	0.36	12.8
43	8	21	53	43	85°06'	15°45'W	2.25	25.96	0.95	2.08	96.1	1.24	54.9
44	9	2	58	33	85°08'	21°20'W	3.00	21.15	1.85	2.77	100	0.78	25.9
45	9	7	56	31	85°08'	26°26'W	3.03	27.17	1.85	3.05	97.4	0.40	13.1
46	9	12	55	32	85°05'	31°28'W	3.93	27.56	2.05	3.43	100	0.68	17.3
47	9	17	31	7	85°01'	36°51'W	3.61	21.42	2.15	2.89	92.0	0.51	14.1
48	9	22	9	46	85°05'	41°29'W	2.82	22.34	1.65	3.13	99.9	1.43	50.8
49	10	2	54	26	85°07'	46°45'W	4.28	25.83	2.35	3.52	86.0	0.85	19.8
50	10	7	34	27	85°05'	51°50'W	5.00	31.48	2.45	3.48	100	0.46	9.2
51	10	12	45	4	85°05'	57°03'W	5.62	27.11	2.85	3.81	100	-0.08	-1.4
52	10	17	28	14	85°02'	62°23'W	6.60	24.22	2.85	3.73	100	0.10	1.6
53	10	22	26	34	84°50'	64°44'W	5.15	29.09	2.95	3.12	100	0.23	4.5
54	11	2	2	10	84°56'	66°31'W	5.90	28.22	2.95	4.06	100	0.06	1.0
55	11	5	35	12	84°59'	63°25'W	6.00	28.47	3.05	3.82	96.3	0.23	3.9
56	11	9	9	7	85°07'	64°44'W	5.78	32.26	2.95	4.13	100	-0.66	-11.4
57	11	13	16	43	85°10'	61°33'W	6.52	25.66	2.95	3.43	100	-0.91	-14.0
58					85°20'	56°35'W	5.65	31.17	2.75	4.18	100	---	---
59	11	20	20	37	85°29'	52°02'W	3.95	26.43	1.75	3.57	97.7	0.43	10.9
60	12	0	56	23	85°41'	46°30'W	2.66	28.05	1.45	5.12	97.8	2.25	84.8
61	12	3	34	50	85°52'	40°56'W	2.08	31.57	0.95	4.15	98.7	2.86	137.5

<b>62</b>	12	6	10	58	85°58'	34°54'W	3.29	37.39	1.05	7.25	97.1	1.58	48.2
<b>63</b>					86°00'	28°35'W	2.18	25.39	1.25	2.49	57.0	---	---
<b>67</b>					85°36'	04°59'W	2.79	17.65	1.35	2.01	21.6	---	---
<b>70</b>					85°34'	04°48'E	3.69	16.17	2.15	3.09	17.4	---	---
<b>71</b>					85°37'	04°02'E	3.90	17.96	2.25	3.27	38.8	---	---
<b>72</b>					85°25'	02°58'E	2.21	14.41	1.65	2.11	18.6	---	---
<b>74</b>					85°31'	00°02'E	3.86	35.66	1.65	2.86	29.2	---	---
<b>75</b>					85°26'	00°57'W	4.21	28.05	2.05	3.37	25.2	---	---
<b>78</b>					85°31'	00°35'E	3.42	16.88	1.85	2.22	26.0	---	---
<b>79</b>					85°31'	00°50'E	4.19	19.78	1.75	3.37	8.4	---	---
<b>83</b>					85°38'	00°22'E	2.43	7.74	1.65	3.18	3.7	---	---
<b>101</b>	18	14	37	2	89°56'	149°36'W	4.12	24.59	2.15	3.63	59.8	-0.03	-0.6
<b>102</b>	18	21	5	37	89°58'	142°07'W	3.05	17.30	1.75	2.91	45.2	1.74	57.3

Table 5-17. Ice draft statistics in the 2004 cruise from AP2077 records for sections 38-102. Draft, coefficient  $\alpha$  and  $\Delta D$  in metres.  $\Delta D/D(2077)$  as a percentage.

## 6 The 2007 *Tireless* Cruise

### 6.1 Description of the cruise – the outbound journey

HMS *Tireless* returned to the Arctic in March 2007. Scientists Peter Wadhams, of the University of Cambridge, and Nick Hughes, then at the Scottish Association for Marine Science, were on board during the full outbound journey, whose track is shown in Figure 6-1. The track of the homebound journey was almost coincident.

A considerable amount of ice draft data was collected in both the outbound and the homebound parts of the cruise with an Admiralty Pattern 780 system identical to the one used three years earlier. The sonar equipment also included an Admiralty Pattern 2077 system but its upward-looking component malfunctioned throughout most of the voyage and the collected ice draft data were judged to have too low quality. In addition, a Kongsberg EM3002 multibeam sonar was installed in a sonar dome on the submarine's bow. It was the first time that a multibeam sonar was fitted to a submarine, and from it came the first three-dimensional images of the underside of the ice in the central Arctic Ocean. At the time of writing, processing of multibeam data is still ongoing and will not be considered in this report.

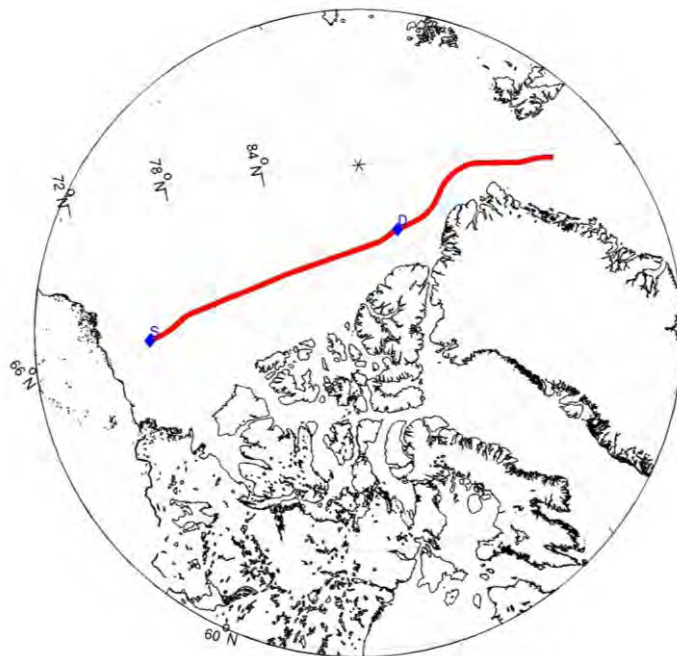


Figure 6-1. Track of the outgoing part of the March 2007 cruise.

We start counting time and along-track distance at 15:20:39 on 10 March 2007 which, according to the log books and the annotations on paper roll number 1, roll section 41, was when ice was detected for the first time. The boat was then at position (77°48'N, 2°45'W), which also marks the start of section 1. However, this section was almost entirely in the marginal ice zone, as we can see in the detailed track of the boat in Fram Strait depicted in Figure 6-2. The quality of the records for this section was not satisfactory and it was decided to ignore it for the statistics.

Once under the ice-pack the *Tireless* followed a S-N path roughly along the 4°W meridian until approximately 83°15'N when it started turning W to go round NE Greenland. The boat crossed the 78°N parallel at 16:13:59 on the 10 March, longitude 2°32'W; then the 80°N parallel at 00:25:22 on 11 March, longitude 4°00'W; then the 82°N parallel at 08:34:56, longitude 4°04'W; then the 83°N parallel at 12:36:56, longitude 4°07'W; then the 84°N parallel later on that day but it is not possible to say exactly when or where because there is a gap in the navigation files. The colours of the track in Figure 6-2 represent the three regions (south, central and north) of Fram Strait as defined in Table 6-2.

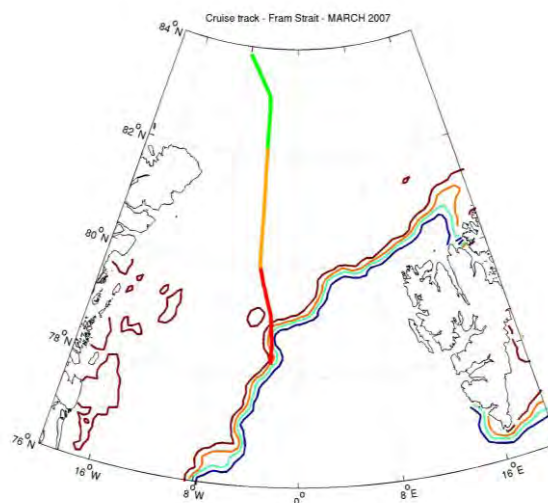


Figure 6-2. Track of the submarine in Fram Strait during the outwards part of the 2007 cruise.

From approximately 03:00 on 12 March, when it was at position (84°41'N, 21°00'W), the boat headed approximately W (sometimes WNW) and it crossed the 85°N parallel at 13:45:44 on the same day, at longitude 48°13'W. It then continued with the same heading for a few more hours.

The DAMOCLES Survey, so named because its location roughly coincided with that of an ice camp erected at the same time of the voyage by the DAMOCLES Consortium, and whose 203km track is shown in Figure 6-3, started on 12 March at 20:36:27, position (85°20'N, 63°30'W), roll/roll section/pixel=13/20/759, and ended on 13 March at 11:44:18, position (85°21'N, 65°01'W), roll/roll section/pixel=12/36/720. The centroid of the survey, marked with the letter *D* in Figure 6-1, had coordinates (85°20'N, 64°08'W). The E-W lines were spaced by 100m. There is a certain ambiguity concerning the depth of the submarine during the survey. The handwritten notes in the paper rolls suggest that the average depth was around 120m while navigation files provided with multibeam

data indicate that the boat was more often than not between 60 and 80m. In any case, the average depth was certainly lower than the average depth of the voyage (see Table 6-7 and Table 6-8). The survey includes the final part of section 27, sections 28, 29, 30 in full and the initial part of section 31. It involves AP780 paper rolls 13 (roll sections 20-32), 14 (roll sections 3-12) and 12 (roll sections 2-36). Note that, unfortunately, the rolls are not chronologically numbered.



Figure 6-3. Track of the DAMOCLES Survey on 12-13 March 2007.

Shortly after the end of the DAMOCLES Survey, when the boat was still cruising westwards a few miles N of 85°N, the sonars stopped recording data, which explains why there is nothing to show for sections 33 and 34. They restarted a few hours later and there is data available for most of section 35. The quality of the data deteriorated in section 36, and in section 37 no data could be used. At 19:07:03 on 13 March the *Tireless* crossed the 85°N parallel at longitude 85°42'W. It then headed SW towards the Beaufort Sea, passing the 80°N parallel at longitude 135°56'W at 04:51:21 on 15 March. We processed data until the end of section 64, position (75°07'N, 144°30'W), at the N edge of the Beaufort Sea, reached at 04:30:59 on 16 March.

The outbound part of the cruise ended at the site of the SEDNA (Sea ice Experiment: Dynamic Nature of the Arctic) ice camp, position (73°07'N, 145°44'W), marked with the letter S in Figure 6-1. The so-called SEDNA Survey took place in the waters surrounding this ice camp between 00:06:59 and 17:31:00 on 18 March. The submarine followed the gridded track shown in Figure 6-4 and collected 241km of ice draft data of which 204km (84.5%) were considered of good quality to generate statistics. The AP780 rolls used were numbers 28 (roll sections 7-56), 31 (roll sections 03-25), 32 (roll sections 03-19), 34 (roll sections 01-15) and 35 (roll sections 02-13).

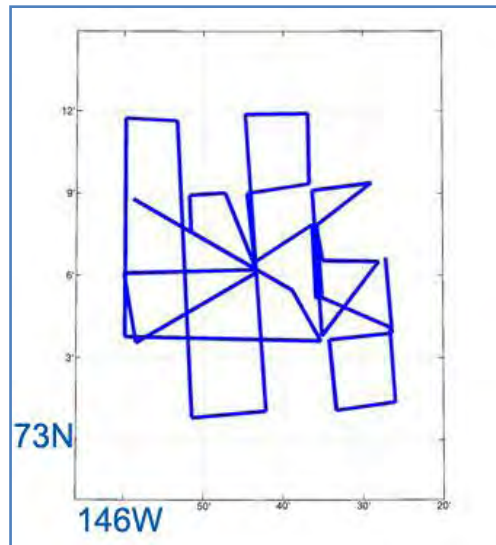


Figure 6-4. Track of the SEDNA Survey on 18 March 2007.

Table 6-1 shows the start and end times of each of the eight regions into which we divided the outbound journey of the *Tireless*, the numbers of the 50km-long sections that form each region and the corresponding portions of the AP780 rolls in the form roll/roll section/pixel. In Table 6-2 we have the exact boundaries of these regions, the length of the track with valid data and the percentage of valid data in each of them.

Region	Start time	End Time	Sections	AP780 Rolls
South Fram Strait	10 Mar 17:09	11 Mar 00:24	02-05	01/45/1459 – 03/02/1322
Central Fram Strait	11 Mar 00:24	11 Mar 09:12	06-10	03/02/1323 – 04/16/1349
North Fram Strait	11 Mar 09:12	11 Mar 16:03	11-14	04/16/1350 – 05/30/3117
Northeast Greenland	11 Mar 16:03	12 Mar 03:16	15-18	05/30/3118 – 09/16/0499
North Greenland	12 Mar 03:16	13 Mar 14:07	19-32	09/16/0500 – 15/10/1124
North Ellesmere Island	13 Mar 17:34	13 Mar 21:26	35-36	15/22/2115 – 17/06/3221
Canadian Basin	13 Mar 23:01	15 Mar 04:28	38-52	17/18/0424 – 22/19/2881
Beaufort Sea	15 Mar 04:28	16 Mar 04:31	53-64	22/19/2882 – 27/07/3016

Table 6-1. Regions covered by the outgoing part of the 2007 cruise, their start and end times, sections involved, and AP780 rolls used.

Region	Lat. (N) limits	Lon. (W) limits	Length	% Valid data
South Fram Strait	78°15' – 80°00'	02°27' – 03°59'	97	48.5
Central Fram Strait	80°00' – 82°11'	03°59' – 04°05'	239	95.6
North Fram Strait	82°11' – 83°51'	04°04' – 07°54'	175	87.7
Northeast Greenland	83°51' – 84°42'	07°36' – 21°43'	152	75.7
North Greenland	84°42' – 85°23'	21°48' – 71°23'	516	73.7
North Ellesmere Island	84°52' – 85°02'	81°39' – 91°35'	48	47.8
Canadian Basin	80°06' – 84°44'	96°22' – 135°37'	439	58.5

<b>Beaufort Sea</b>	75°07' – 80°05'	135°38' – 144°41'	426	71.0
---------------------	-----------------	-------------------	-----	------

Table 6-2. Regions covered by outbound part of the 2007 cruise, their boundaries, length of track with valid data (in km), and percentage of valid data.

We considered three regions in Fram Strait, corresponding to latitudes 78-80°N, 80-82°N, and 82-84°N. From the N entrance of Fram Strait and longitude 65°W the boat followed a track similar to the one three years before. The region designated by North Greenland was cruised at about 85°N and, by convention, it began at approximately 22°W, and finished at about 71.5°W. It comprises 14 sections, of which about four formed the DAMOCLES Survey. After this the boat proceeded westwards and sections 35 and 36, together with less than 50km of valid data, were located north of Ellesmere Island.

## 6.2 Description of the cruise – the homebound journey

As mentioned earlier, the track of the *Tireless* on its way home coincided almost exactly with that of the outgoing part of the journey. Only this time there were no surveys. Due to a grave accident that occurred at the site of the SEDNA camp the boat returned home faster and deeper than it did on its way to the N coast of Alaska. Contrary to what has been suggested, the data collected during the return journey are of superior quality than the data obtained during the outgoing journey, in spite of the absence of scientists on board.

We start counting the time at 16:08:50 on 22 March, position (73°15'N, 145°46'W), just after the boat left the site of the SEDNA camp and stopped the analysis when the boat left the ice in S Fram Strait at 11:17:25 on 27 March, position (76°13'N, 4°04'W). Between those two points the transect was divided into 67 sections, and there are valid data for each of them. The boat reached its northernmost point (85°15'N, 75°01'W) at 04:50 on 25 March. It then crossed the 84°N parallel at 04:07 on 26 March, longitude 10°01'W; the 82°N parallel at 13:39 on the same day, longitude 4°07'N; the 80°N parallel at 21:14 later on that day, longitude 3°56'W; and the 78°N parallel at 05:15 on the following day, longitude 3°19'W.

Even the track in fram strait appears to be similar to the outbound journey, with the boat going south at approximately 4°W at least until it crossed the 80°N parallel. It then diverted a bit to the E, having some stretches at 3°W, only to return to 4°W at about 77°N.

While for the outgoing journey we were provided by the Navy with very detailed navigation data, with positions every 10 seconds, for the return leg we only have access to positions every half an hour. Thus, the start and end times of the sections and those of the crossings of the parallels just mentioned are only approximate.

We tried to define nine regions as similar as possible to the ones of the outbound journey. However, the last region, which is the part of Fram Strait S of 78°N, has no counterpart in the outbound journey. Table 6-3 and Table 6-4 describe the start and end times of these regions, sections involved, AP780 rolls used, boundaries, length and percentage of valid data.

Region	Start time	End Time	Sections	AP780 Rolls
Beaufort Sea	22 Mar 16:09	23 Mar 20:57	01-17	42/46/0271 – 43/19/3359
Canadian Basin	23 Mar 20:57	24 Mar 23:01	18-32	43/19/3360 – 46/10/0090
North Ellesmere Island	24 Mar 23:01	25 Mar 05:43	33-36	46/10/0091 – 46/34/0712
North Greenland	25 Mar 05:43	25 Mar 23:16	37-46	46/34/0713 – 49/19/0525
Northeast Greenland	25 Mar 23:16	26 Mar 05:52	47-50	49/19/0526 – 49/42/3309
North Fram Strait	26 Mar 05:52	26 Mar 13:42	51-54	49/42/3310 – 48/21/0377
Central Fram Strait	26 Mar 13:42	26 Mar 22:03	55-59	48/21/0378 – 50/17/0217
South Fram Strait I	26 Mar 22:03	27 Mar 05:15	60-63	50/17/0218 – 49/64/0988
South Fram Strait II	27 Mar 05:15	27 Mar 11:17	64-67	49/64/0989 – 51/20/0502

Table 6-3. Regions covered by the homebound part of the 2007 cruise, their start and end times, sections involved, and AP780 rolls used.

Region	Lat. (N) limits	Lon. (W) limits	Length	% Valid data
Beaufort Sea	73°15' – 80°22'	134°51' – 145°46'	778	91.6
Canadian Basin	80°29' – 84°57'	93°17' – 134°26'	695	92.7
North Ellesmere Island	85°00' – 85°14'	73°16' – 91°47'	191	95.3
North Greenland	84°41' – 85°13'	22°43' – 71°35'	381	76.2
Northeast Greenland	83°41' – 84°40'	07°39' – 21°12'	191	95.7
North Fram Strait	81°59' – 83°35'	03°56' – 06°53'	128	63.8
Central Fram Strait	79°48' – 81°51'	03°43' – 04°03'	226	90.5
South Fram Strait I	77°59' – 79°42'	02°40' – 03°35'	165	82.4
South Fram Strait II	76°14' – 77°52'	03°27' – 04°04'	168	83.8

Table 6-4. Regions covered by homebound part of the 2007 cruise, their boundaries, length of track with valid data (in km), and percentage of valid data.

### 6.3 Ice draft distribution: general results – outbound journey

The presentation of the results follows the procedure described in Section 5.2 for the 2004 cruise.

Table 6-5 and Table 6-6 show the basic statistics for each section of the cruise with valid data as well as their starting times, centroids and percentages of valid data. The mean, maximum and modal drafts shown were the observed ones (not beamwidth corrected).

Section	Start time				Centroid		Draft			$\alpha$	% valid data
	d	h	m	s	Lat (N)	Lon (W)	Mean	Max	Mode		
2	10	17	9	16	78°28'	02°28'	2.66	11.82	1.85	1.43	43.0
3	10	18	45	31	78°55'	02°34'	2.30	11.80	1.75	1.43	27.9
4	10	20	19	15	79°21'	03°00'	1.92	18.85	0.35	2.18	62.7

5	10	21	57	2	79°44'	03°34'	3.05	15.05	1.35*	2.74	60.4
6	11	0	24	22	80°12'	04°01'	4.34	22.12	1.65*	2.52	88.3
7	11	2	12	49	80°37'	04°02'	3.55	17.86	1.95*	2.88	100
8	11	3	50	33	81°04'	04°01'	3.74	20.84	1.65	2.50	92.3
9	11	6	0	48	81°31'	04°03'	3.58	20.93	1.95*	3.04	98.4
10	11	7	36	37	81°58'	04°04'	4.72	20.39	1.95*	2.79	98.9
11	11	9	12	52	82°24'	04°07'	3.76	22.28	1.85	2.23	91.8
12	11	10	49	37	82°49'	04°06'	3.31	15.69	1.75	2.35	59.0
13	11	12	52	15	83°18'	05°02'	3.62	17.51	1.65	2.01	100
14	11	14	29	17	83°40'	06°52'	3.36	17.87	1.55	2.53	100
15	11	16	3	24	83°58'	08°23'	3.35	18.05	1.55	2.14	36.3
16	11	20	18	52	84°17'	11°42'	3.22	25.84	1.45	3.03	92.6
17	11	22	19	16	84°29'	14°50'	2.72	14.91	1.15	2.49	76.3
18	12	1	40	50	84°40'	19°23'	4.10	21.06	1.65	2.76	97.8
19	12	3	15	38	84°43'	24°08'	4.21	21.70	1.45*	3.19	89.7
20	12	4	51	39	84°45'	28°59'	4.12	20.28	1.65*	2.66	99.4
21	12	6	25	27	84°44'	33°26'	4.76	22.17	1.65	3.88	82.4
22	12	9	33	20	84°49'	38°35'	4.63	21.74	1.85*	3.15	90.2
23	12	11	9	27	84°53'	43°25'	4.85	21.42	1.55	2.82	37.4
24	12	13	2	1	85°01'	48°20'	5.19	22.69	1.05*	3.44	57.6
25	12	14	36	23	85°09'	53°08'	5.34	20.58	1.05	3.41	72.0
26	12	16	19	11	85°16'	58°26'	4.88	19.55	1.85*	3.32	98.3
27	12	17	52	39	85°20'	63°08'	5.89	20.92	1.25	2.93	38.9
28	12	21	35	5	85°20'	64°10'	6.75	23.98	4.35	3.61	60.0
29	13	1	12	16	85°20'	64°04'	6.52	29.52	2.05	4.00	99.1
30	13	4	44	23	85°21'	64°08'	6.38	24.78	2.25	3.85	91.3
31	13	9	5	46	85°21'	64°16'	6.60	27.89	2.25	3.85	73.4
32	13	12	3	56	85°19'	68°52'	5.88	17.57	5.25	2.08	36.4
35	13	17	34	28	85°01'	83°55'	6.57	21.34	6.25*	2.87	85.0
36	13	19	26	53	84°56'	88°52'	3.99	14.30	0.75	2.63	10.5

Table 6-5. Ice draft statistics for the outbound part of the 2007 cruise, sections 2-36 (Fram Strait, Northeast Greenland, North Greenland and North Ellesmere Island). Draft and coefficient  $\alpha$  in metres.

Section	Start time				Centroid		Draft			$\alpha$	% valid data
	d	h	m	s	Lat (N)	Lon (W)	Mean	Max	Mode		
38	13	23	1	0	84°41'	97°43'	4.87	20.21	1.85	2.31	28.4
39	14	0	36	45	84°26'	103°35'	5.09	26.20	2.05	2.61	76.1
40	14	2	59	24	84°16'	106°42'	5.62	19.89	2.25	3.01	90.7
41	14	5	13	22	84°01'	110°39'	5.67	20.89	2.35	3.04	92.8
42	14	6	46	50	83°45'	114°02'	4.85	17.25	1.55	2.63	58.3
44	14	9	55	13	83°11'	119°49'	6.64	25.76	2.15	5.05	18.3
45	14	11	52	50	82°51'	122°34'	5.33	21.47	2.65	2.98	34.6
46	14	13	28	13	82°32'	124°52'	4.43	22.29	2.25	3.05	47.2
47	14	15	27	36	82°11'	127°05'	4.70	27.72	1.15	4.15	66.0
48	14	17	2	13	81°50'	129°05'	4.99	29.89	1.65	3.21	85.3
49	14	18	44	12	81°27'	130°47'	4.63	28.42	2.15	3.30	94.3
50	14	20	18	32	81°05'	132°13'	4.47	19.69	2.05	3.10	64.8

51	14	23	41	50	80°42'	133°33'	3.73	19.04	2.95	3.02	30.3
52	15	2	52	20	80°17'	134°58'	3.80	22.95	2.05	2.90	90.6
53	15	4	28	10	79°54'	136°14'	4.09	24.00	1.85	3.15	97.2
54	15	6	3	23	79°30'	137°20'	4.00	21.46	1.65	2.91	81.7
55	15	7	38	8	79°06'	138°25'	3.28	15.67	1.35	2.19	19.1
56	15	9	12	1	78°40'	139°32'	4.49	23.12	1.55	3.50	72.7
57	15	11	31	44	78°17'	140°23'	4.05	23.28	1.65	2.65	100
58	15	13	6	16	77°52'	141°11'	2.98	20.56	1.55	2.26	81.6
59	15	14	40	32	77°25'	142°02'	3.36	16.83	1.15	3.13	81.9
60	15	16	59	9	77°02'	142°43'	3.11	32.44	1.55	3.31	100
61	15	19	0	0	76°38'	143°24'	2.80	14.87	1.05	2.01	100
62	15	21	4	53	76°14'	144°04'	2.23	11.60	1.35	2.57	41.0
63	15	23	6	15	75°46'	144°38'	1.58	9.60	1.05	2.67	35.8
64	16	0	46	17	75°24'	144°36'	1.99	13.42	0.55	2.15	41.4

Table 6-6. Ice draft statistics for the outbound part of the 2007 cruise, sections 38-64 (Canadian Basin and Beaufort Sea). Draft and coefficient  $\alpha$  in metres.

Figure 6-5 shows the mean ice draft of each section of the outgoing part of the cruise.

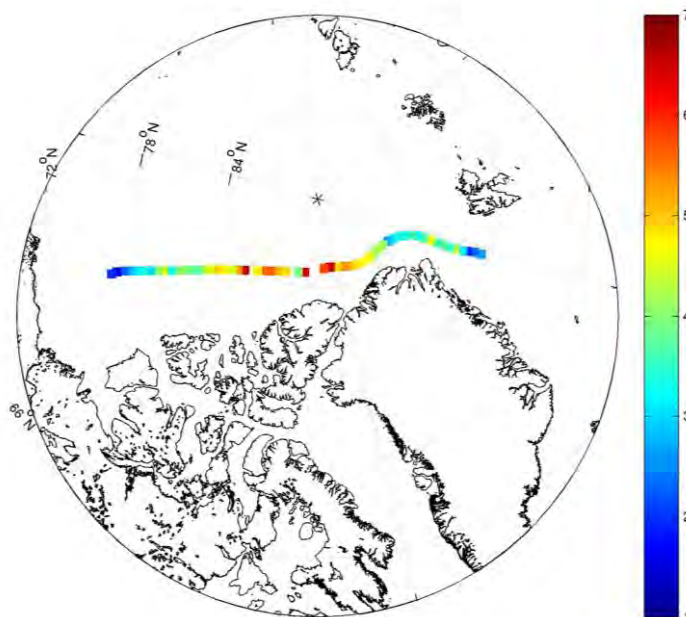


Figure 6-5. Mean ice draft (in metres) for each 50km section of the outbound part of the 2007 cruise.

Table 6-7 and Table 6-8 show the beamwidth corrections (for two possible values of the beamwidth) for sections where the data recorded in paper rolls have sufficient quality to render them relevant.

Section	Mean depth	Observed mean draft	$bw=3^\circ$			$bw=6^\circ$		
			$d_{real}$	$\Delta d$	$\Delta d/d_{real}$	$d_{real}$	$\Delta d$	$\Delta d/d_{real}$
2	150	2.66	---	---	---	---	---	---
3	---	2.30	---	---	---	---	---	---
4	150	1.92	---	---	---	---	---	---
5	---	3.05	---	---	---	---	---	---
6	150	4.34	3.65	0.70	19.2	2.88	1.46	50.7
7	150	3.55	3.00	0.54	18.0	2.41	1.14	47.3
8	147	3.74	3.01	0.73	24.3	2.21	1.53	69.2
9	150	3.58	3.14	0.44	14.0	2.66	0.91	34.2
10	150	4.72	4.17	0.55	13.2	3.57	1.15	32.2
11	150	3.76	3.28	0.47	14.3	2.76	0.99	35.9
12	150	3.31	2.92	0.39	13.4	2.49	0.82	32.9
13	150	3.62	3.05	0.57	18.7	2.43	1.19	49.0
14	150	3.36	2.85	0.50	17.5	2.30	1.05	45.7
15	96	3.35	3.00	0.35	11.7	2.60	0.75	28.8
16	150	3.22	2.64	0.58	22.0	2.01	1.21	60.2
17	147	2.72	2.21	0.51	23.1	1.64	1.08	65.9
18	150	4.10	3.65	0.45	12.3	3.16	0.95	30.1
19	150	4.21	3.72	0.48	12.9	3.20	1.01	31.6
20	150	4.12	3.62	0.50	13.8	3.08	1.04	33.8
21	141	4.76	4.24	0.52	12.3	3.67	1.08	29.4
22	150	4.63	4.11	0.52	12.7	3.55	1.08	30.4
23	150	4.85	4.26	0.59	13.9	3.62	1.23	34.0
24	150	5.19	4.49	0.70	15.6	3.73	1.46	39.1
25	150	5.34	4.73	0.62	13.1	4.05	1.30	32.1
26	150	4.88	4.22	0.66	15.6	3.50	1.38	39.4
27	---	5.89	---	---	---	---	---	---
28	120	6.75	6.31	0.43	6.8	5.82	0.93	16.0
29	120	6.52	6.05	0.47	7.8	5.52	1.00	18.1
30	115	6.38	5.93	0.44	7.4	5.42	0.95	17.5
31	120	6.60	6.11	0.50	8.2	5.54	1.07	19.3
32	---	5.88	---	---	---	---	---	---
35	150	6.57	6.19	0.39	6.3	5.76	0.81	14.1
36	---	3.99	---	---	---	---	---	---

Table 6-7. Beamwidth corrections for the outbound part of the 2007 cruise, sections 2-36. Drafts and depths in metres,  $\Delta d/d_{real}$  as a percentage.

Section	Mean depth	Observed mean draft	$bw=3^\circ$			$bw=6^\circ$		
			$d_{real}$	$\Delta d$	$\Delta d/d_{real}$	$d_{real}$	$\Delta d$	$\Delta d/d_{real}$
38	---	4.87	---	---	---	---	---	---
39	---	5.09	---	---	---	---	---	---
40	150	5.62	5.06	0.56	11.1	4.44	1.18	26.6

41	154	5.67	5.04	0.63	12.5	4.36	1.32	30.0
42	230	4.85	4.25	0.60	14.1	3.69	1.17	31.4
44	220	6.64	6.13	0.51	8.3	5.64	0.99	17.7
45	200	5.33	4.93	0.40	8.1	4.53	0.80	17.7
46	---	4.43	---	---	---	---	---	---
47	180	4.70	4.22	0.48	11.4	3.73	0.97	26.0
48	197	4.99	4.41	0.58	13.2	3.83	1.16	30.3
49	192	4.63	4.07	0.55	13.8	3.51	1.12	31.9
50	178	4.47	3.99	0.48	12.0	3.50	0.97	27.7
51	230	3.73	3.01	0.73	23.9	2.32	1.41	60.8
52	214	3.80	2.69	1.11	41.3	1.62	2.17	134.6
53	150	4.09	3.48	0.61	17.5	2.82	1.28	45.0
54	150	4.00	3.52	0.48	13.6	2.99	1.02	33.8
55	---	3.28	---	---	---	---	---	---
56	---	4.49	---	---	---	---	---	---
57	150	4.05	3.71	0.34	9.2	3.34	0.71	21.3
58	150	2.98	2.53	0.45	17.8	2.03	0.95	46.8
59	148	3.36	2.98	0.38	12.8	2.57	0.79	30.7
60	120	3.11	2.75	0.36	13.1	2.33	0.78	33.5
61	120	2.80	2.50	0.30	12.0	2.16	0.64	29.6
62	120	2.23	2.01	0.22	10.9	1.75	0.47	27.4
63	---	1.58	---	---	---	---	---	---
64	120	1.99	1.64	0.35	21.3	1.24	0.76	61.3

Table 6-8. Beamwidth corrections for the outbound part of the 2007 cruise, sections 38-64. Drafts and depths in metres,  $\Delta d/d_{real}$  as a percentage..

## 6.4 Ice draft distribution: general results - homebound journey

Table 6-9 and Table 6-10 show the basic statistics for each section of the homebound part of the 2007 cruise. We note that there is valid data in all sections of the transect, and in general high percentages of good quality data.

Section	Start time				Centroid		Draft			$\alpha$	% valid data
	d	h	m	s	Lat (N)	Lon (W)	Mean	Max	Mode		
1	22	16	8	50	73°26'	145°31'	3.12	23.02	1.25	2.50	100
2	22	17	44	4	73°55'	144°58'	2.13	20.69	0.55*	2.86	100
3	22	19	19	35	74°20'	144°41'	2.44	15.54	1.95*	2.11	80.7
4	22	20	54	32	74°47'	144°23'	3.41	25.72	2.55	3.72	81.9
5	22	22	51	14	75°12'	144°02'	2.55	15.17	1.65	1.66	100
6	23	0	25	4	75°37'	143°40'	2.74	14.92	1.65	2.29	100
7	23	1	58	47	76°02'	143°17'	2.70	13.30	1.85	1.92	97.9
8	23	3	33	2	76°31'	142°49'	3.04	19.67	1.65	2.40	82.5

9	23	5	33	34	76°55'	142°27'	2.41	12.09	0.45*	2.14	86.7
10	23	7	19	56	77°23'	141°59'	3.58	21.37	2.05	2.25	100
11	23	8	55	47	77°47'	141°17'	2.76	18.79	1.75	1.90	100
12	23	10	33	31	78°13'	140°24'	3.48	21.37	2.05	2.88	89.8
13	23	12	14	31	78°38'	139°31'	3.47	16.42	2.15	2.79	60.3
14	23	14	10	1	79°05'	138°29'	4.16	21.02	2.35	2.54	100
15	23	15	46	54	79°27'	137°32'	4.37	17.76	2.25	2.50	92.1
16	23	17	23	17	79°51'	136°26'	4.20	24.55	1.65	3.32	84.7
17	23	19	20	50	80°14'	135°14'	3.93	22.95	1.95	2.94	100
18	23	20	56	46	80°36'	134°01'	4.55	23.92	1.85	3.07	100
19	23	22	32	10	80°58'	132°41'	4.73	21.27	1.85	2.60	100
20	24	0	7	38	81°23'	130°58'	5.51	36.12	1.95	3.69	86.5
21	24	2	12	24	81°43'	129°21'	5.09	22.61	2.05	3.39	84.8
22	24	4	12	34	82°06'	127°19'	6.47	29.08	2.55	3.09	92.4
23	24	5	48	29	82°26'	125°21'	6.11	23.88	2.45	3.22	100
24	24	7	24	3	82°48'	122°52'	6.10	21.43	2.35	2.95	95.7
25	24	9	1	31	83°07'	120°27'	6.24	31.84	2.45	3.92	90.7
26	24	10	48	53	83°26'	117°33'	5.11	25.19	2.25	2.58	100
27	24	12	23	16	83°46'	114°23'	5.28	20.09	1.45	3.33	100
28	24	13	59	33	84°03'	111°04'	5.28	22.22	2.35	2.86	79.4
29	24	15	56	47	84°17'	107°36'	5.55	26.30	1.75	3.31	100
30	24	17	31	54	84°30'	103°50'	6.51	28.48	1.95	3.28	100
31	24	19	6	57	84°42'	99°51'	5.78	28.09	1.45	3.09	89.7
32	24	20	42	14	84°52'	95°29'	5.18	25.11	1.65	2.76	71.0

Table 6-9. Ice draft statistics for the homebound part of the 2007 cruise, sections 1-32 (Beaufort Sea and Canadian Basin). Draft and coefficient  $\alpha$  in metres.

Section	Start time				Centroid		Draft			$\alpha$	% valid data
	d	h	m	s	Lat (N)	Lon (W)	Mean	Max	Mode		
33	24	23	0	32	85°02'	90°16'	5.24	26.59	1.85	3.73	100
34	25	0	36	57	85°08'	85°28'	5.48	32.78	2.15	3.62	97.7
35	25	2	11	15	85°12'	80°13'	5.04	22.51	1.65	3.43	83.5
36	25	4	8	37	85°13'	74°59'	4.90	22.81	1.75	3.11	100
37	25	5	43	28	85°12'	69°54'	7.25	28.93	7.15	1.85	97.5
38	25	7	18	42	85°08'	64°07'	6.22	27.01	1.55	3.13	100
39	25	8	53	41	85°01'	58°45'	7.70	30.87	6.95	3.27	85.8
40	25	10	43	25	85°02'	54°31'	5.59	20.98	6.35	3.58	32.5
41	25	12	19	40	85°05'	48°58'	6.52	31.85	2.75	3.38	85.8
42	25	13	58	33	85°05'	43°22'	6.31	31.57	2.05	3.48	95.3
43	25	15	35	52	85°02'	38°41'	5.46	22.28	1.85	3.10	20.8
44	25	18	10	55	84°58'	33°48'	5.26	19.99	2.05	2.88	59.0
45	25	19	47	27	84°51'	28°26'	4.86	19.94	2.25	2.93	100
46	25	21	22	41	84°43'	23°48'	3.86	18.55	1.85	3.00	85.0
47	25	23	16	6	84°38'	19°43'	3.17	18.81	1.55	2.20	100
48	26	0	49	58	84°29'	15°17'	4.14	28.42	1.75	3.10	100
49	26	2	27	10	84°10'	11°52'	4.62	26.24	1.85	3.55	97.1
50	26	4	5	42	83°50'	8°55'	3.23	15.20	1.55	2.39	85.7

<b>51</b>	26	5	51	56	83°28'	6°05'	4.54	19.11	1.25	2.69	27.1
<b>52</b>	26	7	27	46	83°07'	4°28'	6.92	21.19	6.25	2.89	47.9
<b>53</b>	26	9	4	37	82°41'	4°03'	4.78	17.96	1.75	2.29	80.1
<b>54</b>	26	12	1	53	82°11'	4°09'	4.78	20.90	2.15	2.52	100
<b>55</b>	26	13	41	48	81°43'	3°59'	4.41	21.81	1.75	2.65	96.3
<b>56</b>	26	15	17	56	81°19'	3°57'	4.25	15.70	1.75	2.32	83.7
<b>57</b>	26	17	7	53	80°53'	3°57'	5.28	21.17	2.05	2.97	93.7
<b>58</b>	26	18	44	54	80°22'	4°01'	5.63	23.58	2.25	3.46	97.5
<b>59</b>	26	20	22	57	79°57'	3°53'	4.22	23.38	0.55*	3.06	81.1
<b>60</b>	26	22	2	37	79°34'	3°24'	3.76	19.16	0.35*	3.28	80.1
<b>61</b>	26	23	42	58	79°05'	2°48'	3.53	15.71	2.55	2.14	80.2
<b>62</b>	27	1	18	3	78°37'	2°49'	3.09	16.10	2.35	2.00	100
<b>63</b>	27	2	52	44	78°07'	3°13'	3.03	17.70	2.35	2.02	69.3
<b>64</b>	27	5	15	11	77°44'	3°33'	2.77	13.46	1.45	1.53	86.1
<b>65</b>	27	6	53	43	77°18'	3°54'	2.52	15.33	1.55	1.63	100
<b>66</b>	27	8	27	33	76°52'	4°02'	3.48	13.73	2.15	1.81	100
<b>67</b>	27	9	54	30	76°24'	4°04'	2.84	11.80	2.25	1.64	48.9

Table 6-10. : Ice draft statistics for the homebound part of the 2007 cruise, sections 33-67 (North Ellesmere Island, North Greenland, Northeast Greenland and Fram Strait). Draft and coefficient  $\alpha$  in metres.

Figure 6-6 shows the mean ice draft for each section of the homebound part of the journey. Note that the colour scheme is slightly different than that of Figure 6-5. In both cases the observed (uncorrected) draft is shown.

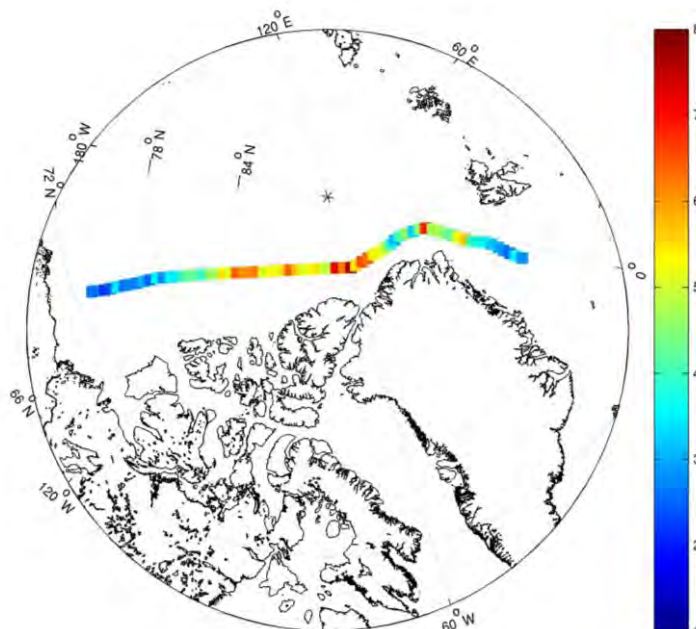


Figure 6-6. Mean ice draft (in metres) for each 50km section of the homebound part of the 2007 cruise.

At the time of writing no beamwidth corrections have been computed for the homebound journey.

## 6.5 Pressure ridge distribution: general results

The basic statistics for the distribution of pressure ridges in each section of the outbound and homebound journeys is presented in the form of tables. These contain information on the number of ridges found in each section, the number of ridges per km (also called ridge frequency or ridge density, which is the number of ridges divided by the length of the track with valid data inside the section), the mean draft of the keels, the number of spacings between consecutive ridges, and the average and modal value of the latter. As explained in Section 5.3, the number of spacings is, in general, different from the number of ridges minus one.

The following tables show these statistics for keels deeper than 5m, 9m, and 15m. For the computation of the mode of the ridge spacing we used a variety of sizes of bins, which seemed plausible after considering several possibilities. Bins of 20m for the stats of 5m keels, 100m for 9m keels, and 200m for 15m keels.

The counting of the ridges was done directly from the observed profiles. No beamwidth corrections were taken into account. As shown before, the actual number of ridges is likely to be slightly larger.

Section	Number of ridges	Ridge frequency	Mean draft	Ridge spacing		
				Number	Mean	Mode
2	48	2.23	6.69	47	447	50
3	20	1.43	7.33	18	297	30
4	85	2.71	7.38	82	333	10
5	141	4.67	7.81	135	178	70
6	266	6.02	8.31	264	156	90
7	221	4.42	8.02	220	225	70
8	260	5.63	7.86	256	178	70
9	175	3.56	8.67	173	275	110
10	234	4.73	8.84	232	208	90
11	191	4.16	8.05	189	239	90
12	103	3.49	7.36	101	285	170
13	237	4.74	7.67	236	211	90
14	191	3.82	7.56	190	261	70
15	97	5.35	7.94	88	160	70
16	184	3.97	8.08	182	247	150
17	166	4.35	7.57	159	217	50
18	227	4.64	8.38	226	216	70
19	236	4.95	8.51	232	192	110

20	256	5.15	8.91	254	192	70
21	218	5.29	9.50	213	178	90
22	272	6.03	8.67	270	165	70
23	107	5.72	9.24	105	174	90
24	200	6.95	9.28	198	137	70
25	197	5.47	9.23	194	181	150
26	252	5.13	9.29	250	195	110
27	123	6.32	9.57	120	158	110
28	177	5.90	10.78	175	171	90
29	338	6.82	10.25	336	146	90
30	321	7.03	10.30	316	142	70
31	253	6.89	10.89	252	145	110
32	70	3.84	9.58	69	264	150
35	195	4.59	10.70	194	218	130
36	20	3.79	8.89	19	235	150

Table 6-11. 5m keel spacing statistics for the outbound part of the 2007 cruise, sections 2-36. Ridge frequency in  $\text{km}^{-1}$ , mean draft, mean and modal spacings in metres.

Section	Number of ridges	Ridge frequency	Mean draft	Ridge spacing		
				Number	Mean	Mode
38	73	5.13	8.92	72	194	110
39	174	4.58	8.99	172	218	130
40	270	5.96	9.03	267	168	90
41	262	5.65	9.25	260	178	170
42	132	4.53	8.71	130	221	130
44	32	3.50	11.67	31	289	130
45	62	3.59	9.62	61	279	210
46	106	4.49	8.57	104	216	90
47	141	4.28	9.41	140	232	130
48	216	5.07	9.26	214	197	150
49	268	5.68	8.44	266	176	110
50	169	5.21	8.59	164	190	90
51	58	3.82	8.48	55	249	50
52	243	5.36	7.92	239	181	10
53	242	4.98	8.35	241	198	110
54	191	4.67	8.67	188	211	90
55	38	3.98	7.34	36	237	70
56	139	3.83	9.06	135	245	110
57	172	3.44	8.79	171	288	130
58	125	3.07	7.71	121	303	190
59	119	2.91	8.50	117	334	90
60	164	3.28	8.09	163	307	90
61	140	2.80	7.32	139	359	90
62	33	1.61	6.90	31	630	70

<b>63</b>	11	0.62	7.08	9	1399	110
<b>64</b>	43	2.08	7.51	42	478	30

Table 6-12. 5m keel spacing statistics for the outbound part of the 2007 cruise, sections 38-64. Ridge frequency in  $\text{km}^{-1}$ , mean draft, mean and modal spacings in metres.

Section	Number of ridges	Ridge frequency	Mean draft	Ridge spacing		
				Number	Mean	Mode
2	3	0.14	10.17	2	4718	---
3	2	0.14	10.55	1	2133	---
4	17	0.54	11.37	16	1353	150
5	41	1.36	11.15	35	546	150
6	84	1.90	11.93	82	494	150
7	60	1.20	11.82	59	811	150
8	69	1.49	11.87	66	597	150
9	68	1.38	11.65	66	669	250
10	87	1.76	12.13	85	557	150
11	45	0.98	11.79	43	939	250
12	16	0.54	11.83	14	1930	150
13	47	0.94	11.33	46	1057	150
14	34	0.68	11.93	33	1462	350
15	27	1.49	11.67	20	408	150
16	49	1.06	12.38	47	955	150
17	40	1.05	11.06	35	638	150
18	73	1.49	12.15	72	647	250
19	79	1.66	12.38	75	573	150
20	105	2.11	12.22	103	458	150
21	94	2.28	13.21	91	393	150
22	97	2.15	12.19	95	462	150
23	45	2.40	12.48	43	408	150
24	87	3.02	12.47	85	314	150
25	94	2.61	11.64	91	386	150
26	116	2.36	12.25	114	423	150
27	59	3.03	12.48	56	320	150
28	108	3.60	13.04	106	275	150
29	175	3.53	13.38	173	284	150
30	165	3.62	13.39	160	275	150
31	138	3.76	13.98	137	267	150
32	39	2.14	11.97	38	465	150
35	123	2.89	12.64	122	329	150
36	8	1.52	11.30	7	545	250

Table 6-13. 9m keel spacing statistics for the outbound part of the 2007 cruise, sections 2-36. Ridge frequency in  $\text{km}^{-1}$ , mean draft, mean and modal spacings in metres.

Section	Number of ridges	Ridge frequency	Mean draft	Ridge spacing		
				Number	Mean	Mode
38	28	1.97	11.75	27	483	150
39	73	1.92	12.02	71	512	150
40	106	2.34	12.12	103	384	150
41	113	2.44	12.17	111	405	250
42	47	1.61	11.64	45	615	150
44	23	2.51	13.68	22	407	150
45	29	1.68	12.46	28	608	550
46	33	1.40	12.19	31	631	150
47	60	1.82	12.74	59	550	150
48	91	2.13	12.80	89	439	150
49	84	1.78	12.39	82	540	150
50	55	1.70	12.58	50	523	50
51	20	1.32	12.43	17	731	350
52	64	1.41	11.90	60	608	250
53	74	1.52	12.39	73	650	150
54	71	1.74	12.39	69	528	150
55	6	0.63	10.84	4	955	---
56	52	1.43	13.02	49	555	250
57	61	1.22	12.43	60	765	250
58	30	0.74	11.30	26	1225	350
59	43	1.05	11.75	41	914	150
60	41	0.82	12.02	40	1241	150
61	25	0.50	10.96	24	1674	250
62	5	0.24	10.55	4	1437	---
63	2	0.11	9.49	1	11473	---
64	10	0.48	10.87	9	2010	50

Table 6-14. 9m keel spacing statistics for the outbound part of the 2007 cruise, sections 38-64. Ridge frequency in  $\text{km}^{-1}$ , mean draft, mean and modal spacings in metres

Section	Number of ridges	Ridge frequency	Mean draft	Ridge spacing		
				Number	Mean	Mode
2	0	0	---	0	---	---
3	0	0	---	0	---	---
4	1	0.03	18.55	0	---	---
5	1	0.03	15.05	0	---	---
6	10	0.23	16.47	8	3681	1500
7	10	0.20	16.35	9	4151	1100
8	9	0.19	17.13	7	4564	900
9	7	0.14	17.14	5	2247	300
10	14	0.28	16.94	13	2821	300
11	6	0.13	17.58	4	5093	---

12	1	0.03	15.69	0	---	---
13	4	0.08	16.58	3	6226	---
14	5	0.10	16.83	4	8147	---
15	1	0.06	18.05	0	---	---
16	8	0.17	18.68	7	2535	1700
17	0	0	---	0	---	---
18	8	0.16	17.66	7	6495	900
19	14	0.29	17.31	10	2166	100
20	15	0.30	16.78	13	3072	300
21	23	0.56	18.18	20	1467	100
22	15	0.33	17.91	13	2462	500
23	10	0.53	16.91	8	1517	500
24	12	0.42	18.69	10	921	100
25	8	0.22	17.19	5	5094	300
26	18	0.37	16.64	16	2079	1500
27	11	0.57	16.96	8	1464	1100
28	22	0.73	18.07	20	1071	500
29	46	0.93	18.63	44	1007	300
30	45	0.99	18.06	41	981	900
31	42	1.14	19.91	41	868	300
32	1	0.05	17.57	0	---	---
35	24	0.56	17.28	23	1552	
36	0	0	---	0	---	

Table 6-15. 15m keel spacing statistics for the outbound part of the 2007 cruise, sections 2-36. Ridge frequency in  $\text{km}^{-1}$ , mean draft, mean and modal spacings in metres.

Section	Number of ridges	Ridge frequency	Mean draft	Ridge spacing		
				Number	Mean	Mode
38	2	0.14	18.21	1	2550	---
39	8	0.21	18.27	6	2412	100
40	14	0.31	17.18	13	2061	2500
41	15	0.32	17.55	13	2525	300
42	6	0.21	15.86	5	3739	300
44	5	0.55	20.21	4	1003	---
45	6	0.35	18.06	5	3041	3100
46	5	0.21	17.67	3	4750	---
47	10	0.30	19.43	9	1934	900
48	17	0.40	18.73	16	1905	100
49	16	0.34	18.63	15	2319	100
50	10	0.31	17.75	5	1464	300
51	4	0.26	17.10	3	1915	---
52	7	0.15	18.31	3	8132	---
53	12	0.25	17.78	11	2763	700

54	12	0.29	16.84	10	3061	300
55	1	0.10	15.67	0	---	---
56	9	0.25	18.50	6	2206	300
57	13	0.26	16.84	12	2309	300
58	4	0.10	16.82	2	4753	---
59	4	0.10	16.25	3	6477	---
60	3	0.06	21.76	2	19036	---
61	0	0	---	0	---	---
62	0	0	---	0	---	---
63	0	0	---	0	---	---
64	0	0	---	0	---	---

Table 6-16. 15m keel spacing statistics for the outbound part of the 2007 cruise, sections 38-64. Ridge frequency in  $\text{km}^{-1}$ , mean draft, mean and modal spacings in metres.

Section	Number of ridges	Ridge frequency	Mean draft	Ridge spacing		
				Number	Mean	Mode
1	139	2.78	7.89	138	356	110
2	71	1.42	8.07	70	696	230
3	76	1.88	7.28	74	512	90
4	105	2.56	7.50	101	352	90
5	100	2.00	6.95	99	484	90
6	104	2.08	7.28	103	470	150
7	88	1.80	7.17	86	555	150
8	101	2.45	7.48	100	409	70
9	87	2.01	7.49	86	499	130
10	168	3.36	7.78	167	298	130
11	94	1.88	7.50	93	520	70
12	125	2.78	7.97	122	359	130
13	76	2.52	8.23	74	374	130
14	188	3.76	8.24	187	266	150
15	170	3.69	8.26	168	271	190
16	175	4.13	8.64	173	239	90
17	180	3.60	8.11	179	276	90
18	204	4.08	8.71	203	244	110
19	222	4.44	8.69	221	226	110
20	206	4.76	9.26	204	209	110
21	229	5.40	8.65	227	183	50
22	216	4.68	10.11	214	213	110
23	231	4.62	9.48	230	216	110
24	217	4.54	9.74	216	221	110
25	224	4.94	9.85	223	203	110
26	219	4.38	9.09	218	229	150
27	248	4.96	9.22	247	202	110
28	216	5.44	9.25	214	183	110

<b>29</b>	262	5.24	9.15	261	191	150
<b>30</b>	260	5.20	10.15	259	192	130
<b>31</b>	194	4.33	9.56	193	231	150
<b>32</b>	183	5.16	9.55	180	193	90

Table 6-17. 5m keel spacing statistics for the homebound part of the 2007 cruise, sections 1-32. Ridge frequency in  $\text{km}^{-1}$ , mean draft, mean and modal spacings in metres.

Section	Number of ridges	Ridge frequency	Mean draft	Ridge spacing		
				Number	Mean	Mode
<b>33</b>	239	4.78	9.69	238	210	110
<b>34</b>	255	5.22	9.13	253	191	150
<b>35</b>	208	4.98	8.96	206	198	130
<b>36</b>	226	4.52	8.85	225	221	150
<b>37</b>	226	4.64	10.69	224	214	130
<b>38</b>	212	4.24	9.75	211	235	90
<b>39</b>	186	4.33	11.47	183	232	150
<b>40</b>	57	3.51	9.77	53	273	110
<b>41</b>	174	4.05	10.38	170	247	130
<b>42</b>	233	4.89	10.16	231	205	130
<b>43</b>	53	5.10	9.58	51	188	90
<b>44</b>	142	4.81	8.88	141	205	110
<b>45</b>	199	3.98	8.93	198	248	190
<b>46</b>	175	4.12	8.45	173	240	70
<b>47</b>	188	3.76	7.47	187	266	90
<b>48</b>	160	3.20	8.17	159	313	270
<b>49</b>	181	3.73	9.16	180	268	170
<b>50</b>	135	3.15	7.99	134	319	150
<b>51</b>	47	3.47	7.81	46	276	130
<b>52</b>	75	3.13	10.22	73	319	350
<b>53</b>	191	4.77	8.64	188	210	110
<b>54</b>	216	4.32	8.67	215	232	130
<b>55</b>	192	3.99	8.59	189	250	150
<b>56</b>	170	4.06	8.16	167	241	110
<b>57</b>	182	3.88	9.22	179	258	150
<b>58</b>	215	4.41	8.72	213	225	210
<b>59</b>	139	3.43	9.09	135	294	170
<b>60</b>	109	2.72	9.01	105	367	130
<b>61</b>	136	3.39	7.78	134	293	130
<b>62</b>	137	2.74	7.21	136	364	130
<b>63</b>	85	2.45	6.88	84	408	250
<b>64</b>	134	3.11	6.79	130	225	90
<b>65</b>	101	2.02	7.16	100	443	150
<b>66</b>	164	3.28	7.31	163	305	90
<b>67</b>	56	2.29	6.89	54	330	70

Table 6-18. 5m keel spacing statistics for the homebound part of the 2007 cruise, sections 33-67. Ridge frequency in  $\text{km}^{-1}$ , mean draft, mean and modal spacings in metres.

Section	Number of ridges	Ridge frequency	Mean draft	Ridge spacing		
				Number	Mean	Mode
1	35	0.70	11.28	34	1404	350
2	16	0.32	12.75	15	3122	250
3	11	0.27	11.21	9	2513	150
4	21	0.51	11.78	18	1421	250
5	11	0.22	10.89	10	2804	150
6	21	0.42	10.77	20	2141	850
7	13	0.27	11.18	11	3957	350
8	19	0.46	11.81	18	2124	250
9	20	0.46	10.31	19	1774	150
10	39	0.78	11.93	38	1276	350
11	17	0.34	11.47	16	2411	250
12	32	0.71	12.02	29	1189	550
13	23	0.76	11.77	21	978	150
14	59	1.18	11.92	58	858	150
15	56	1.22	11.63	54	787	350
16	54	1.28	12.73	52	707	150
17	43	0.86	12.44	42	1088	250
18	68	1.36	12.47	67	739	150
19	77	1.54	12.16	76	642	150
20	89	2.06	12.44	87	469	150
21	76	1.79	12.51	74	552	350
22	112	2.43	13.02	110	400	250
23	109	2.18	12.52	108	446	250
24	110	2.30	12.60	109	429	150
25	100	2.20	13.65	99	424	150
26	95	1.90	12.24	94	519	150
27	97	1.94	12.69	96	510	250
28	90	2.27	12.65	88	419	150
29	96	1.92	12.91	95	515	250
30	127	2.54	13.37	126	386	250
31	96	2.14	12.15	95	469	150
32	88	2.48	12.58	85	402	150

Table 6-19. 9m keel spacing statistics for the homebound part of the 2007 cruise, sections 1-32. Ridge frequency in  $\text{km}^{-1}$ , mean draft, mean and modal spacings in metres.

Section	Number of ridges	Ridge frequency	Mean draft	Ridge spacing		
				Number	Mean	Mode
33	114	2.28	12.72	113	442	150

34	102	2.09	12.26	100	471	150
35	81	1.94	12.23	79	475	150
36	87	1.74	11.95	86	570	250
37	139	2.85	12.92	137	343	150
38	104	2.08	12.71	103	470	250
39	117	2.73	13.89	114	369	250
40	30	1.85	12.50	26	529	350
41	93	2.17	13.32	89	445	250
42	114	2.39	13.51	112	419	250
43	25	2.40	12.68	23	406	150
44	55	1.86	11.94	54	536	250
45	81	1.62	12.26	80	594	150
46	53	1.25	12.34	51	764	250
47	34	0.68	11.31	33	1490	250
48	46	0.92	12.27	45	1066	650
49	69	1.42	13.02	68	673	150
50	43	1.00	11.22	42	1005	50
51	9	0.66	11.80	8	1351	250
52	43	1.80	12.82	41	543	350
53	71	1.77	11.35	68	559	150
54	81	1.62	11.70	80	603	250
55	68	1.41	12.16	65	677	150
56	54	1.29	10.87	51	715	450
57	83	1.77	12.11	80	561	150
58	84	1.72	11.89	82	571	150
59	57	1.40	11.95	53	721	150
60	46	1.15	11.99	42	699	250
61	36	0.90	11.22	34	1122	150
62	22	0.44	10.94	21	2080	150
63	8	0.23	10.84	7	4232	1250
64	15	0.35	10.20	13	1087	350
65	16	0.32	10.35	15	1729	350
66	29	0.58	10.55	28	1671	350
67	8	0.33	10.20	6	1422	50

Table 6-20. 9m keel spacing statistics for the homebound part of the 2007 cruise, sections 33-67. Ridge frequency in  $\text{km}^{-1}$ , mean draft, mean and modal spacings in metres.

Section	Number of ridges	Ridge frequency	Mean draft	Ridge spacing		
				Number	Mean	Mode
1	2	0.04	19.14	1	18683	---
2	4	0.08	18.36	3	13328	---
3	1	0.02	15.54	0	---	---
4	2	0.05	20.41	1	3254	---

5	1	0.02	15.17	0	---	---
6	0	0	---	0	---	---
7	0	0	---	0	---	---
8	2	0.05	17.75	1	15574	---
9	0	0	---	0	---	---
10	6	0.12	16.73	5	9408	300
11	2	0.04	16.93	1	8212	---
12	7	0.16	17.09	4	1338	---
13	3	0.10	15.60	2	3373	---
14	9	0.18	17.06	8	3472	300
15	6	0.13	16.22	5	4707	1500
16	10	0.24	18.81	8	3777	100
17	10	0.20	17.53	9	4929	100
18	12	0.24	17.91	11	4425	100
19	13	0.26	16.97	12	3181	700
20	12	0.28	19.26	11	2729	2500
21	14	0.33	18.28	13	3021	100
22	29	0.63	17.77	27	1510	300
23	20	0.40	17.83	19	2478	900
24	22	0.46	17.30	21	2079	900
25	32	0.71	18.98	31	1323	500
26	12	0.24	17.43	11	3694	2900
27	23	0.46	17.29	22	2223	300
28	18	0.45	17.41	16	2012	2700
29	24	0.48	17.94	23	1974	700
30	37	0.74	18.47	36	1239	300
31	14	0.31	18.27	13	2781	300
32	18	0.51	17.82	16	1972	100

Table 6-21. 15m keel spacing statistics for the homebound part of the 2007 cruise, sections 1-32. Ridge frequency in  $\text{km}^{-1}$ , mean draft, mean and modal spacings in metres.

Section	Number of ridges	Ridge frequency	Mean draft	Ridge spacing		
				Number	Mean	Mode
33	21	0.42	18.95	20	2483	300
34	13	0.27	20.11	11	2919	900
35	12	0.29	18.06	10	2180	100
36	12	0.24	18.33	11	2228	300
37	30	0.62	17.49	28	1490	300
38	18	0.36	18.61	17	2585	700
39	31	0.72	19.64	28	1204	300
40	6	0.37	17.46	3	1605	---
41	23	0.54	17.97	19	1713	100
42	29	0.61	19.49	27	1691	100
43	5	0.48	18.85	3	2121	---

44	5	0.17	18.80	4	6070	---
45	16	0.32	17.28	15	3077	1100
46	11	0.26	17.18	9	1809	300
47	3	0.06	16.60	2	19682	---
48	5	0.10	18.66	4	8008	---
49	14	0.29	19.53	13	3024	100
50	1	0.02	15.20	0	---	---
51	2	0.15	17.41	1	5768	---
52	8	0.33	17.66	6	2363	300
53	3	0.07	16.80	1	3529	---
54	7	0.14	17.23	6	6404	300
55	12	0.25	17.36	9	1762	900
56	2	0.05	15.43	0	---	---
57	11	0.23	17.89	8	3259	100
58	12	0.25	18.18	10	4059	300
59	8	0.20	17.94	5	1374	500
60	5	0.12	17.41	2	2157	---
61	2	0.05	15.40	0	---	---
62	1	0.02	16.10	0	---	---
63	1	0.03	17.70	0	---	---
64	0	0	---	0	---	---
65	1	0.02	15.33	0	---	---
66	0	0	---	0	---	---
67	0	0	---	0	---	---

Table 6-22. 15m keel spacing statistics for the homebound part of the 2007 cruise, sections 33-67. Ridge frequency in  $\text{km}^{-1}$ , mean draft, mean and modal spacings in metres.

## 6.6 Regional analysis

Time has come to report in more detail the characteristics of the ice thickness distribution in each of the eight regions traversed by the *Tireless* (we shall not comment on the part of Fram Strait S of 78°N). A summary of the statistics for the outgoing leg, before and after beamwidth corrections, is presented in Table 6-23. Not all sections were used for the calculation of the average beamwidth corrections. Instead we selected only those with data of good quality. These are found in the third column of the table below.

The coefficient  $\beta$  was calculated from the observed (uncorrected) draft frequency distribution. At the time of writing the corrections for the return journey have not yet been done. All plots and maps show observed (uncorrected) values for the draft and the number of ridges.

Region	Mean (all)	Selected sections	Mean (selected)	Mean ( $bw=3^\circ$ )	Mean ( $bw=6^\circ$ )	Mode	Maximum	$\beta$
--------	------------	-------------------	-----------------	-----------------------	-----------------------	------	---------	---------

	sections)		sections)					
<b>South Fram Strait</b>	2.49	---	---	---	---	0.35*	18.85	0.53
<b>Central Fram Strait</b>	3.98	6-10 (all)	3.98	3.39	2.75	1.95*	22.12	0.40
<b>North Fram Strait</b>	3.53	11-14 (all)	3.53	3.03	2.49	1.65	22.28	0.49
<b>Northeast Greenland</b>	3.39	15-18 (all)	3.39	2.90	2.36	1.45	25.84	0.38
<b>North Greenland</b>	5.36	19-26, 28-31	5.32	4.71	4.21	1.65*	29.52	0.32
<b>North Ellesmere Island</b>	6.29	35	6.57	6.19	5.76	6.25*	21.34	0.35
<b>Canadian Basin</b>	4.87	40-42, 44,45, 47-52	4.88	4.26	3.62	2.05	29.89	0.34
<b>Beaufort Sea</b>	3.35	53, 54, 57-62, 64	3.33	2.93	2.48	1.55	32.44	0.38

Table 6-23. Ice draft statistics before and after beamwidth corrections for the regions of the outgoing part of the 2007 cruise. Draft in metres, coefficient  $\beta$  in metres<sup>-1</sup>.

Region	Mean	Mean (bw=3°)	Mean (bw=6°)	Mode	Maximum	$\beta$
<b>Beaufort Sea</b>	3.20			1.85	25.72	0.37
<b>Canadian Basin</b>	5.57			2.15	36.12	0.32
<b>North Ellesmere Island</b>	5.17			1.75	32.78	0.31
<b>North Greenland</b>	6.00			2.05	31.80	0.30
<b>Northeast Greenland</b>	3.81			1.65	28.42	0.33
<b>North Fram Strait</b>	5.16			2.15	21.19	0.37
<b>Central Fram Strait</b>	4.79			2.05*	23.58	0.33
<b>South Fram Strait I</b>	3.35			2.35*	19.16	0.43
<b>South Fram Strait II</b>	2.92			1.55	15.33	0.65

Table 6-24. Ice draft statistics before and after beamwidth corrections for the regions of the homebound part of the 2007 cruise. Draft in metres, coefficient  $\beta$  in metres<sup>-1</sup>.

Table 6-25 and Table 6-26 show basic pressure ridge statistics for each of the regions of the outbound and homebound legs, respectively. They were generated without taking into account beamwidth corrections.

Region	5m		9m		15m	
	N	N/km	N	N/km	N	N/km
<b>South Fram Strait</b>	294	3.03	63	0.65	2	0.02
<b>Central Fram Strait</b>	1155	4.83	368	1.54	50	0.21
<b>North Fram Strait</b>	722	4.12	142	0.81	16	0.09
<b>Northeast Greenland</b>	673	4.44	188	1.24	17	0.11
<b>North Greenland</b>	3016	5.85	1398	2.71	282	0.55

<b>North Ellesmere Island</b>	215	4.50	131	2.74	24	0.50
<b>Canadian Basin</b>	2206	5.03	826	1.88	125	0.28
<b>Beaufort Sea</b>	1416	3.32	419	0.98	58	0.14

Table 6-25. Numbers of keels deeper than 5, 9 and 15m for the regions of the outbound part of the 2007 cruise.

Region	5m		9m		15m	
	N	N/km	N	N/km	N	N/km
<b>Beaufort Sea</b>	2044	2.63	489	0.63	65	0.08
<b>Canadian Basin</b>	3330	4.79	1431	2.06	300	0.43
<b>North Ellesmere Island</b>	927	4.86	384	2.01	58	0.30
<b>North Greenland</b>	1656	4.35	810	2.13	174	0.46
<b>Northeast Greenland</b>	664	3.47	192	1.00	23	0.12
<b>North Fram Strait</b>	529	4.15	204	1.60	20	0.16
<b>Central Fram Strait</b>	899	3.97	347	1.53	45	0.20
<b>South Fram Strait I</b>	467	2.83	112	0.68	9	0.05
<b>South Fram Strait II</b>	455	2.72	68	0.41	1	0.01

Table 6-26. Numbers of keels deeper than 5, 9 and 15m for the regions of the homebound part of the 2007 cruise.

In the rest of this chapter we shall be mostly concerned with the outbound journey, though histograms for the return journey will also be shown.

## CHAPTER DONE UP TO HERE.

### 6.6.1 South Fram Strait

The plot in Figure 6-7 shows the mean and the modal draft for each of the sections in S, Central and N Fram Strait for the outbound part of the journey, with different colours for each region. As mentioned before, we opted for not showing the statistics for Section 1. Sections 2 and 3 are partially in the marginal ice zone while 4 and 5 are already inside the ice pack. These four sections form what we call the S portion of Fram Strait.

There is a certain ambiguity in the definition of the sea ice thickness distribution in the marginal ice zone because it is unclear if one should take into account the vast areas of open water. The value of the mean ice thickness for section 2 (shown in Table 6-5) was calculated excluding all roll sections under open water. Had we taken these into account the mean ice draft would drop to 1.45m. If the same procedure is applied to section 3 we would find a mean of 1.32m. This ambiguity, added to the fact that the quality of the records is very low, makes the results for these two sections quite unreliable. This is why we haven't determined beamwidth corrections.

Section 4 is the first one within the 95% ice concentration contour. Unfortunately, the record is again of low quality. Section 5 is even worse. In view of these problems, the results for the southern part of Fram Strait cannot be considered reliable.

A modal ice draft typically between 1.5 and 2m in all three sectors of the strait suggests that first-year ice is the dominant ice type. The value of 0.35m for the mode in section 4 indicates probably a large number of refrozen leads. The histogram for this section also shows a secondary peak at 1.75m. The mean draft is considerably higher in central and N Fram Strait than in S Fram Strait.

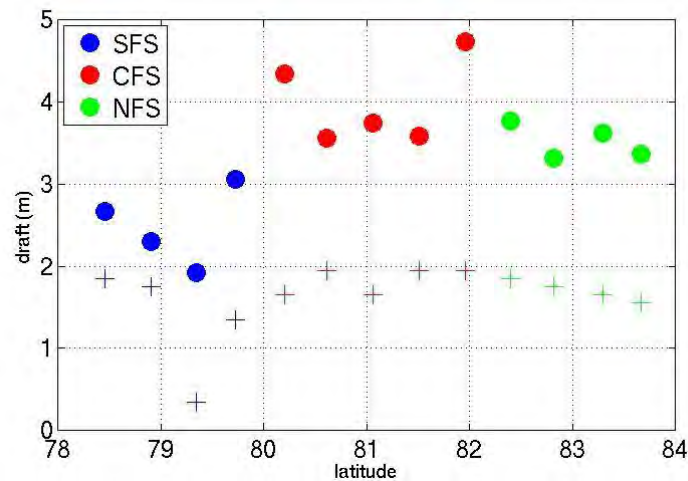


Figure 6-7. Mean (circles) and modal (crosses) ice draft for each section of the outbound part of the 2007 cruise in Fram Strait.

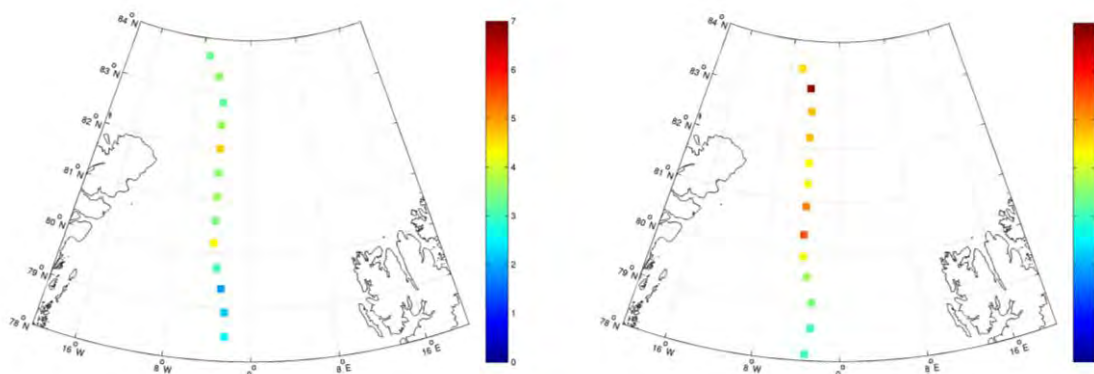


Figure 6-8. Mean ice draft for each section of the outbound (left) and homebound (right) parts of the 2007 cruise in Fram Strait.

Histograms for the full ice draft distribution in S Fram Strait for the outbound and homebound journeys are in the figures below.

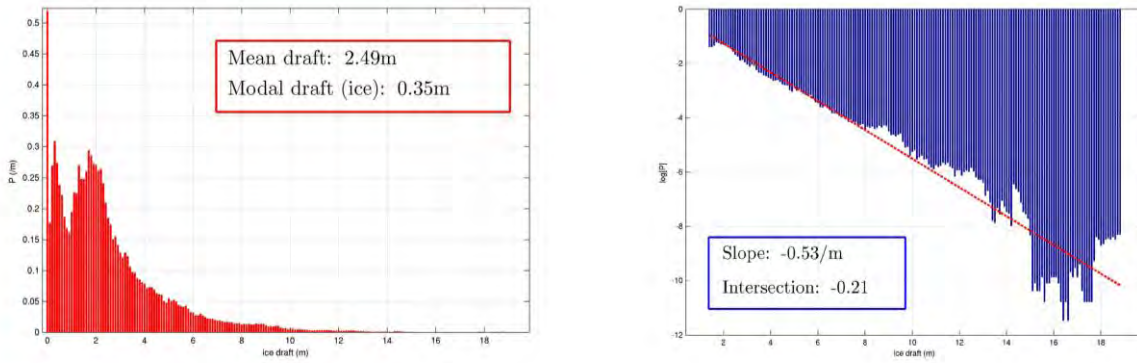


Figure 6-9. Ice draft histograms in linear (L) and semi-logarithmic (R) scales for the outbound part of the 2007 cruise in South Fram Strait (sections 2-5).

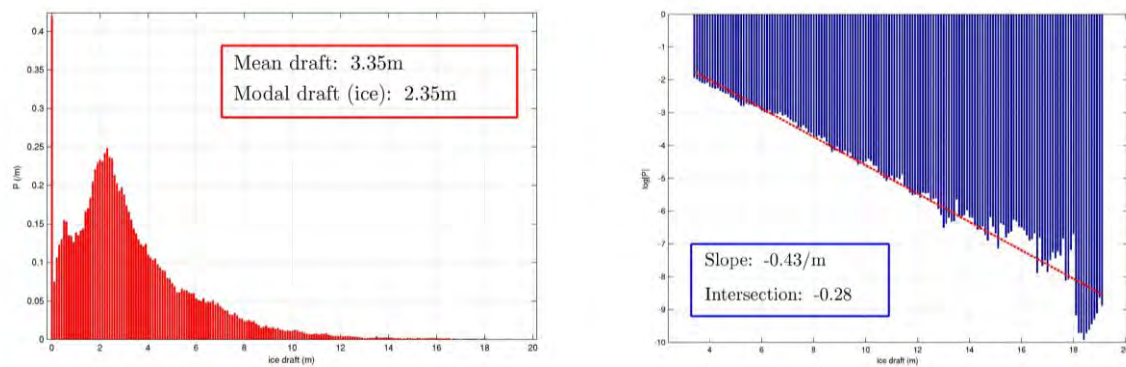


Figure 6-10. Ice draft histograms in linear (L) and semi-logarithmic (R) scales for the homebound part of the 2007 cruise in South Fram Strait (sections 60-63).

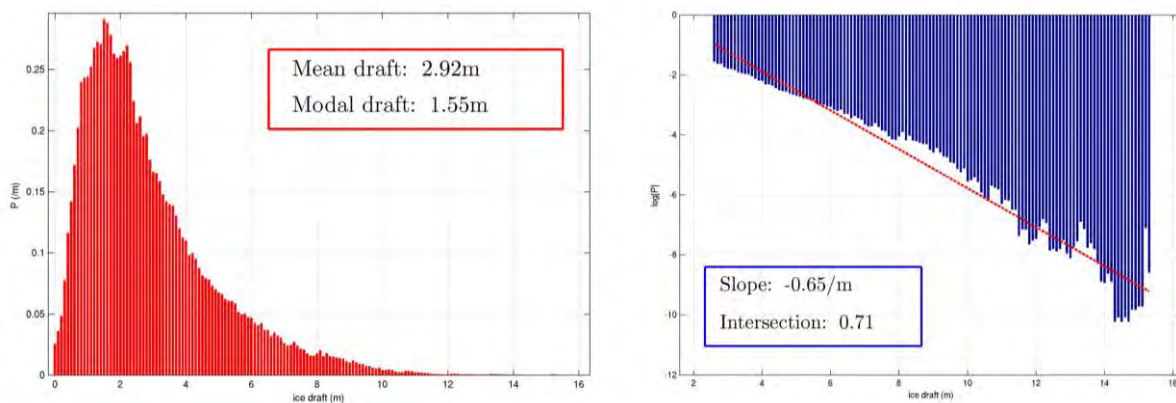


Figure 6-11. Ice draft histograms in linear (L) and semi-logarithmic (R) scales for the homebound part of the 2007 cruise in South Fram Strait (sections 64-67).

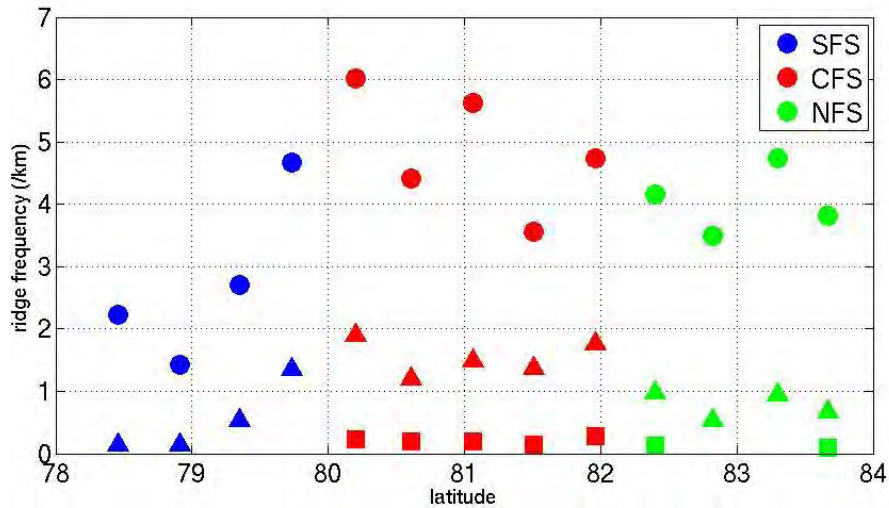


Figure 6-12. 5m (circles), 9m (triangles) and 15m (squares) ridge frequency in each section of the outbound part of the 2007 cruise in Fram Strait.

**Error! Reference source not found.** depicts the mean number of keels deeper than 5m and m per km for each section of the outgoing transect in Fram Strait.

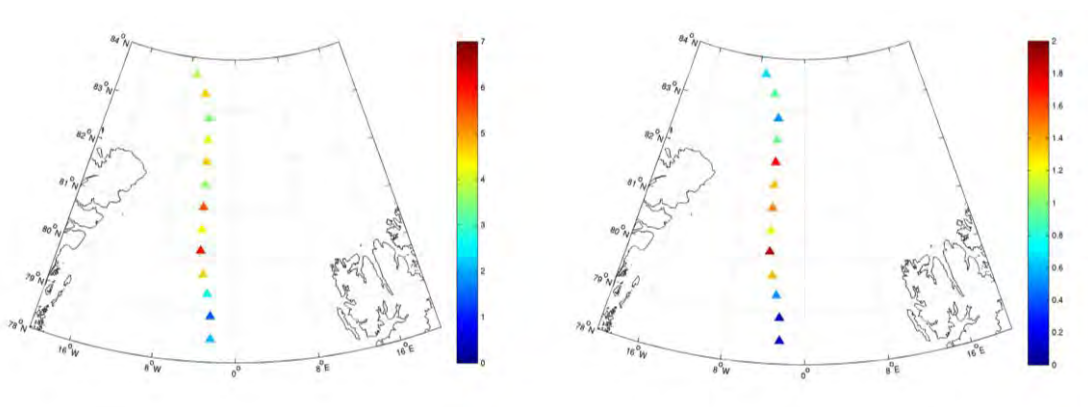


Figure 6-13. Mean number of 5m (L) and 9m (R) keels per km for each section of the outbound part of the 2007 cruise in Fram Strait.

### 6.6.2 Central Fram Strait

The AP780 records for sections 6-10, which compose the central part of Fram Strait, by which we mean points between 80 and 82°N, have much better quality than those of previous sections. In fact, of all the regions, this is the one with the highest percentage of valid data. The mean draft is significantly higher than in S (and N) Fram Strait and so is the number of ridges per km. The usual histograms are shown in Figure 6-14 for the outbound journey and in Figure 6-15 for the return.

There is a large difference in average draft in the two situations. This may be due to the higher depth of the submarine in the return leg but we cannot know for sure.

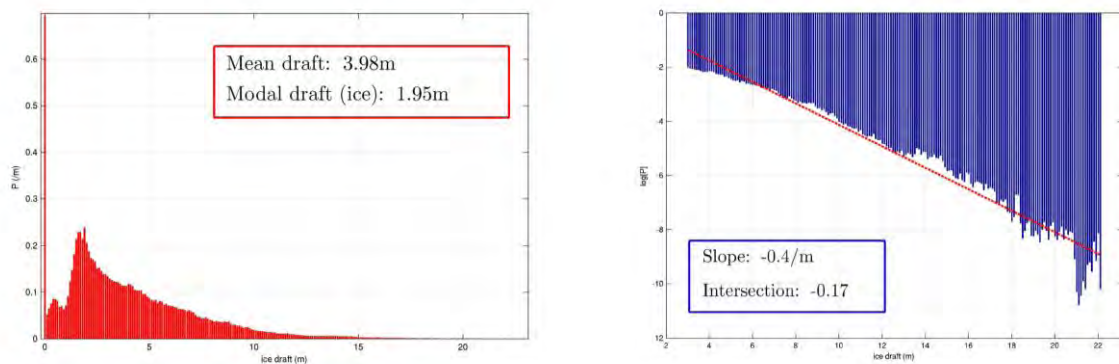


Figure 6-14. Ice draft histograms in linear (L) and semi-logarithmic (R) scales for the outbound part of the 2007 cruise in Central Fram Strait (sections 6-10).

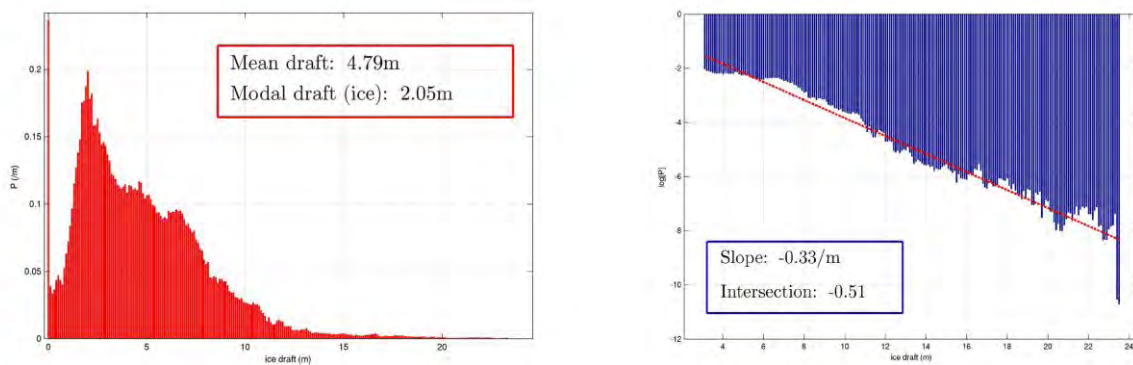


Figure 6-15. Ice draft histograms in linear (L) and semi-logarithmic (R) scales for the homebound part of the 2007 cruise in Central Fram Strait (sections 55-59).

Figure 6-16 shows the histogram for the number of ridges deeper than 15m per km in Central Fram Strait during the outbound part of the cruise, with observations in red and the Poisson fit in blue. The mean number of keels per km was 0.21, which was the parameter used to construct the corresponding Poisson distribution.

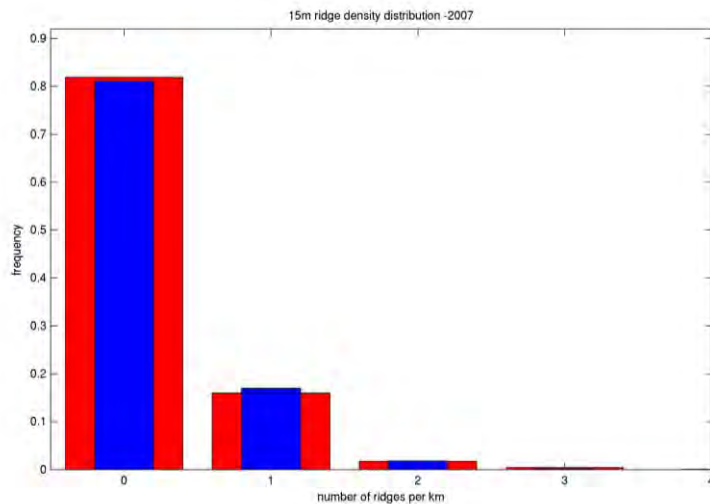


Figure 6-16. Distribution of the number of ridges deeper than 15m per km in Central Fram Strait (sections 6-10) during the outbound part of the 2007 cruise.

In Figure 6-17 we show the histogram for the keel depth distribution, where the reader can observe the approximately exponential behaviour.

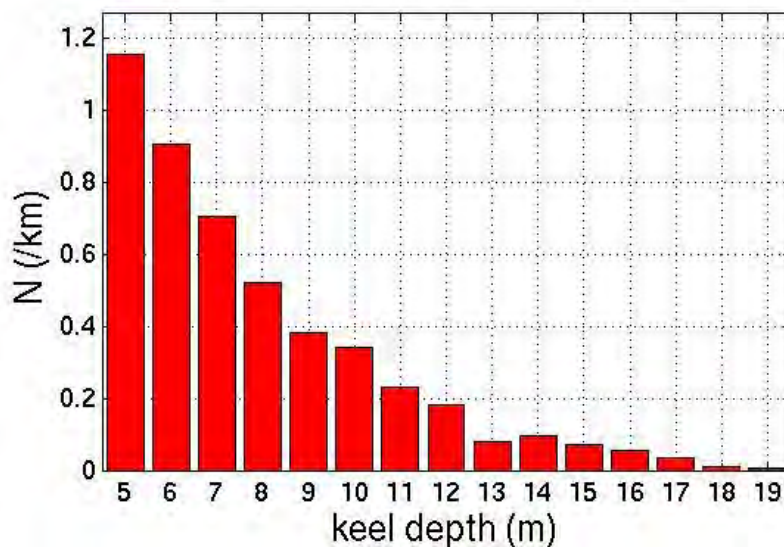


Figure 6-17. Keel depth distribution histogram cruise in Central Fram Strait (sections 6-10) for the outbound part of the 2007.

### 6.6.3 North Fram Strait

The most striking feature of the ice distribution in this region is the disparity between the mean and the modal drafts observed in the outbound and in the homebound journeys. This and the

differences in the histograms are difficult to explain. We note, however, that N Fram Strait is the region of the return leg for which we have the lowest percentage of valid data.

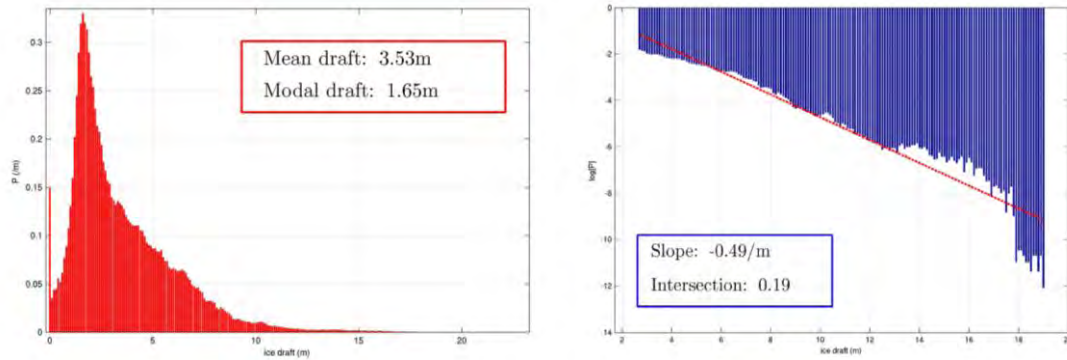


Figure 6-18. Ice draft histograms in linear (L) and semi-logarithmic (R) scales for the outbound part of the 2007 cruise in North Fram Strait (sections 11-14).

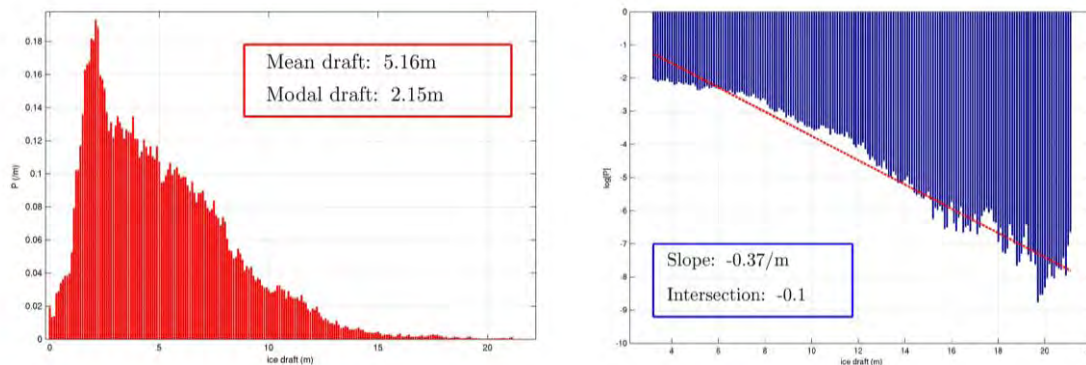


Figure 6-19. Ice draft histograms in linear (L) and semi-logarithmic (R) scales for the homebound part of the 2007 cruise in North Fram Strait (sections 51-54).

### 6.6.4 Northeast Greenland

Figure 6-20 gives the mean and modal drafts in each section of the transect of the outgoing voyage in Northeast Greenland, North Greenland (including the DAMOCLES Survey) and North Ellesmere Island. Maps in Figure 6-21 and Figure 6-22 give the similar information, this time also for the return voyage.

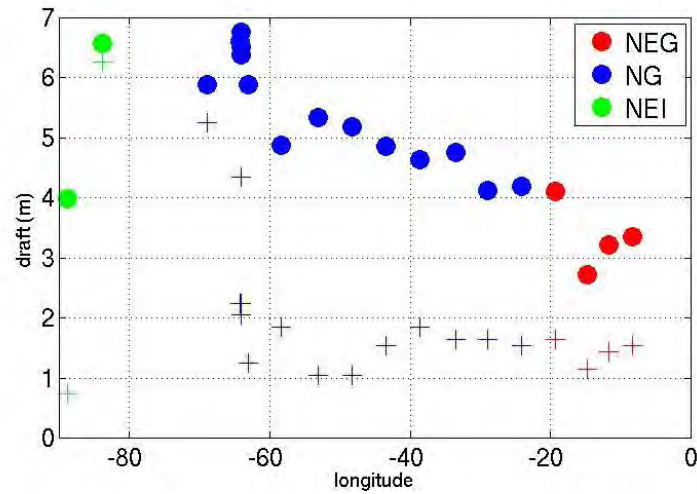


Figure 6-20. Mean (circles) and modal (crosses) ice draft for each section of the outbound part of the 2007 cruise in Northeast Greenland, North Greenland and North Ellesmere Island.

The records on paper rolls for sections 15 to 18 are of good quality and we can trust the results for this region.

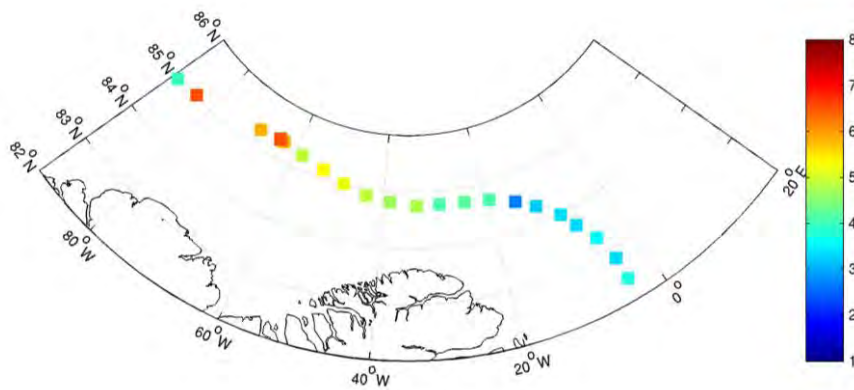


Figure 6-21. Mean ice draft for each section of the outbound part of the 2007 cruise in Northeast Greenland, North Greenland and North Ellesmere Island.

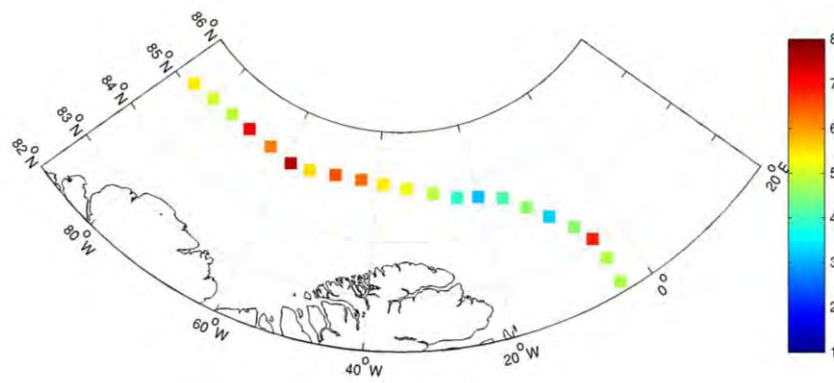


Figure 6-22. Mean ice draft for each section of the homebound part of the 2077 cruise in North Ellesmere Island, North Greenland and Northeast Greenland.

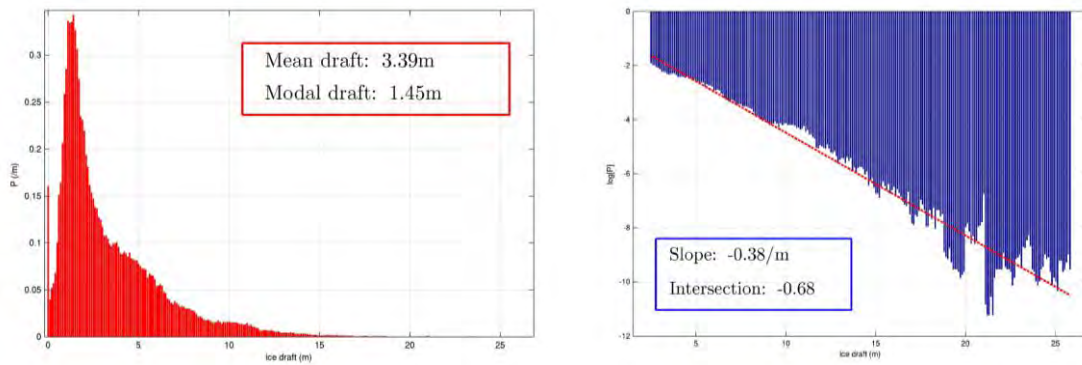


Figure 6-23. Ice draft histograms in linear (L) and semi-logarithmic (R) scales for the outbound part of the 2077 cruise in Northeast Greenland (sections 15-18).

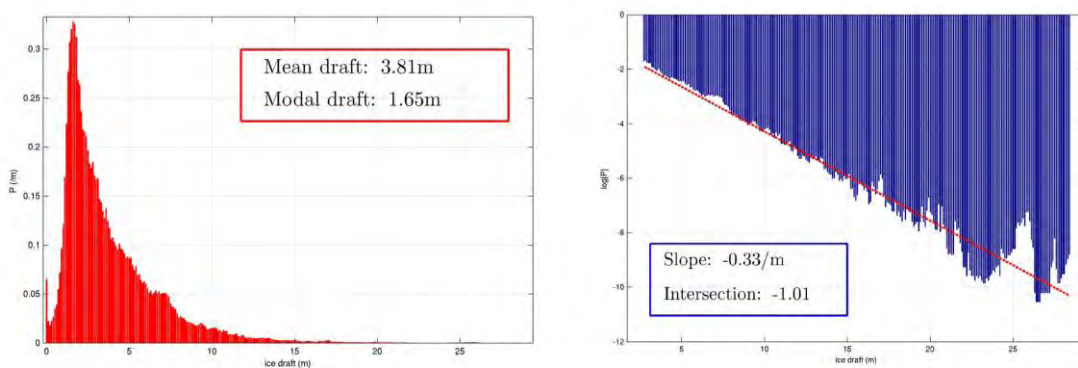


Figure 6-24. Ice draft histograms in linear (L) and semi-logarithmic (R) scales for the homebound part of the 2077 cruise in Northeast Greenland (sections 47-50).

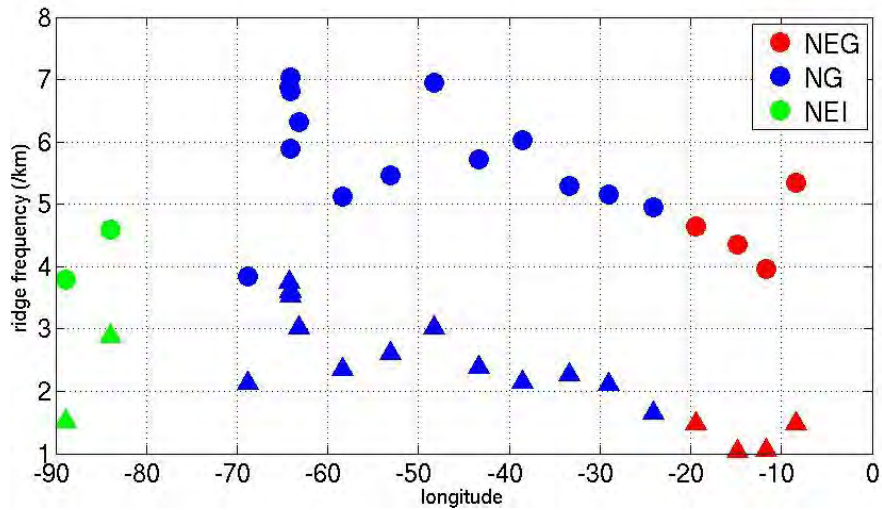


Figure 6-25. 5m (circles) and 9m (triangles) ridge frequency in each section of the outbound part of the 2007 cruise in Northeast Greenland, North Greenland and North Ellesmere Island.

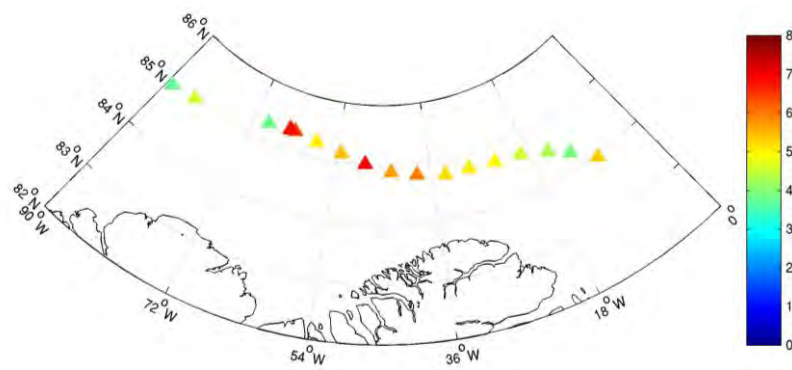


Figure 6-26. Mean number of 5m keels per km for each section of the outbound part of the 2007 cruise in Northeast Greenland, North Greenland and North Ellesmere Island.

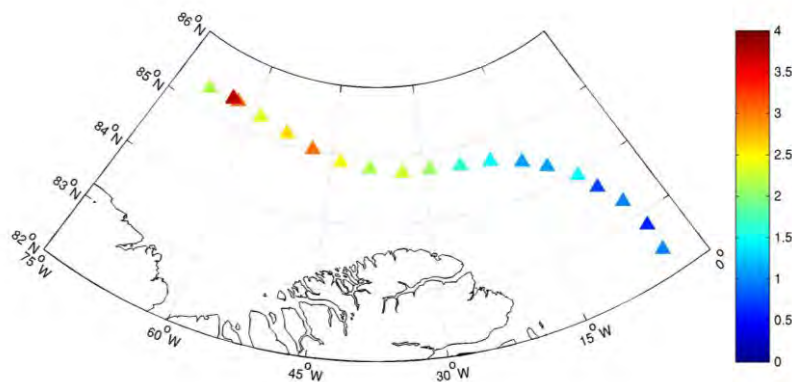


Figure 6-27. Mean number of 9m keels per km for each section of the outbound part of the 2007 cruise in Northeast Greenland, North Greenland and North Ellesmere Island.

### 6.6.5 North Greenland

North Greenland is an area of fundamental importance because it is here (as well as N of Ellesmere Island) that one finds some of the thickest ice in the Arctic. Moreover, according to most climate models, it is also where some ice is likely to remain after the rest of the Arctic Ocean will have ice-free summers.

Sections 19 to 26 have reasonably good quality records. That is not the case of section 27, which was left out for the calculations of the beamwidth corrections. Section 28, directly N of Cape Columbia, has the thickest ice of all the sections of the outgoing voyage. Sections 29 to 31 have also good data but not section 32, which was not considered good enough to deserve beamwidth corrections.

On the return journey there are several sections with mean drafts higher than 6m and two sections with mean drafts (all before beamwidth corrections) above 7m. Although drafts are in general higher in the return leg, these values appear to be too high and some measurement or processing errors cannot be excluded.

The histograms in Figure 6-28 (for the outbound) and Figure 6-29 (for the homebound journey) show clearly a large amount of highly deformed ice. The modal drafts, on the other hand, are quite reasonable.

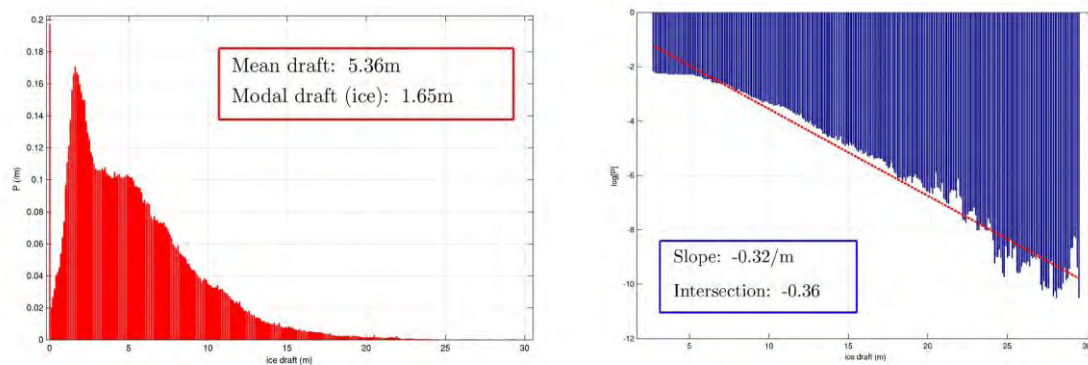


Figure 6-28. Ice draft histograms in linear (L) and semi-logarithmic (R) scales for the outbound part of the 2007 cruise N of Greenland (sections 19-32).

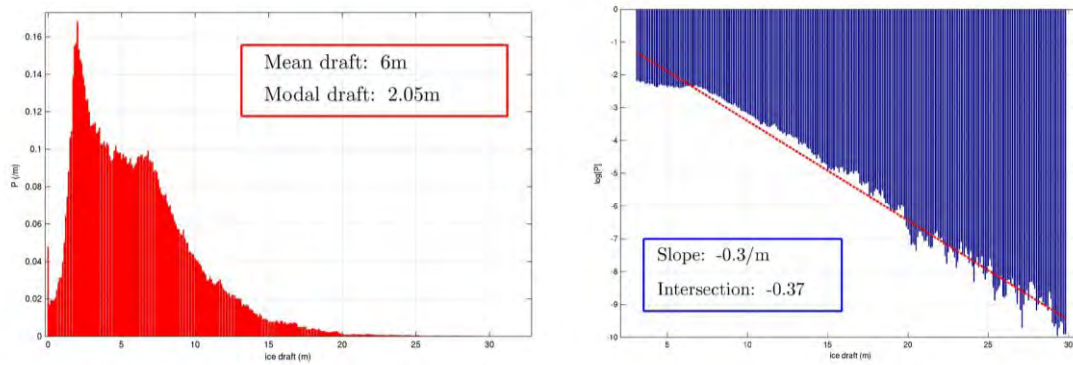


Figure 6-29. Ice draft histograms in linear (L) and semi-logarithmic (R) scales for the homebound part of the 2007 cruise N of Greenland (sections 37-46).

This is also the region with the highest number of keels per unit length (together with N Ellesmere Island for keels deeper than 9m). Figure 6-30 gives the observed ridge spacing distribution (in violet) and the corresponding best lognormal fit (in yellow) for keels deeper than 5m (L) and 9m (R). the parameters of the lognormal were determined as described in Section 2.2.

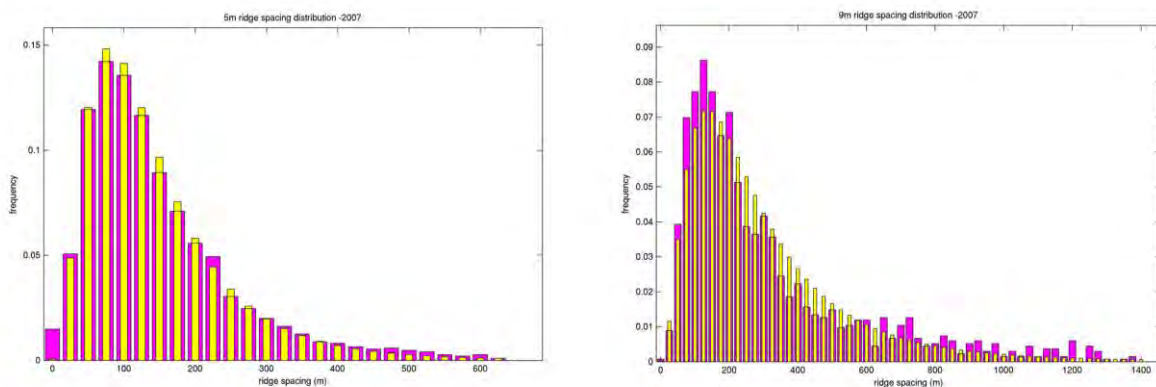


Figure 6-30. Ridge spacing distribution for keels deeper than 5m (L) and 9m (R) for the outbound part of the 2007 cruise in North Greenland (sections 19-32). Observations in violet, best lognormal fit in yellow.

The histogram in Figure 6-31 represents the keel depth distribution for the outgoing part of the 2007 cruise in North Greenland and North Ellesmere Island (sections 19-36), with the observed frequencies in red and the best exponential fit in yellow. According to Section 2.2, the parameter that defines the exponential is the mean draft of the ridges deeper than 5m, in this case 9.67m. The author leaves for the reader the task of deciding if the fit is good or useless.

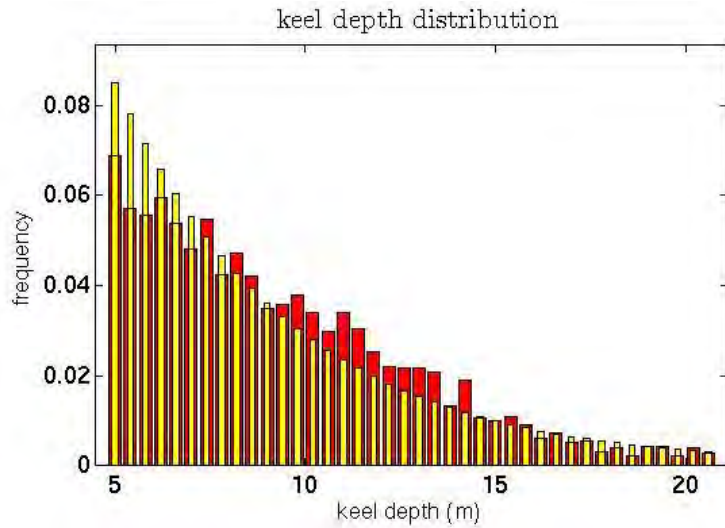


Figure 6-31. Keel depth distribution histogram for the outgoing part of the 2007 cruise in North Greenland and North Ellesmere Island (sections 19-36). Observations in red, exponential fit in yellow.

### 6.6.6 The DAMOCLES Survey

The track of the submarine and complementary information about the DAMOCLES Survey can be found in Section 6.1. The mean and modal ice drafts, uncorrected for beamwidth effects, were 6.55m and 2.25m, respectively. Once those corrections were made, the mean draft (for sections 28-31) dropped to 6.08m and 5.55m for sonar beams 3 and 6° wide, respectively.

The histograms in Figure 6-32 show the ice draft frequency distribution in linear and semi-logarithmic scale. It is clear that there is large amount of thick deformed ice in this area.

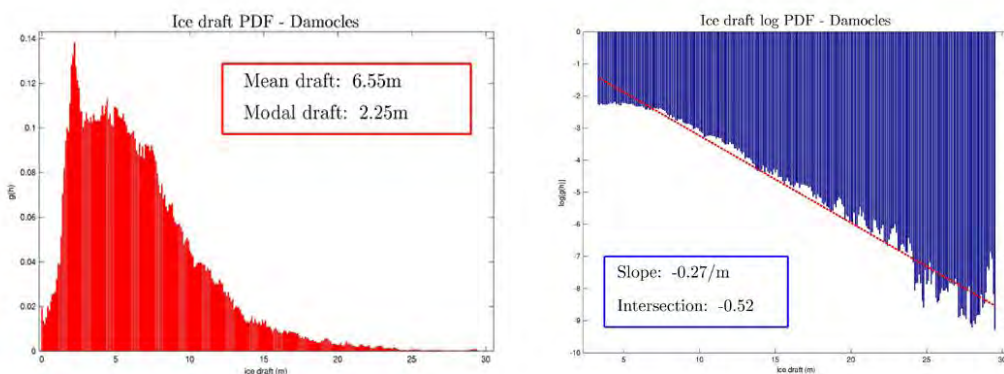


Figure 6-32. Ice draft histograms for the DAMOCLES Survey in linear (L) and semi-logarithmic (R) scales.

### 6.6.7 North Ellesmere Island

As mentioned before, the sonars stopped collecting data shortly after the DAMOCLES Survey which means that we have only a limited amount of data for the area N of Ellesmere Island during the outbound journey and what we have is not of good quality. In section 36, for instance, only 10% of the track has data considered acceptable. In view of these problems, the results for this section, notably the histograms shown below, have to be taken with caution. The histogram is totally different from the histograms for any other region. There appears to be a lot of open water and also a lot of ridged ice. If we exclude the peak at 6.25m, the mode has the more reasonable value of 1.75m, more in line with the modes for North Greenland and the Canadian Basin.

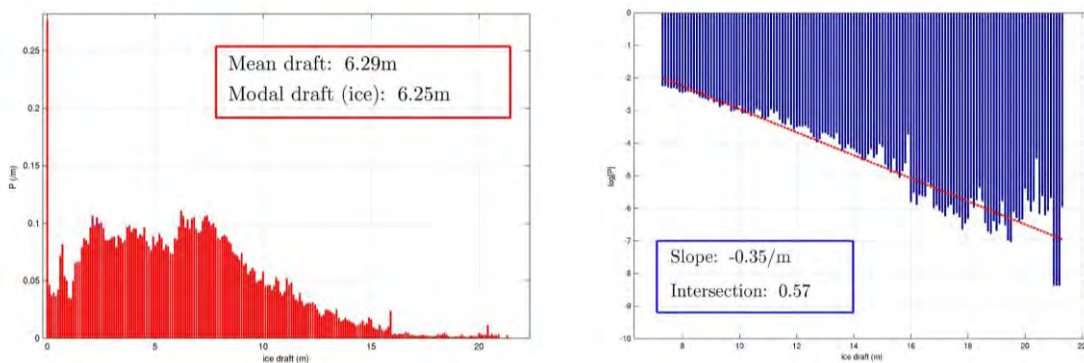


Figure 6-33. Ice draft histograms in linear (L) and semi-logarithmic (R) scales for the outbound part of the 2007 cruise N of Ellesmere Island (sections 35-36).

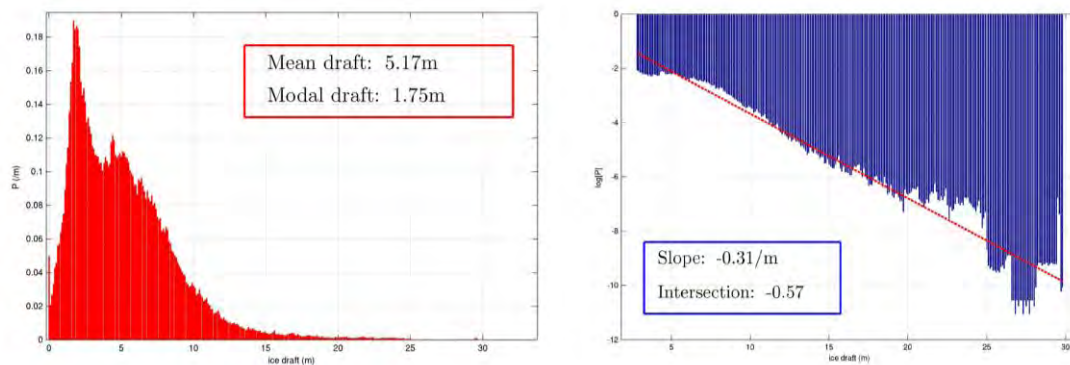


Figure 6-34. Ice draft histograms in linear (L) and semi-logarithmic (R) scales for the homebound part of the 2007 cruise N of Ellesmere Island (sections 33-36).

### 6.6.8 Canadian Basin

The segment that we are going to study now, to which we gave the not so appealing name of Canadian Basin, is composed by sections 38 to 52 of the outbound journey and sections 18 to 32 of the homebound journey.

AP780 records for sections 38 and 39 are of bad quality. In some roll sections the marking of the water points was particularly tricky and two different analyses led to quite different values for the draft. We have a low, or even very low, level of confidence in the results for these sections. Things improve a bit in sections 40 and 41, where the level of confidence is medium, but still the draft appears to be too high. Sections 42, 44 and 45 have not particularly good records and nothing could be extracted for section 43. Sections 46 and 47 seem unproblematic though just over half of the recorded data could be used. Sections 48, 49, 50 and 52 have medium level of confidence while 51 is somewhere between medium and low. Based on this we conclude that the overall quality of the data for this region is not satisfactory and the resulting mean draft may have been overestimated.

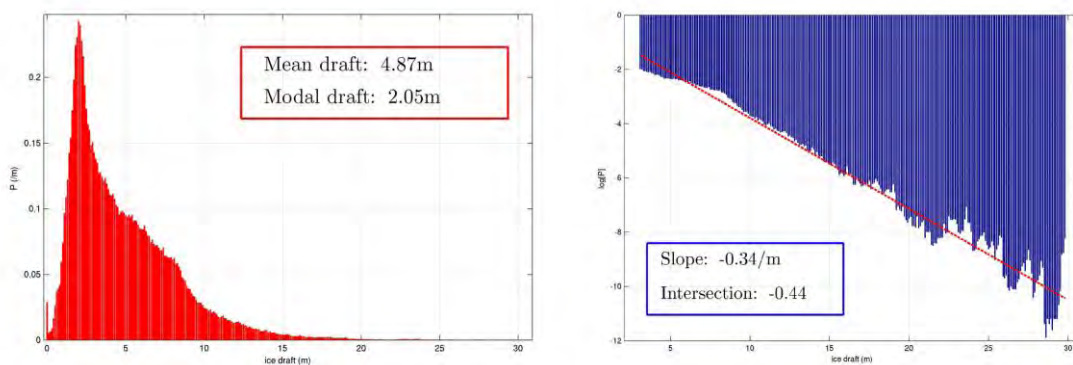


Figure 6-35. Ice draft histograms in linear (L) and semi-logarithmic (R) scales for the outbound part of the 2007 cruise in the Canadian Basin (sections 38-52).

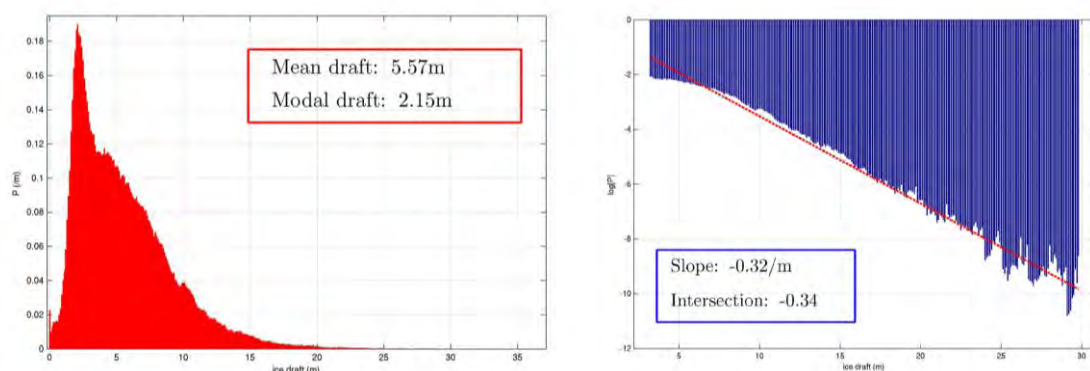


Figure 6-36. Ice draft histograms in linear (L) and semi-logarithmic (R) scales for the homebound part of the 2007 cruise in the Canadian Basin (sections 18-32).

Maps in Figure 6-37 show the spatial distribution of the ridge frequency in this part of the Arctic based on data gathered in the outbound journey.

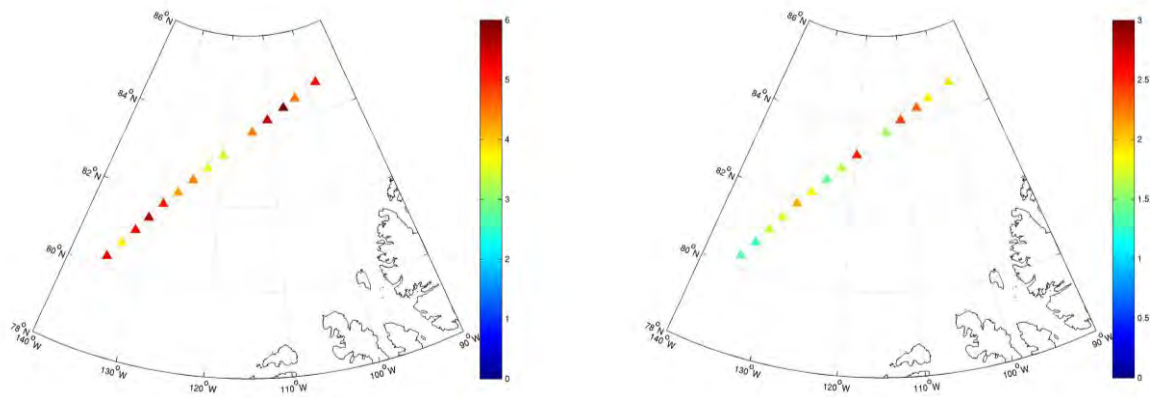


Figure 6-37. Mean number of 5m (L) and 9m (R) keels per km for each section of the outbound part of the 2007 cruise in the Canadian Basin.

### 6.6.9 Beaufort Sea

The segment of the outgoing journey that we take as being in the Beaufort Sea (though technically most of it is actually N of the N boundary of the Beaufort Sea) stretches between latitudes 75 and 80°N. The corresponding sections are 53 to 64 for the outwards journey and 1 to 17 for the return.

The quality of the records of the outbound journey are not exactly satisfactory and that may be one of the reasons why the overall mean draft (3.35m) is possibly overestimated. Of the 12 sections that compose this segment, there is good data for sections 53, 54, 57, 58, 60 and 61 and the corresponding results can be accepted with some confidence. For all other sections the level of confidence is low and the results have to be considered with caution. For instance in section 55 we could only use less than 20% of the data and even that was of poor quality.

There appears to be a transition in the ice regime from section 57 to section 58. The latter has a much lower mean draft than in previous sections, though not so different from that of the following sections.

In spite of these reservations, some of the results make sense: for instance the mean ice draft possesses a clear southwards gradient and the histogram built from all valid data exhibits a very nice exponential tail, as the reader can see in Figure 6-38 and Figure 6-40.

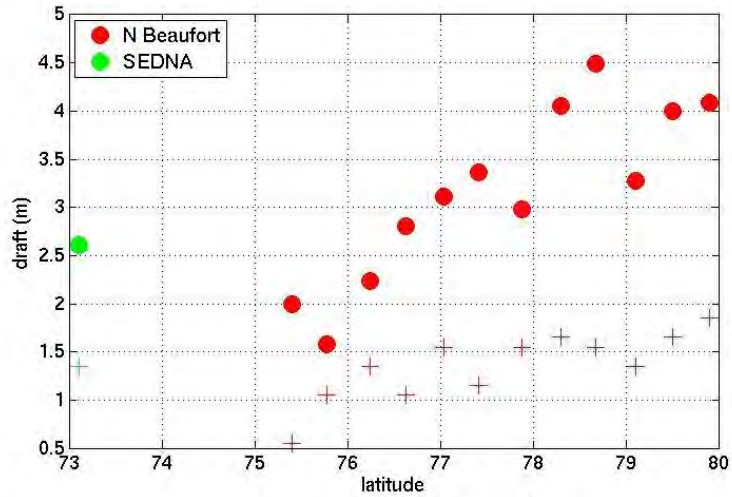


Figure 6-38. Mean (circles) and modal (crosses) ice drafts for each section of the outbound of the 2007 cruise in the Beaufort Sea.

The quality of the data of the return journey seems to be better. Note, for example, the high percentage of valid data that were used for the analysis. The mean draft was slightly lower than that of the outgoing journey, which only happened in one other region. The modal draft, however, was higher in the return. It is unclear if these differences have any statistical relevance.

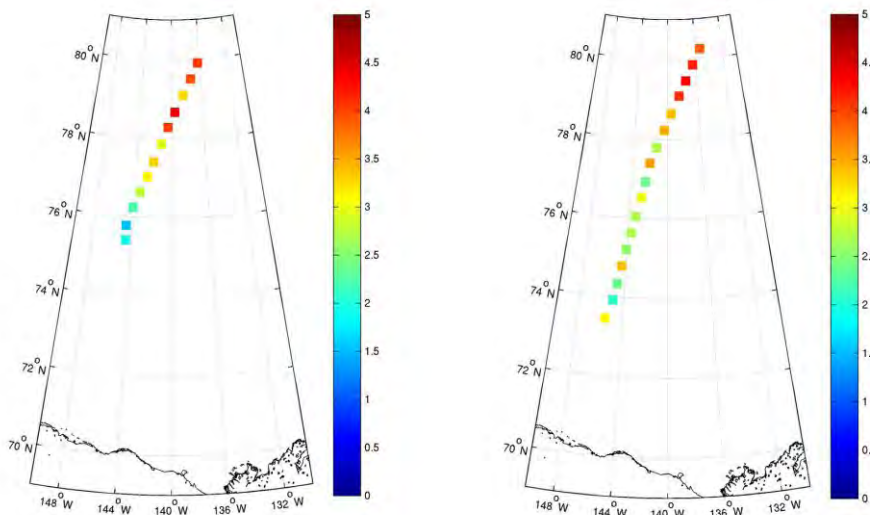


Figure 6-39. Mean ice draft for each section of the outbound (left) and homebound (right) parts of the 2007 cruise in the Beaufort Sea.

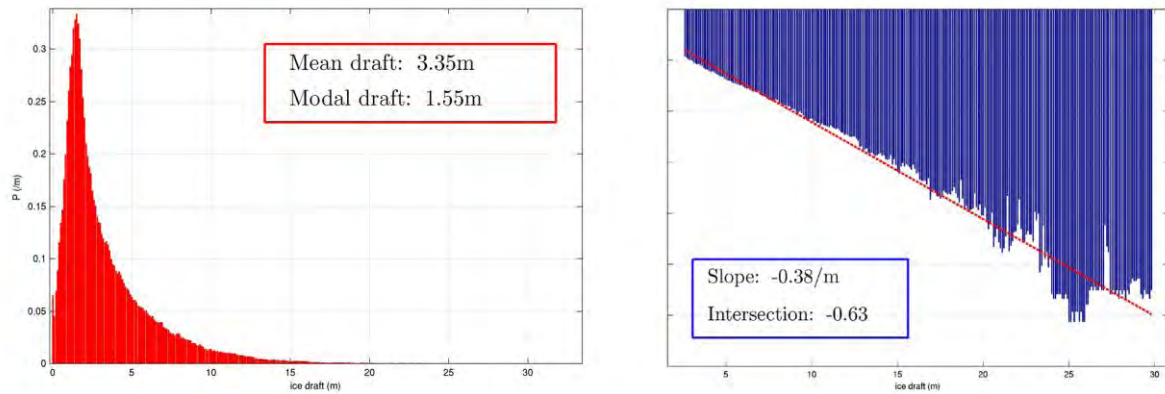


Figure 6-40. Ice draft histograms in linear (L) and semi-logarithmic (R) scales for the outgoing part of the 2007 cruise in the Beaufort Sea (sections 53-64).

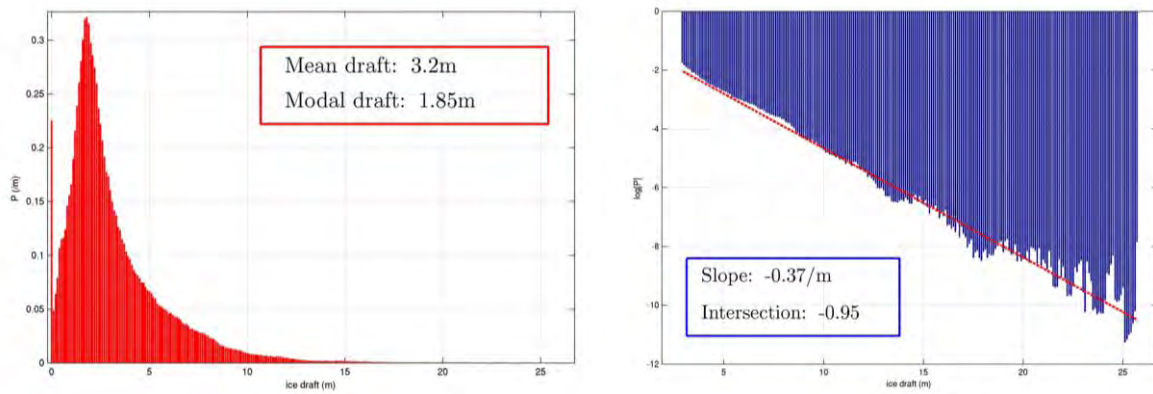


Figure 6-41. Ice draft histograms in linear (L) and semi-logarithmic (R) scales for the homebound part of the 2007 cruise in the Beaufort Sea (sections 1-17).

The maps in Figure 6-42 show the spatial distribution of the number of keels deeper than 5m and deeper than 9m per unit length (km).

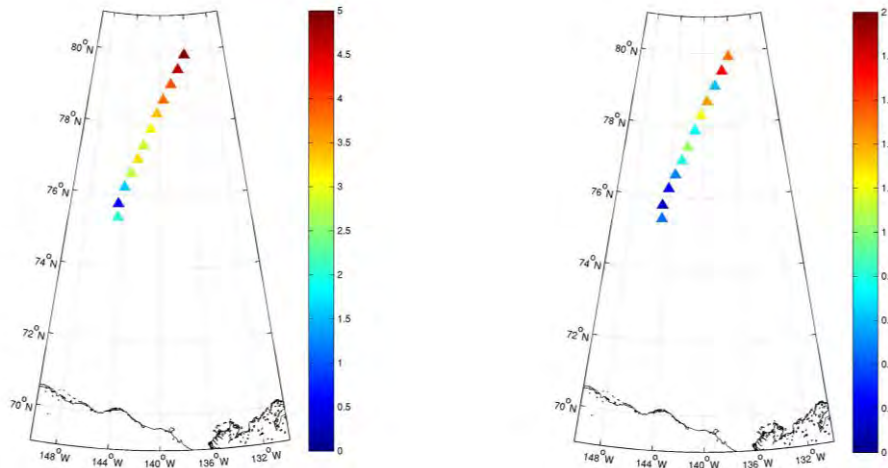


Figure 6-42. Mean number of 5m (L) and 9m (R) keels per km for each section of the outbound part of the 2007 cruise in the Beaufort Sea.

Figure 6-43 shows the best exponential fit of the keel depth distribution of the whole voyage. It belongs to the transect in the Beaufort Sea at the beginning of the homebound journey. The mean depth of the keels used to construct the exponential fit was 7.82m.

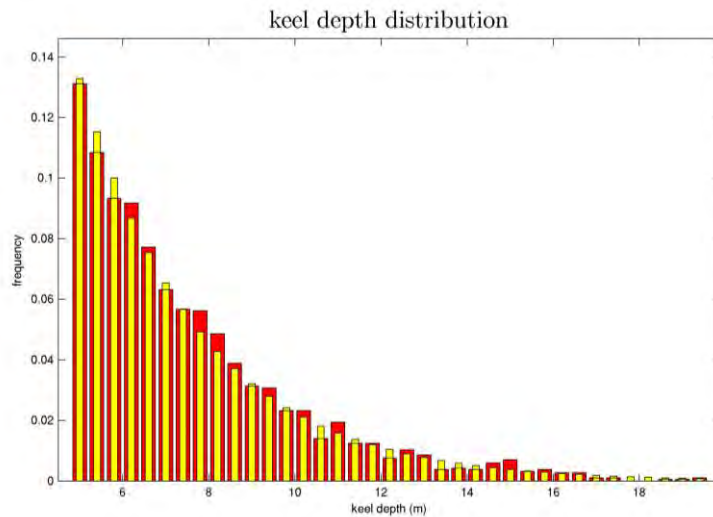


Figure 6-43. Keel depth distribution histogram for the homebound part of the 2007 cruise in the Beaufort Sea (sections 1-16). Observations in red, exponential fit in yellow.

Plots in Figure 6-44 and Figure 6-45 compare the keel depth distribution for the Beaufort Sea and North Greenland during the outbound journey in linear and semi-logarithmic scales, respectively. It is evident the larger amount of ridging in the area N of Greenland.

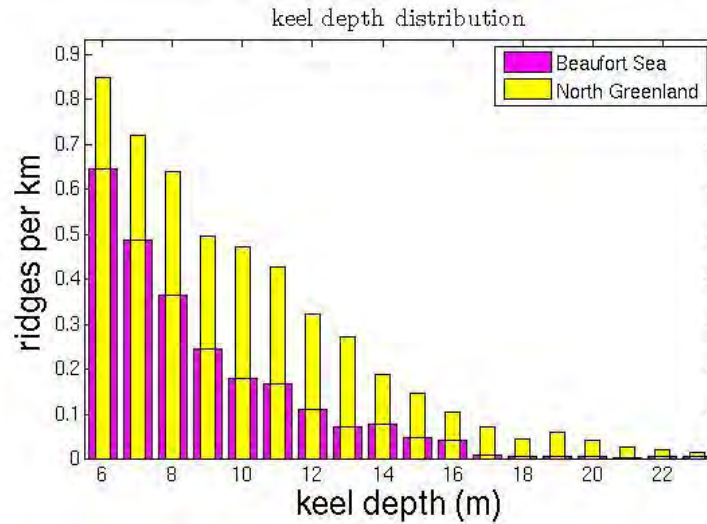


Figure 6-44. Comparison of the keel depth distribution in the Beaufort Sea and North Greenland in the outbound part of the 2007 cruise.

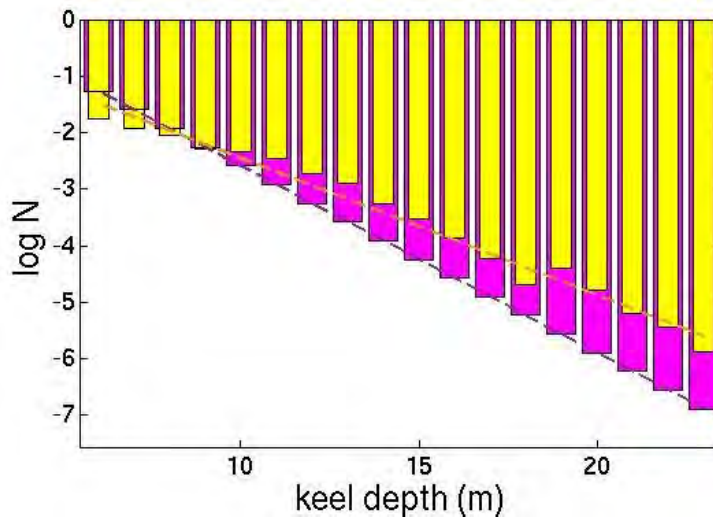


Figure 6-45. Comparison of the keel depth distribution in the Beaufort Sea (violet) and North Greenland (yellow) in the outbound part of the 2007 cruise (this time in semi-logarithmic scale).

### 6.6.10 The SEDNA Survey

The mean, modal and maximum ice drafts were 2.61m, 1.35m and 21.80m. The value of the modal ice draft is in good agreement with the mean thickness of the undeformed ice floes (1.5m) as measured by drilling. Figure 6-46 shows the histogram of the ice draft distribution in linear and in semi-logarithmic scales.

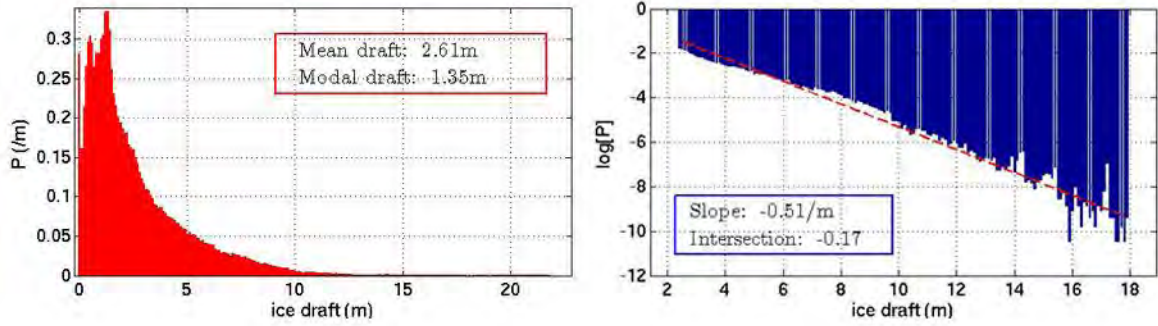


Figure 6-46. Ice draft histograms for the SEDNA Survey in linear (L) and semi-logarithmic (R) scales.

The pressure ridge statistics is as follows: the frequency of keels deeper than 5m was 3.84/km, with a mean draft of 7.23m; that of keels deeper than 9m was 0.64/km, with a mean draft of 11.16m. Figure 6-47 shows the histograms of the keel depth distribution in linear and semi-logarithmic scales.

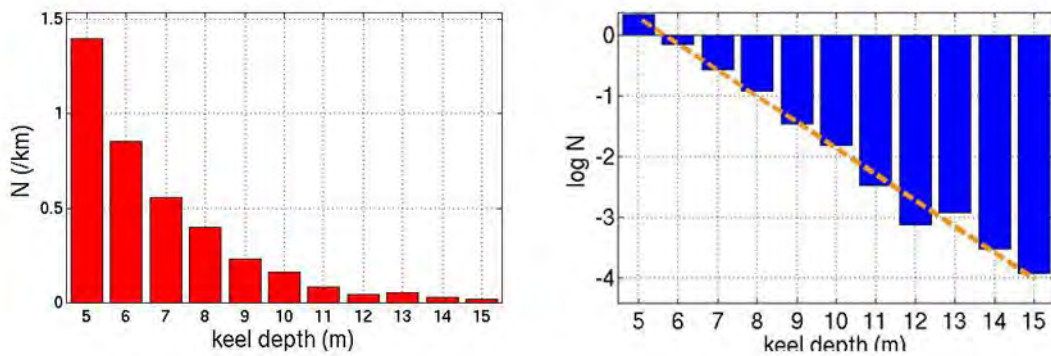


Figure 6-47. Keel depth distribution of the SEDNA Survey in linear (L) and semi-logarithmic (R) scales.

## 7 Long term changes in Arctic sea ice thickness

In the preceding three chapters we described the valuable collection of sea ice draft data obtained by British submarines during the 31 year period between 1976 and 2007. The number of cruises may not be large but hopefully it is sufficient to give an idea of how the ice thickness in the Arctic Ocean and Fram Strait evolved in the last three decades.

The first evidence of thinning of the Arctic sea ice was provided by Wadhams (1990) after comparing cruises with similar tracks in the region N of Greenland in October 1976 and May 1987. The loss of ice was estimated in 15% (in volume).

Some years later Wadhams and Davis (2000) announced what they call “further evidence of ice thinning in the Arctic Ocean”. The evidence was based on the calculation of mean drafts for ice profiles obtained during cruises in October 1976 and September 1996 which had similar paths on the way from the North Pole towards Fram Strait along the Prime meridian. It was found that on average the ice in 1996 was 43% thinner (41% after corrections for seasonality) than in 1976. Such a decline in ice thickness was in good quantitative agreement with observations made by US submarines over the same period of time.

And yet, in my view, the importance of Wadhams and Davis’ result must not be overstated. Differences in tracks, time of cruises, equipment, analysts criteria, etc., make the comparison between the two cruises a tricky task. We also have to consider the well-known interannual variability of the Arctic sea ice cover, which makes it impossible to infer a concrete trend from two isolated observations. But what makes the result essentially invalid from the scientific point of view is the absolute impossibility of an independent verification.

In the next sections we concentrate in four different regions of the Arctic: Fram Strait, North Greenland and Ellesmere Island, the North Pole and the Beaufort Sea. For the first two we compare the ice draft distributions of 2004 and 2007, and try to figure out if there is any well defined by looking at the results of earlier cruises. For the last two we simply quote the results of the available measurements.

### 7.1 Fram Strait

We start by summarizing the observations of the winters of 2004 and 2007 (outbound part only for the latter) in Table 7-1. We find it necessary to study separately the E and the W tracks, due to the peculiar ice distribution in the strait, which has much more ice in its W half than in its E half.

Latitude	Track	April 2004		March 2007	
		Longitude	Draft (m)	Longitude	Draft (m)
80-82°N	West	1°E-2°W	3.00	4°W	3.98
	East	5°E	1.89		
	All	5°E-2°W	2.77		
82-84°N	West			4-8°W	3.53
	East	5°E	2.62		
	All				

Table 7-1. Mean ice drafts in Fram Strait in 2004 and the outbound part of 2007.

One can see from this table that a reliable comparison between the observations of 2004 and 2007 cannot be made because the tracks were not at all coincident. In 2007 the trajectory of the *Tireless* was much more to the W than three years earlier and that can well explain the apparent increase in ice thickness.

Because Fram Strait is the gateway to the Arctic Ocean used by British submarines, we actually have data for this part of the Arctic from all seven cruises described earlier. A summary of the observations can be seen in Table 7-2. For a good understanding of the table we need to clarify a few points denoted by the superscript (.) in the table.

- (1) Average of sections 1, 36, 37 and 38 of Table 4-3.
- (2) Average of sections 2, 3, 34 and 34 of Table 4-3.
- (3) Value quoted by Wadhams and Davis (2001).
- (4) 83-84°N only.

Latitude	Track	October 1976		April/May 1979		June/July 1985		May 1987		September 1996	
		Lon	Draft	Lon	Draft	Lon	Draft	Lon	Draft	Lon	Draft
80-82°N	West	1°E-4°W <sup>(1)</sup>	4.81	4-7°W	4.19					5°W	1.25
	East			0-5°E	3.10					5°E	2.12
	All	5°E-5°W <sup>(3)</sup>	5.84	5°E-7°W	3.65	1°E-2°W	3.75	5°E-1°W	3.62	5°E, 5°W	1.69
82-84°N	West	7-12°W <sup>(2)</sup>	4.78							5°W	2.61
	East					2.5-7.5°E	4.97			5°E <sup>(4)</sup>	2.76
	All	5°E-5°W <sup>(3)</sup>	5.39	2°E-3°W	4.62						

Table 7-2. Mean ice drafts (in metres) in Fram Strait in 1976, 1979, 1985, 1987 and 1996.

The 1996 value of the mean draft is very low, especially in the W Fram Strait. If we ignore for a moment this point, which does not fit the overall picture, we see that in the region 80-82°N there is a steady decline of ice draft between 1976 and 2004, which can also be seen in Figure 7-1. The same also holds, though not so clearly, for the Northern sector of the strait. The 2007 looks very high but, on the other hand, we know that there was an unusually high amount of ice in Fram Strait in that year.

These results for Fram Strait as a whole confirm that this is a complex region, with distinct regimes in the W and E halves, and no particular dependence on the latitude. This is known to be an area of the Arctic where most of the sea ice is not locally formed but advected from higher latitudes. Ice transported from the W, from the central Arctic (through the Transpolar Drift) and, sometimes, from the E, exits the Arctic Ocean through Fram Strait. The thickness of this ice depends very much on its history.

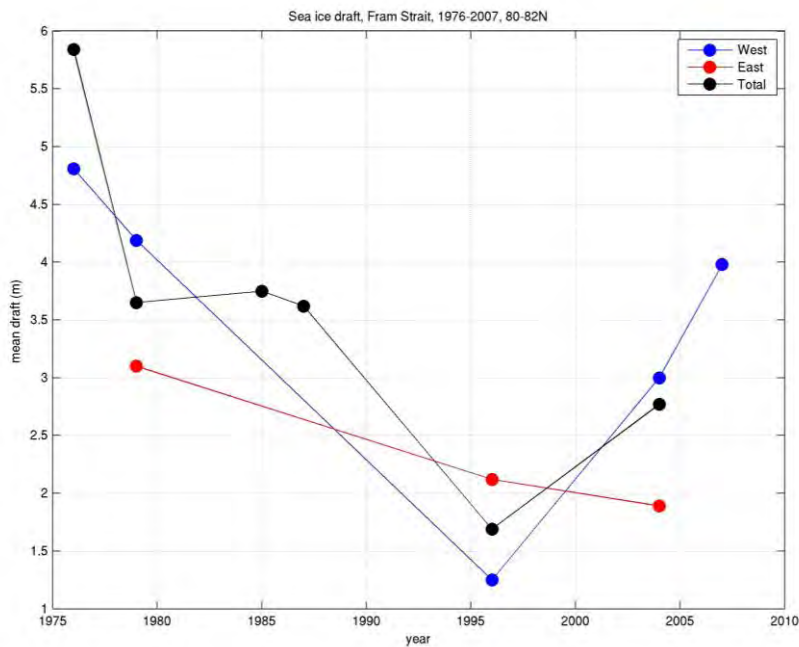


Figure 7-1. Mean sea ice draft in Central Fram Strait between 1976 and 2007.

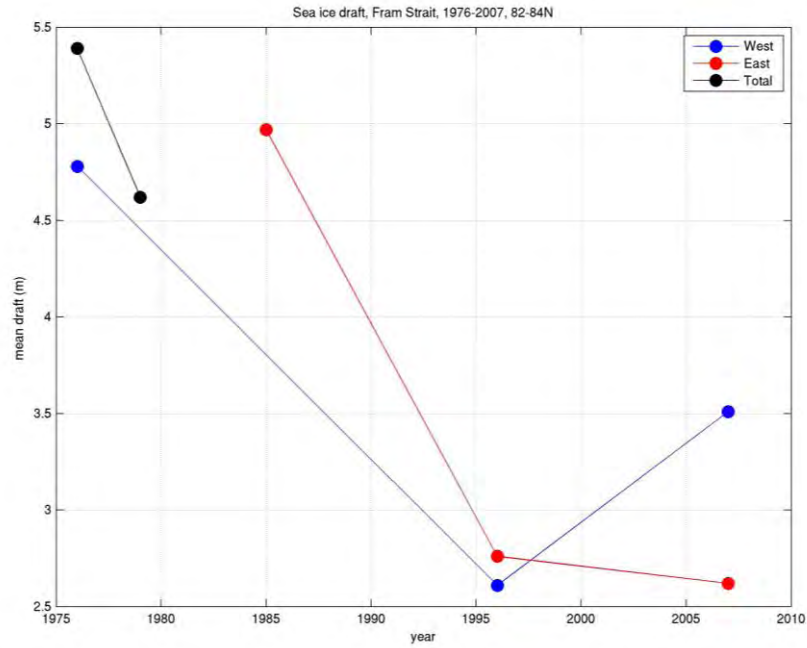


Figure 7-2. Mean sea ice draft in North Fram Strait between 1976 and 2007.

## 7.2 North Greenland and Ellesmere Island

The *Tireless* had very similar tracks in the vicinity of the 85°N parallel in 2004 and 2007 and this allows a direct comparison between the results of the two cruises in this area of the Arctic. It is perhaps worth to put together in the same figure some of the histograms already shown in the previous chapter.

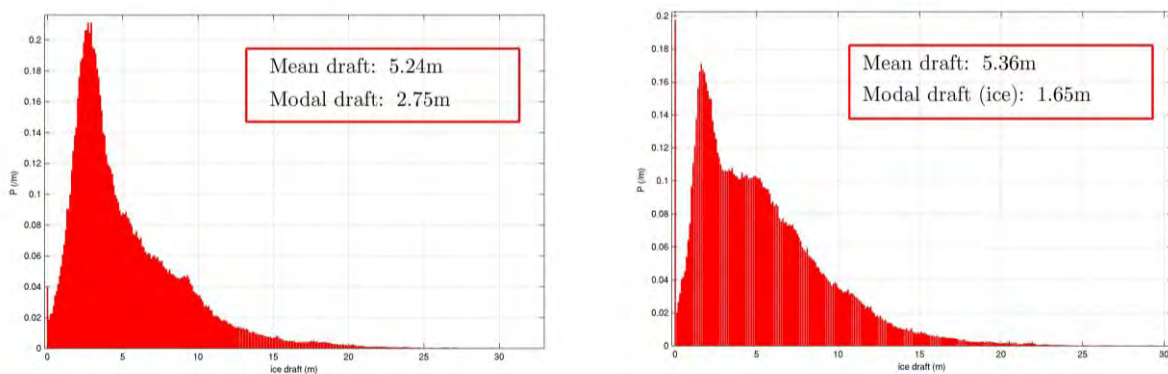


Figure 7-3. Ice draft histograms for North Greenland in 2004 (L) and 2007 outgoing (R).

We observe that although the mean ice draft (whose values shown in Figure 7-3 are uncorrected for beamwidth effects) is approximately the same in the two situations, the actual ice draft distribution is quite different (the ability to study the full ice distribution instead of only mean values has actually been hailed as one of the great advantages of submarines over satellites). The modal ice draft is much lower in 2007, which suggests that what was in 2004 a region dominated by multi-year ice is in 2007 a place where first-year ice is predominant. There is also much more open water in 2007 and, more importantly, much more thick, deformed ice, reflecting a more dynamic ice cover in 2007.

More or less the same conclusions could be drawn from a comparison between the ice distributions of the GreenICE and DAMOCLES Surveys. The location and timing (end of winter) of the two surveys was approximately the same.

A study of the pressure ridge distribution in this area shows an increase of 7% and 6% in the number of ridges per km, for keels deeper than 5m and 9m, respectively, while the frequency of deep keels was approximately the same in 2004 and 2007.

We must now summarize the long term evolution of the sea ice in this part of the world by putting together the results for the four cruises which visited N Greenland and Ellesmere Island. That is done in Table 7-3 and Figure 7-4.

<b>Longitude</b>	<b>Oct 76</b>	<b>May 87</b>	<b>April 04</b>	<b>Mar 07</b>
<b>10-70°W</b>	6.34	4.72	4.85	5.06
<b>10-55°W</b>	6.17	4.72	4.35	4.31
<b>22-55°W</b>	6.17	4.60	4.61	4.73

*Table 7-3. Mean ice draft (in metres) in the region north of Greenland (85°N).*

The table above (for which no beamwidth corrections were done, except for the 1976 cruise, when the beamwidth was 17°) shows that there is really no evidence of thinning since 1987 in this part of the Arctic. This conclusion holds if we consider the first line (all data from the four cruises), the second line (taking into account only the portion where the 1987, 2004 and 2007 tracks coincided), or the third line (taking into account the portion where the tracks of the four cruises coincided).

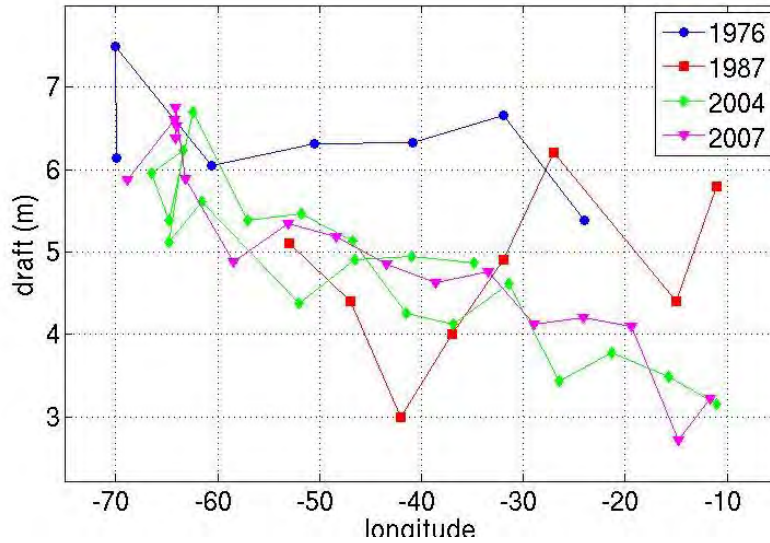


Figure 7-4. Mean ice draft in each section of four cruises in North Greenland (latitude ~ 85°N).

### 7.3 The North Pole

We have four records of british submarines in the vicinity of the North Pole. Table 7-4 shows the mean ice draft recorded in each of those cruises in the region 89-90°N. The first thing to note is that all cruises took place in different months so a direct comparison is not possible. The reader has noticed that the 1996 value is substantially lower than all the others and that the 2004 mean draft appears to be too high, even for the end of the winter, if we accept that there has been a thinning of the ice in recent decades. However, as mentioned earlier, the records of 2004 are of very low quality and the confidence in the value obtained is low.

Cruise	Mean draft (m)
October 1976	4.21
May 1987	4.50
September 1996	1.99
April 2004	4.10

Table 7-4. Mean ice draft in the vicinity of the North Pole (latitude>89N).

### 7.4 The Beaufort Sea

For the Beaufort Sea we can only compare the results of the 1976 *Gurnard* cruise described in Section 4.1 with the results of the 2007 *Tireless* cruise that were shown in Section 6.6.10. As we can see from Figure 4-1, the size of the surveys are not the same but at least they were located in the

same region of the Beaufort Sea. Table 7-5 shows the mean and modal drafts of both surveys. The decline in mean draft is about 32% while the modal draft in 2007 was roughly one half of what it was about thirty years earlier. This suggests that in 1976 the region was mostly covered with multi-year ice, while in 2007 first-year ice was the dominating ice type.

<b>Cruise</b>	<b>Ice camp</b>	<b>Mean Draft (m)</b>	<b>Modal Draft (m)</b>
April 1976 (USS <i>Gurnard</i> )	AIDJEX (73°N, 144°W)	3.81	2.7-3.0
April 2007 (HMS <i>Tireless</i> )	SEDNA (73°N, 145°45'W)	2.60	1.35

Table 7-5. Basic ice draft statistics for the location of the AIDJEX and SEDNA ice camps.

## 8 Comparison with other ice thickness measurements

Time has come in this report, which is getting long, too long, some would say, to verify if there is agreement between the sea ice thicknesses retrieved from measurements by British submarines and other type of ice thickness measurements.

Aircraft, helicopters, submarines and satellites have all been used to measure Arctic sea ice thickness and yet the number of coincident or nearly coincident measurements over large areas with different non-fixed platforms is very small.

Simultaneous aircraft and submarine measurements of sea ice thickness occurred for the first time in October 1976 when the British submarine *Sovereign* and an Argus patrol aircraft of the Canadian Forces followed the same track for approximately 2200km (Wadhams, 1981). In May 1987 another British submarine and a NASA P-3A aircraft equipped with an Airborne Oceanographic Lidar performed coincident measurements of Arctic sea ice draft and sea ice freeboard, respectively (Comiso *et al.*, 1991).

### 8.1 Submarine vs ICESat measurements

It is of great interest to take advantage of the rare occasions in which there is an overlap in time of a submarine in the Arctic and a satellite above it. Efforts to combine submarine and satellite altimetry data, namely ICESat data, have been scarce. Some exceptions are the well-known work of Kwok *et al.* (2009) and the more modest attempt by the author and two collaborators (Calvao *et al.*, 2011). In the former it appears that there is a good agreement between the ice thicknesses obtained from ICESat freeboards and from ice draft measurements by a US submarine in November 2005. In the latter, however, there are large differences between the mean values of the ice thickness extracted from ICESat freeboards during its L3H phase of operation and from (nearly coincident) ice draft measurements by a British submarine in March 2007, at least in some parts of the Arctic Ocean, notably in the area north of Greenland.

Figure 8-1 displays the results of submarine and ICESat thickness measurements during the April 2004 *Tireless* cruise and the L2B ICESat campaign (17/02/2004 to 21/03/2004). There is no overlap in time between the two operations but because both measurements were made at the end of the winter, when the ice thickness is at or near its annual maximum, a comparison between them is, in our view, legitimate. Sea ice freeboards were obtained from altimetry data with the techniques described in (Calvao *et al.*, 2011). The density of the ice was taken as  $920\text{kg/m}^3$  and that of the snow as  $360\text{kg/m}^3$ , values that are extensively used in the literature. For the depth of the snow cover we used 30cm, in agreement with observations made during winter field campaigns in the Beaufort Sea and the Lincoln Sea around that time. The submarine observations of Figure 8-1 are not corrected for beamwidth effects. Moreover, the author acknowledges that some corrections to the submarine measurements have been performed since this plot was first published in (Calvao *et al.*, 2011).

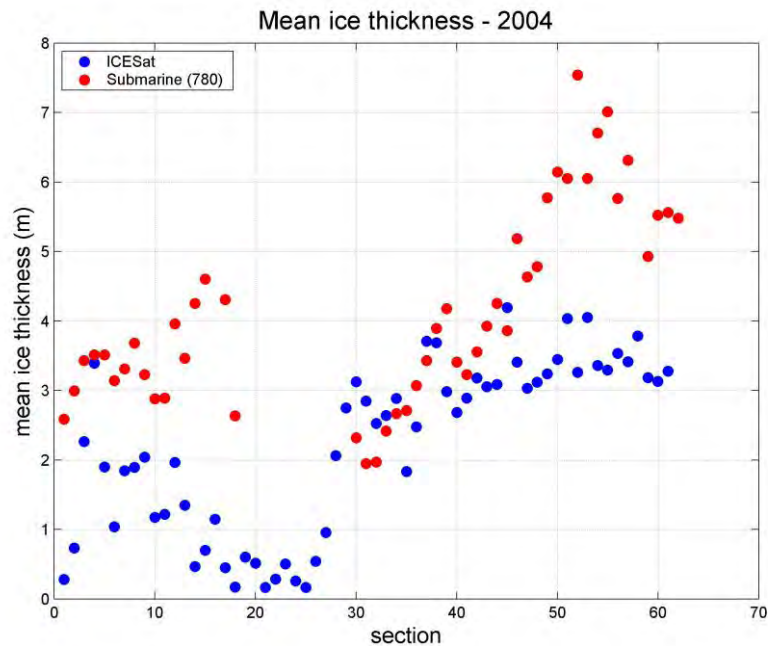


Figure 8-1. Mean ice thickness from submarine and ICESat measurements for each section of the 2004 cruise.

The plot in Figure 8-2 shows the measurements made by the *Tireless* in its outgoing part of the 2007 voyage (with the contribution of the snow ignored and draft converted into thickness using a factor 1.125, which corresponds to an ice density of  $910\text{kg/m}^3$ ) and the almost coincident ICESat retrievals processed by the groups led by Kwok and Zwally. The satellite results used here are those of the whole ICESat campaign, which lasted from 12 March to 14 April 2007. After some consideration, this choice was preferred to the alternative of only using data collected during the period 10-16 March. The values of the draft used in this plot have been corrected for a beamwidth of  $6^\circ$  (which is likely to be slightly above its real value).

A few comments are in order. Perhaps one of the first things that we notice is the difference in the ice thicknesses obtained from the two altimetry groups. While the agreement between Kwok *et al.* and Zwally *et al.* is evident in the region of Fram Strait, it appears to exist an approximately constant difference of 1m in the other sections. But we have nothing to do with that.

What concern us is the large discrepancies that exist between submarine measurements (even after strong beamwidth corrections) and satellite observations in all sections except those in Fram Strait, which is exactly where the agreement was not expected (due to the variable ice conditions in that area).

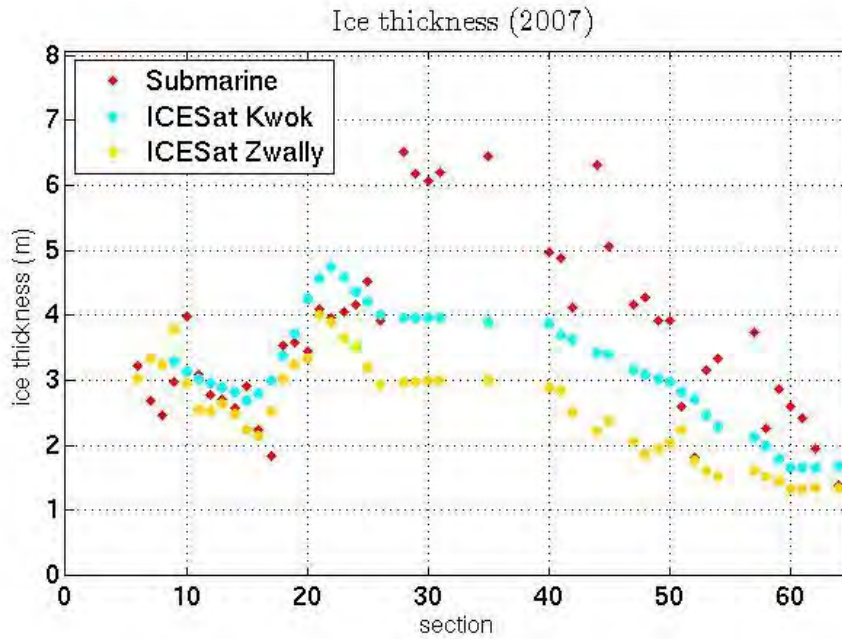


Figure 8-2. Mean ice thickness from submarine and ICESat measurements for each section of the outgoing part of the 2007 cruise.

In Table 8-1 we compare the mean ice thicknesses in the region N of Greenland (84°30'-85°30'N, 22-70°W) obtained from satellite and submarine measurements. In 2007 only observations made during the outgoing leg of the *Tireless* journey were used. For the 2004 cruise used sections 44 to 57 while for the 2007 voyage they were 19 to 32 for the uncorrected drafts and 19-26 and 28-31 for the beamwidth corrected ones.

It is encouraging to note that when the bias due to the beamwidth is removed the submarine measurements lead to thickness values that are in the same interval as the ICESat values calculated by Kwok *et al.*, especially if we take the beamwidth as 6°. As this is likely to be higher than the actual beamwidth of the AT780 used in 2004, we have to conclude that a discrepancy between the satellite and the submarine observations still remains.

Platform	2004	2007	Variation
ICESat (Kwok)	4.68	4.16	-0.52
ICESat (Zwally)	-	3.38	-
Submarine (uncorrected)	5.90	6.02	+0.12
Submarine (6° beamwidth corrected)	4.80	4.74	-0.06

Table 8-1. Mean ice thickness (in metres) from submarine and ICESat measurements in the winters of 2004 and 2007 for the region North of Greenland (84°30'-85°30'N, 22-70°W).

Such discrepancies are clearly evident when we compare the histograms for the ice draft distribution in the region N of Greenland in the winter of 2007 with those shown in Figure 8-3, obtained from data processed by Zwally *et al.* Both the mean and the modal draft are much below the values extracted from our submarine observations.

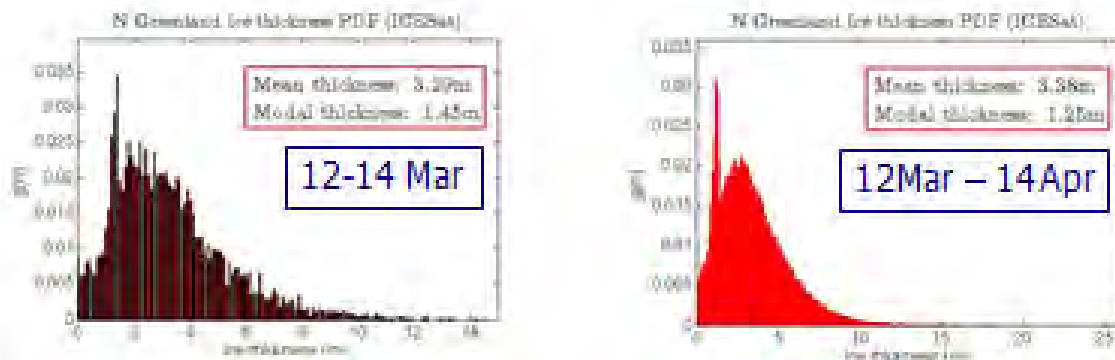


Figure 8-3. Histograms for the sea ice thickness distribution in the region N of Greenland in the winter of 2007 from ICESat measurements.

To understand the causes of such lack of agreement between the sea ice thickness observations made from the two main platforms is, in the author's view, a matter of some urgency.

## 8.2 Submarine vs electromagnetic sounding

A comparison between submarine and airborne electromagnetic sounding measurements is difficult. In first place, there appear to be no flights that coincide in time and space with any of the two last Royal Navy submarine cruises.

A 350km flight in April 2007 between the North Pole and (87°N, 58°W), mostly over second year ice, produced a mean thickness of ice (plus snow) of 3.31m and a mode of 2.35m. Once the snow is subtracted, Haas *et al.* (2008) obtain a mean ice thickness of about 3m, and modal ice thicknesses of 2.05m for second-year ice and 1.60m for first-year ice. Unfortunately, that part of the Arctic Ocean was not visited by our submarine.

The author plans to investigate if the Alfred Wegener Institute, also a partner in the SIDARUS project, has collected ice thickness data during any other flights that may have taken place at the same time of the submarine cruises. At the time of writing, the author is not aware of any such flights.

## 9 Conclusion

Submarines are undoubtedly a privileged platform for the determination of the large-scale Arctic sea ice thickness distribution. For about 50 years US and UK submarines have been cruising the Arctic Ocean regularly and collecting valuable sea ice draft data that have been passed to scientists of the University of Washington in the US and the University of Cambridge in the UK. These data sets proved to be of great importance for a better understanding of the Arctic climate and, in particular, of the properties of the Arctic Ocean sea ice cover and the way it has been changing. Observations of sea ice thinning by Wadhams (1990), Rothrock *et al.* (1999), and Wadhams and Davis (2000), provided early warnings of the profound changes were happening to the Arctic.

However, the use of a variety of sonar equipment, the frequent impossibility of an independent evaluation of the accuracy of the measurements, the sparsity of the voyages, the non-coincidence of the tracks, the varied times of the year of the cruises, and the difficulty in merging UK and US data in a single global data bank suggest that some caution is needed when they are used to derive long-term trends. UK submarine missions with nearly coincident tracks are often several years (sometimes decades) apart. With such a small amount of data it is difficult to correctly interpret the differences of average thickness values obtained in different cruises. They may be the effect of a climate related monotonic (or approximately monotonic) trend or simply the reflection of the well-known pronounced interannual variability of the Arctic sea ice.

Submarine measurements can rarely be compared with simultaneous measurements in the same area by other instruments. Attempts by the author to match ice draft measurements by HMS *Tireless* in March 2007 with nearly coincident freeboard determinations by satellite altimetry, both converted to thickness by the method described in Section 2.8, have not been particularly successful. It is very likely that errors exist in both measurements. In principle they could be identified once a closer collaboration between the submarine and the satellite communities is established. While this certainly happened in the US, it is not yet the case of the UK.

The difficulty in validating submarine data is amplified by the secretive nature of the missions. While the author acknowledges that the Navy may not be willing to distribute raw data or navigation files, the release of processed data would benefit a larger community. Again, while many of the processed ice thickness data collected by the US Navy are now accessible in the National Snow and Ice Data Center archive, little data has been released by the British Navy and the University of Cambridge. This clearly diminishes the scientific value and undermines the authority of UK submarine measurements. Some would go further and, like Popper, claim that if the results are not corroborable, they have nothing of scientific in them. On the contrary, several research groups are making the most of openly available altimetry data. By working independently, these groups' results automatically validate each other.

Submarine missions to the Arctic are likely to become less frequent, at least until the Arctic becomes, again, strategically vital, this time because of its natural resources. The next Royal Navy cruise to the Arctic that will accommodate a scientific component is scheduled for 2013 or 2014. We have plenty of time to plan it carefully in order to make the most of this fantastic opportunity. Beyond

the traditional measurements of sea ice thickness and morphology there is a wealth of oceanography and marine biology observations to be made from such a unique platform (Boyd, 2010). Hopefully, the next UK submarine mission to the Arctic will be richer than ever.

## REFERENCES

- Ackley, S.F., W.B. Hibler, F. Kugrzk, A. Kovacs, and W.F. Weeks (1974). *Thickness and roughness variations of arctic multi-year ice*. Oceans '74, IEEE International Conference on Engineering in the Ocean Environment, vol. 1, pp. 109–117. Halifax, NS, Canada.
- Boyd, T. (2010). Report on the *Arctic Submarine based Science Workshop*, Oban, Scotland, April 2010.
- Calvao, J., J. Rodrigues, and P. Wadhams (2011). *Arctic sea ice thickness in the winters of 2004 and 2007 from coincident satellite and submarine measurements*, in “Geodesy for Planet Earth”, Proceedings of the 2009 IAG symposium, Buenos Aires, Argentina, 2009. ISBN 978-3-642-20337-4. Published by Springer.
- Cavalieri, D.J., and J.C. Comiso (2004). AMSR-E/Aqua daily L3 12.5km Tb, Sea ice concentrations and Snow depth polar grids; NSIDC.
- Collins, W.J., *et al.* (2008). *Evaluation of the HadGEM2 model*. Met Office Hadley Centre Technical Note no. HCTN 74.
- Comiso, J., *et al.* (1991). *Top/bottom multisensor remote sensing of Arctic sea ice*. J. Geophys. Res. 96 (C2), 2693–2709.
- Eisenman, I. (2010). *Geographic muting of changes in the Arctic sea ice cover*; Geophys. Res. Lett., 37, L16501, doi:10.1029/2010GL043741.
- Farrell, S.L., S.W. Laxon, D.C. McAdoo, D. Yi, and H.J. Zwally (2009). *Five years of Arctic sea ice freeboard measurements from the Ice, Cloud and land Elevation Satellite*. J. Geophys. Res., 114, C04008, doi:10.1029/2008JC005074.
- Forsberg, R., and H. Skourup (2005). *Arctic Ocean gravity, geoid and sea ice freeboard heights from ICESat and Grace*. Geophys. Res. Lett. 32, L215502 doi:10.1029/2005GL023711.
- Forsberg, R., *et al.* (2007). *Combination of spaceborne, airborne and in-situ gravity measurements in support of Arctic sea ice thickness mapping*. Danish National Space Centre, Technical Report, 7.
- Forsström, S., S. Gerland, and C.A. Pedersen (2011). *Thickness and density of snow-covered sea ice and hydrostatic equilibrium assumption from in situ measurements in Fram Strait, the Barents Sea and the Svalbard Coast*. Annals of Glaciology 52 (57).
- Gerdes, R., M.J. Karcher, F. Kauker, and U. Schauer (2003). *Causes and development of repeated Arctic Ocean warming events*. Geophys. Res. Lett. 30, 1980, doi:10.1029/2003GL018080.
- Gerdes, R. (2011). ACCESS WP1 Workshop, Bremen. Private communication.
- Giles, K.A., S.W. Laxon, and A.L. Ridout (2008). *Circumpolar thinning of Arctic sea ice following the 2007 record ice extent minimum*. Geophys. Res. Lett., 35, L22502, doi:10.1029/2008GL035710.

- Haas, C., A. Pfaffling, S. Hendricks, L. Rabenstein, J.-L. Etienne, and I. Rigor (2008). *Reduced ice thickness in Arctic Transpolar Drift favors rapid ice retreat*. *Geophys. Res. Lett.*, 35, L17501, doi:10.1029/2008GL034457.
- Haas, C., S. Hendricks, H. Eicken, and A. Herber (2010). *Synoptic airborne thickness surveys reveal state of Arctic sea ice cover*. *Geophys. Res. Lett.*, 37, L09501, doi:10.1029/2010GL042652.
- Heygster, G. (2011). *Arctic sea ice extent small as never before*; Press release from the University of Bremen.
- Hibler, W.D., S. Ackley, W.F. Weeks, and A. Kovacs (1972). *Top and bottom roughness of a multiyear ice floe*. Proceedings of the International Association for Hydraulic Research IAHR Symposium on Ice, pp. 130–142. Leningrad, U.S.S.R.
- Hughes, N., and P. Wadhams (2006). *Measurement of Arctic sea ice thickness by submarine 5 years after SCICEX*; *Ann. Glaciol.*, 44, 200-4.
- Hvidegaard, S.M., and R. Forsberg (2002). *Sea ice thickness from airborne laser altimetry over the Arctic Ocean north of Greenland*. *Geophys. Res. Lett.* 29 (20), 1952, doi:10.1029/2001GL014474.
- Hvidegaard, S.M., R. Forsberg, and H. Skourup (2006). *Sea ice thickness estimates from airborne laser scanning*. In Scientific Report of the International Workshop on Arctic Sea Ice Thickness: Past, Present and Future; Edited by P. Wadhams and G. Amanatidis; European Commission.
- Johns, T.C., et al. (2006). *The new Hadley Centre climate model HadGEM1: Evaluation of coupled simulations*. *J. Clim.*, 19, 1327-1353.
- Karcher, M.J., R. Gerdes, F. Kauker, and C. Köberle (2003). *Arctic warming: Evolution and spreading of the 1990s warm event in the Nordic seas and the Arctic Ocean*. *J. Geophys. Res.*, 108(C2), 3034, doi:10.1029/2001JC001265.
- Kauker, F., R. Gerdes, M. Karcher, C. Köberle, and J.L. Lieser (2003). *Variability of Arctic and North Atlantic sea ice: A combined analysis of model results and observations from 1978 to 2001*. *J. Geophys. Res.*, 108(C6), 3182, doi:10.1029/2002JC001573.
- Kwok, R., and G.F. Cunningham (2008). *ICESat over Arctic sea ice: Estimation of snow depth and ice thickness*. *J. Geophys. Res.*, 113, C08010, doi:10.1029/2008JC004753.
- Kwok, R., G.F. Cunningham, M. Wensnahan, I. Rigor, H.J. Zwally, and D. Yi (2009). *Thinning and volume loss of the Arctic Ocean sea ice cover: 2003-2008*. *J. Geophys. Res.*, 114, C07005, doi:10.1029/2009JC005312.
- Laxon, S., et al. (2003). *High interannual variability of sea ice thickness in the Arctic region*. *Nature* 425, 947–950.
- Markus, T., and D. Cavalieri (1998). *Snow depth distribution over sea ice in the Southern Ocean from satellite passive microwave data*. Antarctic sea ice: physical processes, interactions and variability; Antarctic Research Series 74, 19-39; Washington, DC, USA; American Geophysical Union.

Maslanik, J. A., C. Fowler, J. Stroeve, S. Drobot, H.J. Zwally, D. Yi, and W.J. Emery (2007). *A younger, thinner Arctic ice cover: Increased potential for rapid, extensive sea ice loss*. *Geophys. Res. Lett.*, 34, L24501, doi:10.1029/2007GL032043.

Maslowski, W., J. Clement Kinney, and J. Jakacki (2007a). *Toward prediction of environmental Arctic change*. *Computing in Science and Engineering* 9 (6), 29–34.

Maslowski, W., J. Whelan, J. Clement Kinney, and J. Jakacki (2007b). *Understanding Recent Variability in the Arctic Sea Ice Thickness and Volume — Synthesis of Model Results and Observations*. AGU Invited Talk.

Melling, H., P.H. Johnson, and D.A. Riedel (1995). *Measurement of the topography of sea ice by moored sub-sea sonar*. *J. Atmos. Oceanic Technol.* 12 (3), 589–602.

Melling, H., D.A. Riedel, and Z. Gedalof (2005). *Trends in the draft and extent of seasonal pack ice, Canadian Beaufort Sea*. *Geophys. Res. Lett.* 32, L24501 doi:10.1029/2005GL024483.

Mock, S.J., A.D. Hartwell, and W.D. Hibbler (1972). *Spatial aspects of pressure ridge statistics*. *J. Geophys. Res.* 77 (30), 5945–5953.

National Snow and Ice Data Center (2006). *Submarine upward looking sonar ice draft profile data and statistics*. <http://nsidc.org/data/g01360.html>. Boulder, CO.

Perovich, D.K., J.A. Richter-Menge, K.F. Jones, and B. Light (2008). *Sunlight, water, and ice: Extreme Arctic sea ice melt during the summer of 2007*. *Geophys. Res. Lett.*, 35, L11501, doi:10.1029/2008GL034007.

Rabenstein, L., S. Hendricks, T. Martin, A. Pfaffhuber, and C. Haas (2010). *Thickness and surface-properties of different sea-ice regimes within the Arctic Trans Polar Drift: Data from summers 2001, 2004 and 2007*. *J. Geophys. Res.*, 115, C12059. doi:10.1029/2009JC005846.

Richter-Menge, J., D.K. Perovich, C. Geiger, B.C. Elder, and K. Claffey (2006). *Ice Mass Balance buoy: An instrument to measure and attribute changes in ice thickness*. *Arctic Sea Ice Thickness: Past, Present and Future*, Proceedings of the International Workshop on Arctic Sea Ice Thickness, Rungstedgaard, Denmark, November 2005.

Rodrigues, J. (2009). *The increase in the length of the ice-free season in the Arctic*. *Cold Reg. Sci. Technol.* doi: 10.1016/j.coldregions.2009.05.006.

Rodrigues, J. (2010). *Beamwidth effects on sea ice draft measurements from U.K. submarines*. *Cold Reg. Sci. Technol.* 65 (2011) 160-171, doi:10.1016/j.coldregions.2010.09.005.

Romanov, I.P. (2004). *Morphometric characteristics of ice and snow in the Arctic Basin: aircraft landing observations from the former Soviet Union, 1928-1989*; National Snow and Ice Data Center, Boulder, CO; Digital media.

Rothrock, D.A., Y. Yu, and G.A. Maykut (1999). *Thinning of the Arctic sea-ice cover*. *Geophys. Res. Lett.*, 26 (23), 3469–3472, doi:10.1029/1999GL010863.

Rothrock, D.A., and M. Wensnahan (2007). *The accuracy of sea ice drafts measured from US Navy submarines*. J. Atmos. Oceanic Technol., 24(11), 1936–1949, doi:10.1175/JTECH2097.1.

Rothrock, D., D. Percival, and M. Wensnahan (2008). *Decline in Arctic sea-ice thickness: separating the spatial, annual, and interannual variability in a quarter century of submarine data*. J. Geophys. Res. 113, C05003, doi:10.1029/2007JC004252.

Schwarz, J., and W.F. Weeks (1977). *Engineering properties of sea ice*. J. Glaciol., 19(81), 499– 530.

Schwegmann, S., S. Hendricks, A. Herber, C. Haas, H. Eicken, and A. Mahoney (2011). *Spring and summer 2011 AWI sea ice surveys*. SIDARUS Progress Meeting 2, Bremen, December 2011.

Shimada, K., and T. Kamoshida (2008). *Mechanism on further catastrophic reduction of Arctic sea ice: influence of oceanic change*. Proceedings of The First International Symposium on the Arctic Research (ISAR-1), Drastic Change under the Global Warming, Tokyo, Japan, November 2008.

Skourup, H., and R. Forsberg (2006). *Sea ice freeboard from ICESat — a comparison with airborne lidar measurements*. Arctic Sea Ice Thickness: Past, Present and Future, Proceedings of the International Workshop on Arctic Sea Ice Thickness, Rungstedgaard, Denmark, November 2005.

Spreen, G., S. Kern, D. Stammer, and E. Hansen (2009). *Fram Strait sea ice volume export estimated between 2003 and 2008 from satellite data*. Geophys. Res. Lett. 36, L19502. doi:10.1029/2009GL039591.

Stroeve, J., M.M. Holland, W. Meier, T. Scambos, and M. Serreze (2007). *Arctic sea ice decline: Faster than forecast*. Geophys. Res. Lett., 34, L09501, doi:10.1029/2007GL029703.

Serreze, M. (2011). *Rethinking the sea ice tipping point*. Nature, 471.

Tietsche, S., D. Notz, J.H. Jungclaus, and J. Marotzke (2011). *Recovery mechanisms of Arctic summer sea ice*. Geophys. Res. Lett., 38, L02707, doi:10.1029/2010GL045698.

Timco, G.W., and W.F. Weeks (2010). *A review of the engineering properties of sea ice*. Cold Regions Science and Technology, 60, 107-129, doi:10.1016/j.coldregions.2009.10.003.

Vinje, T., N. Nordlund, and A. Kvambekk (1998). *Monitoring ice thickness in Fram Strait*. J. Geophys. Res. 113, 10437–10449.

Wadhams, P., and R.J. Horne (1980). *An analysis of ice profiles obtained by submarine sonar in the Beaufort Sea*. J. Glaciol., 25, 93.

Wadhams, P. (1981). *Sea-ice topography of the Arctic Ocean in the region 70°W to 25°E*. Phil. Trans. Roy. Soc., London, A302, 45-85.

Wadhams, P. (1983). *Sea ice thickness distribution in Fram Strait*. Nature, vol. 305, No. 5930, pp. 108-111, 8th September.

Wadhams, P., and T. Davy (1986). *On the spacing and draft distributions for pressure ridge keels*. J. Geophys. Res. 91, 10697–10708.

- Wadhams, P. (1989). *Sea-ice thickness distribution in the Trans Polar Drift Stream*. Rapp. P.-v. Reun. Cons. int. Explor. Mer, 188: 59-65.
- Wadhams, P. (1990). *Evidence for thinning of the Arctic ice cover north of Greenland*. Nature, vol. 345, No. 6278, pp. 795-797, 28th June.
- Wadhams, P. (1992). *Sea Ice Thickness Distribution in the Greenland Sea and Eurasian Basin, May 1987*. J. Geophys. Res., 97(C4), 5331-5348.
- Wadhams, P. (1997); *Ice Thickness in the Arctic Ocean: The statistical reliability of experimental data*. J. Geophys. Res., 102 (C13), 27951-27959.
- Wadhams, P., and N.R. Davis (2000). *Further evidence of ice thinning in the Arctic Ocean*. Geophys. Res. Lett., 27(24), 3973–3975, doi:10.1029/2000GL011802.
- Wadhams, P., and N.R. Davis (2001). *Arctic sea-ice morphological characteristics in summer 1996*. Ann. Glaciol., 33, 165-170.
- Wadhams, P., J.P. Wilkinson, and S.D. McPhail (2006). *A new view of the underside of Arctic sea ice*. Geophys. Res. Lett., 33, L04501, doi:10.1029/2005GL025131.
- Wadhams, P., N. Hughes and J. Rodrigues (2011); *Arctic sea ice thickness characteristics in winter 2004 and 2007 from submarine sonar transects*; J. Geophys. Res., 116, C00E02, doi:10.1029/2011JC006982.
- Warren, S.G., I.G. Rigor, N. Untersteiner, V.F. Radionov, N.N. Bryazgin, Y.I. Aleksandrov, and R. Colony (1999). *Snow depth on Arctic sea ice*. J. Clim., 12, 1814 – 1829, doi:10.1175/1520-0442(1999)012<1814:SDOASI>2.0.CO;2.
- Weeks, W. F., and O.S. Lee (1958). *Observation on the physical properties of sea ice at Hopedale, Labrador*. Arctic, 11(3), 134– 155.
- Williams, E., C. Swithinbank, and G. Robin (1975). *A submarine sonar study of Arctic ice pack*. J. Glaciol. 15 (73), 349–362.
- Woodgate, R.A., T. Weingartner, and R. Lindsay (2010). *The 2007 Bering Strait oceanic heat flux and anomalous Arctic sea ice retreat*. Geophys. Res. Lett., 37, L01602, doi:10.1029/2009GL041621.
- Zwally, H.J., D. Yi, R. Kwok, and Y. Zhao (2008). *ICESat measurements of sea ice freeboard and estimates of sea ice thickness in the Weddell Sea*. J. Geophys. Res., 113, C02515, doi:10.1029/2007JC004284.

**END OF DOCUMENT**